Robust optimisation of ethanol yield during fermentation using neural networks.

A thesis submitted to the Faculty of Engineering and the Built Environment, University of the Witwatersrand, Johannesburg, in fulfilment of the requirements for the degree of Doctor of Philosophy

Prepared by

Antony James Higginson

Submitted to

School of Chemical and Metallurgical Engineering, Faculty of Engineering and the Built Environment, University of the Witwatersrand, Johannesburg, South Africa

Supervisors:

Professor Kevin Brooks

Professor Kevin Harding

2025

Declaration

I declare that this thesis is my own unaided work. It is being submitted for the degree of Doctor of Philosophy in Engineering to the University of the Witwatersrand, Johannesburg.

It has not been submitted before for any degree or examination at any other University.

Antony James Higginson

Abstract

The optimisation of ethanol production during fed-batch fermentation by *Saccharomyces cerevisiae* under uncertain conditions was achieved using Artificial Neural Networks (ANN) for parameter estimation and robust optimisation. While yeast has been extensively studied, there is no universally accepted kinetic model to describe ethanol formation during fermentation. In this work a novel simplified model for ethanol production and sugar consumption was developed, indicating that ethanol toxicity was the primary limiting factor determining the final concentration of ethanol.

Online density measurements were used, along with existing correlations related to the relationship between the change in density over a batch and the ethanol and sugar concentrations in the liquid. The equations were adapted to work with fed-batch mode fermentations and were demonstrated to provide an estimate with an average error of 7.23 g/L compared with HPLC measurements.

The fermentation data was modelled analytically, and a new model was developed to predict the total sugar consumed during the fed-batch fermentation. Parameter estimation was performed using ANN to predict the value of P_{max} during the fermentation, and the maximum ethanol concentration was predicted with an R^2 of 0.91 over the dataset.

The developed models were then used to optimise the process. It was found that additional water could be added to obtain the maximum quantity of ethanol from a fermentation, optimising ethanol production. The volume of diluting water can easily be determined for cases where the value of the ethanol toxicity (P_{max}) is known. However, the ANN estimation was used in cases where Pmax is unknown. Due to the uncertainty of the estimate, a robust optimisation framework was used to prevent an “optimal” solution that was sub-optimal for the actual P_{max} value, where the parameter's upper bound was specified. The volume addition determined using the robust optimisation method was within 10% of the optimal volume calculated offline and could increase the sugar conversion to near 100%.

Dedication

To Aneshree and Jayseelan

Acknowledgements

I would like to thank the following people, without them I would not have been able to complete this research.

Professor Kevin Brooks, who guided me to the end.

Professor Kevin Harding, Professor Herman Potgieter and Professor Sunny Iyuke for providing support along the way

All the staff at the School of Chemical and Metallurgical Engineering

Table of Contents

Table of Figures

List of Tables

List of symbols

D: dilution factor h^{-1}

E: Energy used to distil fermentation product to 90% KJ/Kg

G: glycerol concentration g/L

g_1 g_2 g_3 C : constants for calculation of SG from tilt

K_s: half velocity constant g/L

K_I: inhibition constant g/L

K_p: product inhibition constant for biomass growth g/L

K'_P: product inhibition constant for product formation g/L

k_1 k_2 k_3 k_4 k_5 k_6 k_7 k_8 k_9: constants for Starzac model

k_d: specific rate of cell death h^{-1}

$m_{f:}$ mass feed kg

m_w: mass water kg

n: toxic power

OE: original extract

P: Product (ethanol) concentration g/L

P_{max}: maximum ethanol concentration g/L

$P_{max,opt}$: upper bound for maximum ethanol concentration g/L

P_t: total product g

q: attenuation factor

RE: real extract

r_x: rate of product formation g/L.h

S: Substrate concentration g/L

S_0: initial substrate concentration g/L

S_f: Substrate in feed g/L

SG: Specific gravity

S_t: total sugar consumed during fermentation kg

S_{tf}: substrate added to fermenter kg

V: Volume of fermentation L

V_0: initial volume L

V_f: feed volume L

V_{DW}: Volume of dilution water L

V_{max}: Maximum volume L

X: Biomass concentration g/L

X_0: initial biomass concentration g/L

X_t: total biomass g

$Y_{p/s}$: yield g ethanol/kg sugar

θ_1 θ_2: constants for temperature adjustment

μ: specific rate of biomass growth h^{-1}

μ_{max}: maximum specific rate of biomass growth h^{-1}

μ_0: specific rate of biomass growth rate without inhibition h^{-1}

ν_G: specific rate of glycerol production h^{-1}

ν: specific rate of product formation h^{-1}

ν_0: specific rate of product formation without inhibition h^{-1}

ν_{max}: maximum rate of product formation $g.h^{-1}.L^{-1}$

1) Introduction

1.1 Introduction

Ethanol production by Saccharomyces cerevisiae is one of the oldest known biochemical processes, with evidence of this process being used in beverage production dating back several thousand years (McGovern et al., 2005). Modern use of S. cerevisiae to produce ethanol can be split into two main application areas: biofuel and beverage production. In South Africa, fuel ethanol is not currently produced, with limited ethanol production for the beverage, paint, and pharmaceutical industries (Kohler, 2016). However, the country has the potential to produce approximately 274 000 tonnes of bioethanol should surplus sugar from cane production be used to produce fuel (Cartwright, 2007).

The process used to produce ethanol for fuels depends on the feedstock, with the primary feedstock used being corn in the United States of America and sugar cane in Brazil. Ethanol produced from sugar cane feedstock is fermented by yeast in a fed-batch process to 7-9% alcohol by volume (abv) followed by distillation to concentrate the alcohol to greater than 96% purity. The fed-batch process increases yeast cell concentrations during fermentation and reduces contamination (Lucio & Fermentec, 2008). However, high gravity and very high gravity fermentations where greater sugar concentrations of up to 250 g/L and greater than 250 g/L, respectively, increase the final ethanol concentration and could potentially reduce the costs associated with the process by reducing the energy requirements during distillation and reducing water usage. High gravity fermentations, however, place extra stresses on the yeast cells that can affect ethanol production (Gomes et al., 2021). In addition, molasses and cane juice, the primary feedstocks for ethanol production, can vary significantly in terms of the available nutrients and other constituents that can affect the yeast cells (Palmonari et al., 2020). These effects can result in high residual sugar concentrations at the end of the fermentation of up to 60 g/L (Joannis-Cassan et

al., 2014), which in a 300 m^3 fermenter would mean that 18 tonnes of sugar would be unfermented at the end of the fermentation. This residual sugar equates to over 11 kL of ethanol that could have been produced during the fermentation. The effect of nutrient variability and yeast vitality on ethanol toxicity means that it can be difficult to predict the residual sugars present after a high gravity fermentation.

A barrier to the optimisation of ethanol production is the uncertainty in the measurement and modelling of the process. Measurement of key variables is not feasible in many instances due to the cost or complexity of sensors. Other important variables, such as the nutritional requirements and their effect on the process, are poorly understood. Hence, an optimal solution, based on these uncertain parameters, may be unfeasible or suboptimal.

To address the uncertainty of the parameters and to prevent sub-optimal solutions from being implemented, a Robust Optimisation framework is used to determine the solution that is viable for all potential values of the uncertain parameter.

1.2 Problem statement

High gravity fermentations may be used to increase ethanol production during fermentation. In practice, the kinetics are unknown or uncertain and can only be determined from fermentation data during the fermentation process.

1.3 Research Objectives

To increase the amount of ethanol produced during fermentation by manipulating the feed during fed-batch fermentation.

To achieve this objective, the following sub-objectives must be achieved.

1) A method to monitor the sugar and ethanol concentration in real-time during the fermentation must be developed.
2) The development of a method to determine the fermentation kinetics of the yeast during the fermentation.
3) Development of a robust optimisation strategy that can increase the amount of ethanol produced and reduce the residual sugar concentration.

1.4 Structure of the thesis

This thesis is divided into nine chapters.

Chapter 2 Bioethanol production. This chapter reviews the literature related to bioethanol production and looks into the modelling of ethanol fermentations.

Chapter 3 Dynamic optimisation of ethanol yield. This chapter reviews the literature related to optimising ethanol production during fermentation, including aspects of modelling, soft sensors and parameter estimation.

Chapter 4: Data collection from fermentations. This chapter describes the experimental apparatus and the experiments performed to collect data.

Chapter 5: Online monitoring of ethanol concentration during fed-batch fermentations. This chapter details the development of a method that allows for the online measurement of the ethanol concentration during fed-batch ethanol fermentation. The online estimates are compared to offline measurements made using high-performance liquid chromatography to demonstrate the effectiveness of the online soft sensor.

Chapter 6: Modelling of fed-batch fermentations. This chapter uses the experimental data to develop an analytical model for the system, indicating the variables most affecting the ethanol yield. The data is also used to develop a predictive model using artificial neural networks for parameter estimation. The Neural network, trained on the experimental dataset, is then tested against data produced from simulations that use the developed analytical model.

Chapter 7: Robust optimisation of ethanol yield. This chapter examines optimisation strategies that could be implemented and demonstrates the effectiveness of these strategies. Limiting the amount of substrate feed was shown to be an effective optimisation strategy, but it limits the amount of ethanol produced. Adding dilution water was an effective strategy for increasing the total amount of ethanol produced.

Chapter 8: Conclusion. This chapter summarises the findings of the research and provides recommendations for further work.

Appendices. Selected experimental data and MATLAB code relating to the research are presented.

1.5 Novelty of Research

This research covers several novel areas.

1) Online monitoring of ethanol and sugar concentrations during fed-batch fermentations using density measurements. Density measurements have been used for over 150 years to estimate the ethanol concentration during fermentations by *Saccharomyces cerevisiae*. This research developed a method to use these empirical relationships for fed-batch reactions by adjusting the original extract as feed is added to the fermentation.
2) The research proposes a novel model for sugar consumption during fed-batch fermentations. There is little research on anaerobic fermentations, and most research proposes using Monod-type kinetics, which is inappropriate for the reaction as there is little cell growth. The kinetics developed in this research are based on the limitation caused by product inhibition. It allows for calculating the total amount of sugar consumed and the total amount of ethanol produced. By analysing the model, an optimisation strategy was developed where water was added to dilute the ethanol and reduce the inhibition, thus allowing the fermentation to consume more sugar and produce more ethanol overall without reducing the ethanol concentration significantly.
3) The application of robust optimisation to fed-batch fermentations using artificial neural networks to estimate unknown parameters. As it can be assumed that the maximum theoretical ethanol concentration is unknown at the start of the fermentation, a method was developed to use the measurements taken during the fermentation to estimate the final ethanol concentration based on historical data. The dataset used to train the network was relatively small, consisting of only ten fermentations, and shown to be effective for conditions not included in the dataset. As the prediction was uncertain, Robust optimisation was used to prevent the

uncertainty of the estimation from causing an overestimation of the dilution water required.

2) Bioethanol production

2.1 Production of fuel ethanol by fermentation

2.1.1 Industrial Importance

Global ethanol production is over 100 million litres per year (Hoang & Nghiem, 2021), with production primarily located in Brazil and the USA (Parapouli et al., 2020). The feedstocks for production vary by region, with 60% produced using corn as a feedstock, 25% from sugarcane and the remainder from other sugar sources such as wheat and sugar beets (Hoang & Nghiem, 2021). The profit that can be generated is the limiting factor to the potential production of bioethanol. With the competition of fuel vs food and other constraints, maximising ethanol production from the available feedstock is of great importance, as well as the reduction of waste streams. As technologies develop, the need for biofuels may diminish as battery-powered vehicles and hydrogen storage become more widely available. However, ethanol produced through fermentation of sustainable sources such as cellulose can replace fossil based feedstocks, such as polyethylene, where ethanol derived from petroleum products is the primary source (Morschbacker, 2009) (Dagle et al., 2020). Sustainably produced ethanol can also form part of a biorefinery concept where multiple high value products are produced. Hydrogen, which is a promising future energy source could also be produced sustainably using ethanol (Rass-Hansen et al., 2007).

Globally, the feedstocks and technologies used vary by region, with ethanol production in the USA mainly using corn as a feedstock. In Brazil, sugarcane is used as a feedstock, and sugar beet is the primary feedstock for fermentation in Europe.

2.1.2 Ethanol Production in the USA

As of 2021, the USA accounts for more than half of the fuel ethanol produced worldwide (Renewable Fuels Association, n.d.). Nearly all ethanol production in

the USA is derived from start feedstocks, specifically corn (Hoang & Nghiem, 2021). When a starch feedstock is used, additional processing is required as the sugars are in a form that cannot be metabolised by yeast, and yeast does not produce the enzymes to hydrolyse the starch molecules into fermentable sugars such as glucose. Several approaches can be used for this purpose. A dry milling process grinds the corn prior to a stage in which hot water is added to make the starch soluble. Enzymes are then added to hydrolyse the starch molecules into fermentable sugars. In a wet milling process, the corn is steeped in water before grinding, allowing for components such as gluten, corn oil, and corn germ to be removed prior to solubilisation and enzymatic hydrolysis of the starch. 91.1% of ethanol production in the USA is produced using a dry milling process, as it has lower capital costs, higher ethanol yields and energy savings compared to wet milling (J. Li et al., 2022).

An essential factor in the fermentation is the Free Amino Nitrogen (FAN) available for the yeast during fermentation. FAN is mostly consumed by the yeast in the first 24 hours of fermentation during the growth phase, with no consumption during the later stages of fermentation (Arifeen et al., 2009). While the FAN content of the fermentation can be increased by using protease enzymes to break down proteins in the feedstock, this can also be supplemented by adding yeast extract, ammonium salts, urea or spent yeast to increase the ethanol yield (Perez-Carrillo et al., 2012).

After fermentation, the fermentation product contains approximately 15% ethanol and is distilled and processed to anhydrous ethanol. An additional product from the distillation bottoms is the distillers' spent grains, which are dried and sold as animal feed (Hoang & Nghiem, 2021).

2.1.3 Ethanol Production in Brazil

Brazil is the world's second-largest fuel ethanol producer, producing 27% of the world's ethanol in 2021 (Renewable Fuels Association, n.d.). There are 360 1st generation ethanol plants in Brazil with a nameplate capacity of 42.8 billion.

However, only 67% of that capacity is used (Hoang & Nghiem, 2021). Brazil is unique among the leading ethanol producers in that the primary feedstock for ethanol production is sugarcane, with 70-80% of distilleries using fed-batch fermentation (Ccopa Rivera et al., 2017). The fed-batch fermentation mode allows for 99.5% of the cells to be separated and reused in subsequent fermentations. The fed-batch mode of operation allows for high cell densities and short fermentations that last approximately 6-11 hours. The limitation of the technology is that the fermentation is limited to approximately 200 g/L TSAI (Total Sugars As Invert, where sucrose is equivalent to 0.95 of the fructose and glucose formed), and higher sugar concentrations can result in stuck fermentations where not all sucrose is converted to ethanol.

2.1.4 Potential for fuel ethanol production in South Africa

Production of Bioethanol in the Southern African region remains low despite the mandated blending requirements in many countries in the region, as well as large-scale sugarcane farming in the area. However, the cost of ethanol production from sugarcane remains very high, with the cost of ethanol being over $100/bbl (Kohler, 2016). Most of this cost comprises the feedstock, which contributes approximately $67/bbl. Newer technologies such as 2nd and 3rd generation feedstocks have shown promise but are not yet commercially viable due to technological challenges. 2nd generation feedstocks are those that use lignocellulosic feedstocks (woody biomass). While these feedstocks are available in abundance, they are not yet viable options economically and in terms of sustainability criteria due to the expensive and energy-intensive processes required in the pre-treatment hydrolysis processes. The hydrolysis process for 2nd generation feedstocks is complex as the fermentable sugars are polymerised as cellulose fibres and bound in a matrix strengthened by lignin. Hence, the matrix must first be weakened using various technologies, such as steam explosion, prior to either acid or enzymatic hydrolysis of the cellulose. 3rd Generation feedstocks, composed of microalgae, hold great promise to fulfil the energy needs of countries. For example, South

Africa could require only 1% coverage with microalgae cultivation for its energy needs, compared to 6% cultivation with sugarcane (Correa et al., 2019).

As technologies for the production of 2nd and 3rd-generation biofuels are not yet feasible, using 1st-generation feedstocks remains the proven technology to produce biofuels. Due to the cost of feedstock and area required for cultivation, the yield of bioethanol from the feedstock is vitally important, as well as the concentration attainable to reduce capital costs with fed-batch systems reporting a yield of up to 96.8% and an ethanol concentration by fermentation of first generation feedstocks (Ayodele et al., 2020). While research into 2nd and 3rd-generation feedstocks is ongoing, producing ethanol from these feedstocks is not economical due to expensive pre-treatment and low ethanol concentration achieved from these fermentations with 2nd-generation feedstocks (Tesfaw & Assefa, 2014).

South Africa can potentially produce a large quantity of ethanol using sugarcane as a feedstock. It is estimated that to produce 2% of the petroleum consumed by the country in 2013 would require less than 10% of the area planted with sugarcane to provide the feedstock (Kohler, 2016). There are, however, several problems that the country needs to solve for the production of biofuels to be widely adopted, chiefly the uncertainty with which governmental goals regarding biofuel targets need to be treated due to the repeated failures of government programs, for example, aiming to introduce mandatory blending of bio-ethanol which was mandated to commence in 2015 (Arndt et al., 2019)

2.2 Modelling of the production of ethanol by Saccharomyces cerevisiae in fed-batch fermentation

2.2.1 Mode of fermentation

Fermentations can be operated in 3 modes: continuous, batch and fed-batch (Rani & Rao, 1999), as shown in Figure 2.1. Batch fermentations are the simplest, whereby all substrate is available at the start of the fermentation. Generally, the fermentation will go through stages of growth, with a lag phase while the microorganism adapts to the medium, exponential growth occurring when the substrate is plentiful, a stationary phase once the substrate level has been depleted, and death once the cells can no longer sustain themselves (Schuler & Kargi, 2002). Continuous fermentations are fermentations where new medium is constantly added to the fermenter, and effluent is constantly removed. Due to the time that continuous fermenters are operational, sterilisation can become an issue if the fermenter becomes infected by foreign microorganisms. Fed-batch fermentations allow for batch type fermentation, where the conditions during each cycle can be carefully controlled. However, the addition of medium during

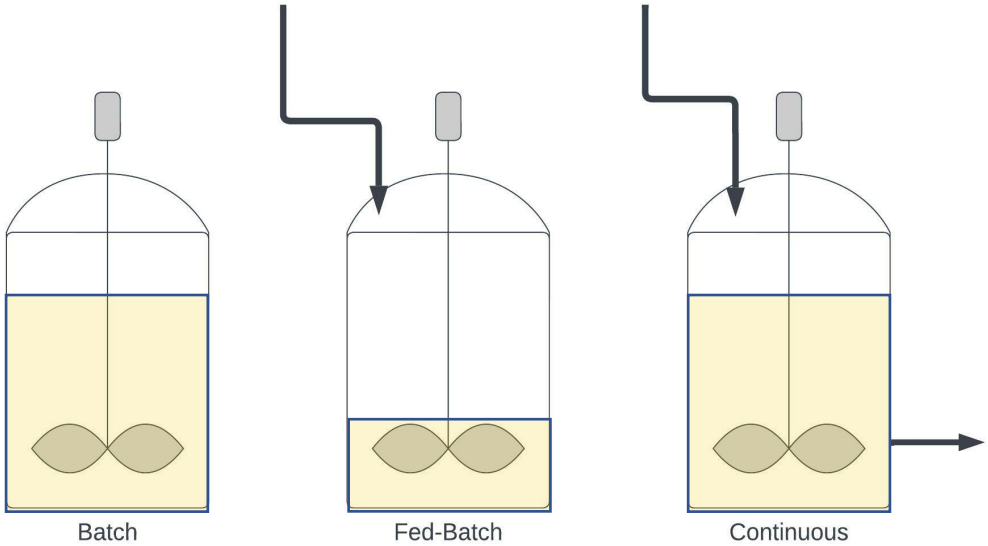

Figure 2.1: Batch, Fed-batch and continuous modes of operation

fermentation allows for greater control of the fermentation conditions than would otherwise be possible during fermentation (Rani & Rao, 1999). Fed-batch fermentations can be further divided into single-cycle fed-batch, where fresh substrate and micro-organisms are added to each cycle, and repeated cycle fed-batch processes, where a small amount of the final product at the end of one batch containing viable micro-organisms is reused as the starter culture for the next batch (Modak & Lim, 1992).

The main benefit of operating a fermentation in batch mode is the lower costs associated with the process (Tse & Wiens, 2021). Continuous fermentations can reduce downtime and cleaning costs, while fed-batch fermentations can maintain a higher viable cell concentration due to the ability to control variables such as pH and nutrients (Zabed et al., 2014).

For ethanol production, fermentation mode depends largely on the feedstock, with those producing ethanol from corn feedstock, such as those in the USA, primarily operating as batch fermenters (Bothast & Schlicher, 2005). Bioethanol fermentations that use sugar cane feedstock, such as those in Brazil, are mainly operated as fed-batch fermentations (De Oliva-Neto et al., 2013).

A method for obtaining higher ethanol concentrations is to use very high gravity fermentations, where the sugar concentration exceeds 180 g/L (Bai et al., 2008). Higher sugar concentrations lead to yeast cell stress due to nutrient limitations, osmotic stress and higher ethanol concentrations (Puligundla et al., 2011).

From an analytical perspective, modelling and optimisation of fed-batch fermentations is challenging. Fed-batch fermentations are differentiated from either batch or continuous fermentations in that the volume of the medium changes during the fermentation. The changing volume and dynamics of the system create challenges for the control and optimisation of the system as variables such as product concentration can be challenging to measure online, and the model often contains many time-varying parameters (Rani & Rao, 1999).

2.3 Modelling of the production of ethanol by Saccharomyces cerevisiae in fed-batch fermentation

2.3.1 Growth, substrate utilisation and product formation

The growth and product formation of Saccharomyces cerevisiae has been widely studied, and it is one of the most industrially important organisms (Parapouli et al., 2020). Modelling biological processes can be complex as several simultaneous pathways can occur during the metabolism of a substrate, as well as mass transfer of the substrate from the bulk liquid into the cells and product from the cell into the bulk liquid. In addition, the result is the totality of the effect of billions of cells simultaneously performing a wide variety of anabolic and catabolic reactions. For this reason, unstructured global models are most often used in the modelling and control of bioprocesses (Shugerl & Bellgardt, 2000). Unstructured models do not differentiate between different types of biomass, as all of the components are combined into a single term, X.

Unstructured global models are often used to describe the change in the growth rate with changing substrate concentration under circumstances where the growth is substrate limited. Many forms of growth kinetics are derived from Monod kinetics (Oliveira et al., 2017), shown in Equation 2.1, where X is the dry biomass, μ_{max} is the maximum specific growth rate, k_s is the half velocity constant, and S is the substrate concentration.

Monod kinetics describes a growth rate approximated by a first-order function of the substrate concentration at low concentrations and saturates to a maximum growth rate at high substrate concentrations. Hence, substrate limitations only become significant at lower substrate concentrations. This effect resembles Michaelis-Menten kinetics as the growth rate is affected dramatically by the substrate concentration at low values but reaches a maximum at higher substrate concentrations, beyond which increasing the substrate concentration further does not increase the growth rate (Monod, 1949). Monod kinetics assumes that other

nutrients and reactants, such as oxygen and nitrogen-containing molecules, are in excess and thus have little effect on the growth rate.

$$\frac{1}{X}\frac{dX}{dt} = \frac{\mu_{max} S}{k_s + S} \qquad 2.1$$

The overall metabolic process followed can generally be divided into Crabtree-positive and Crabtree-negative yeasts. Crabtree-positive yeasts produce the majority of adenosine triphosphate (ATP), the energy-carrying molecule for the cell, through the fermentative pathway shown in Figure 2.2, even in the presence of Oxygen. Crabtree-negative yeasts produce ATP through oxidative respiration, which does not produce ethanol (Hajar et al., 2017). In Crabtree-positive yeasts, once the sugars have been depleted in the medium, the ethanol produced during fermentation is oxidised by the cell to produce ATP, known as diauxic shift.

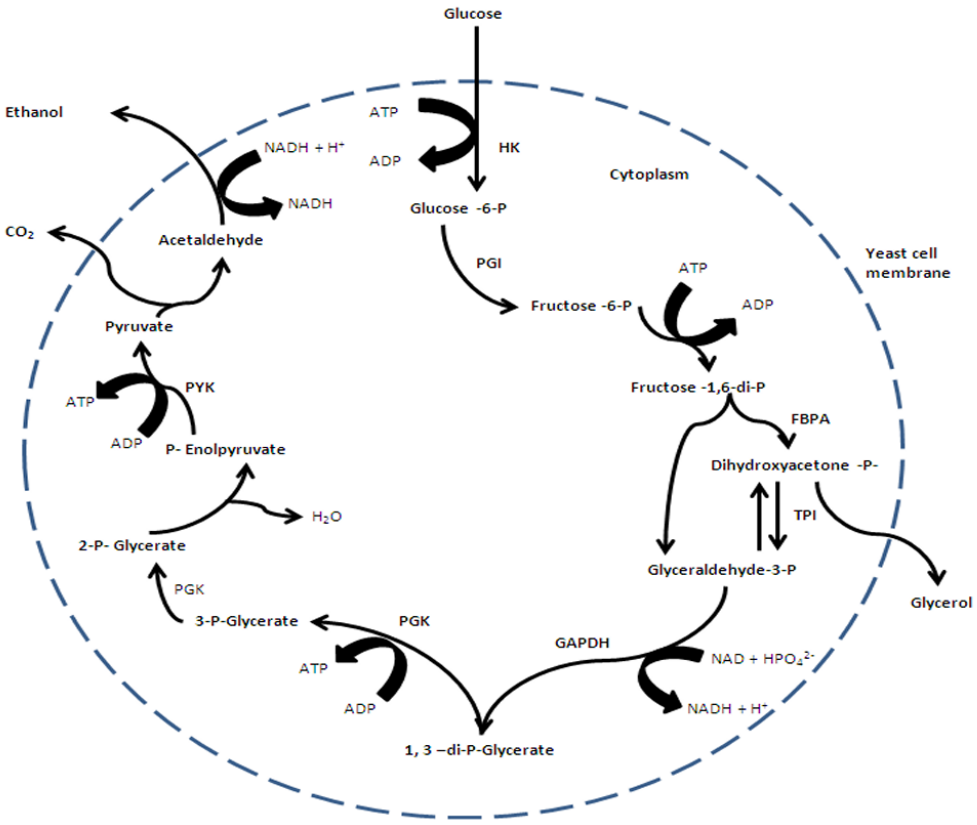

Figure 2.2: Metabolic pathway for the anaerobic formation of ethanol by Saccharomyces cerevisiae adapted from (Bai et al., 2008)

Saccharomyces cerevisiae is used in many industrial processes. However, the major products are yeast itself, in the case of biomass formation for the production of yeast for (among other uses) the baking industry, and ethanol production through alcoholic fermentation (Parapouli et al., 2020). In the case of alcohol fermentation, the formation of biomass is not the primary product, and many different reactions are performed in ethanol production, as shown in Equations 2.2-2.12 (Roels, 1981; Starzak et al., 1994). Equations 2.2 to 2.12 represent some of the important reactions involved in the fermentation of sucrose by *Saccharomyces cerevisiae,* where 'H_2' represents nicotinamide adenine dinucleotide (NADH) + H^+ as the reducing equivalents in the catabolic processes that form ATP. For clarity, some species involved in the reactions, such as ADP, inorganic phosphate and water involved in the phosphorylations and dephosphorylations, have been omitted. Equation 2.2 shows the anabolic metabolism of sucrose to form biomass. Energy is released from the ATP molecule when the phosphate group is removed. These processes are cyclical, and neither ATP nor NADH is consumed in the reaction. Hence, both can essentially be eliminated from the stoichiometry for practical purposes.

$$1.095CH_{11/6}O_{11/12} + 0.15NH_3 + 0.051ATP \rightarrow$$
$$CH_{1.61}O_{0.52}N_{0.15} + 0.13'H_2'^{\square} + 0.095CO_2 + 0.294H_2O \qquad 2.2$$

Equation 2.3 describes the anabolic formation of biomass from ethanol. As ethanol is an energy-rich, carbon-containing molecule, the yeast can metabolise the molecule to produce energy and biomass, although this process is less energy efficient than using sucrose or another sugar as a substrate.

$$1.285CH_3O_{0.5} + 0.15NH_3 + 1.588ATP \rightarrow$$
$$CH_{1.61}O_{0.52}N_{0.15} + 0.795'H_2'^{\square} + 0.285CO_2 \qquad 2.3$$

Equations 2.4, 2.5, 2.6, 2.7, and 2.8 represent the anaerobic fermentation of sucrose to form ethanol, glycerol, acetaldehyde, acetic acid and butanediol, respectively.

$$1.095CH_{11/6}O_{11/12} + 0.125H_2O \rightarrow CH_3O_{0.5} + 0.5\,CO_2 + 0.5ATP \quad 2.4$$

$$CH_{11/6}O_{11/12} + {}^{1}/_{12}\,H_2O + {}^{1}/_{3}\,ATP + {}^{1}/_{3}\,'H_2' \rightarrow CH_{8/3}O \quad 2.5$$

$$1.5CH_{11/6}O_{11/12} + 0.125H_2O \rightarrow CH_2O_{0.5} + 0.5CO_2 + 0.5ATP + 0.5'H_2' \quad 2.6$$

$$1.5CH_{11/6}O_{11/12} + 0.125H_2O \rightarrow CH_2O + 0.5CO_2 + 0.5ATP + 'H_2' \quad 2.7$$

$$1.5CH_{11/6}O_{11/12} + 0.125H_2O \rightarrow CH_{2.5}O_{0.5} + 0.5CO_2 + 0.5ATP + 0.5'H_2' \quad 2.8$$

Equations 2.9 and 2.10 show the catabolic reactions in the oxidation of sucrose and ethanol, respectively.

$$CH_{11/6}O_{11/12} + {}^{13}/_{12}\,H_2O \rightarrow CO_2 + {}^{2}/_{3}\,ATP + 2'H_2' \quad 2.9$$

$$CH_3O_{0.5} + 0.5ATP + 1.5H_2O \rightarrow CO_2 + 2'H_2' \quad 2.10$$

Equation 2.11 shows the oxidative phosphorylation of the reducing equivalents to ATP, produced during the initial redox reactions, which can be used as an energy source for other processes within the cell.

$$0.5O_2 + 'H_2' \rightarrow H_2O + \partial ATP \quad 2.11$$

Equation 2.12 shows the Polymerisation of Biomass precursors, consuming ATP for the anabolic process.

$$CH_{1.61}O_{0.52}N_{0.15} + \kappa ATP \rightarrow Biomass\ + 3'H_2' \qquad 2.12$$

While the substrate and nutrients involved in these reactions are essential in terms of the kinetics of the reactions, several other factors can also affect the rate of these reactions. Effects such as substrate inhibition (Mulchandani & Luong, 1989) and carbon dioxide effects (Jones & Greenfield, 1982) have been shown to decrease the rate of both biomass formation and the rate of ethanol production. The mechanisms of inhibition vary. Substrate inhibition occurs due to high substrate concentration, causing an increase in the osmotic pressure and thus adversely affecting the cell. High product concentration causes competitive inhibition of enzyme activity where the product (ethanol) binds to metabolic enzymes, thus preventing the enzymes from binding with the substrate and preventing the reaction (Mulchandani & Luong, 1989). High carbon dioxide concentrations affect the cell membrane and various metabolic processes (Jones & Greenfield, 1982).

2.2.2 Kinetics of growth, substrate utilisation and product formation by *Saccharomyces cerevisiae*

While there are many approaches that have been investigated, macroscopic approaches offer the benefits of integrating elemental balances and kinetics in the formulation of the model but individual reactions inside the cell do not need to be calculated (Roels, 1981). The model, however, must be chosen to include all relevant components. An example is the model developed from experimental data for the fermentation of sucrose by *Saccharomyces cerevisiae* at 30^{o}C (Starzak et al., 1994). The model includes Monod type substrate limitation without substrate

inhibition, exponential product inhibition, and Herbert's concept of endogenous metabolism. The relevant constants are shown in Table 2.2.

$$(r_x)_{growth} = \frac{k_1 XS}{k_2 F + S} \exp(k_5 P) \quad 2.13$$

$$(r_x)_{endogenous} = -k_6 X \quad 2.14$$

$$r_x = (r_x)_{growth} + (r_x)_{end} \quad 2.15$$

$$r_s = -k_3 (r_x)_{growth} \quad 2.16$$

$$r_P = k_4 (r_x)_{growth} \quad 2.17$$

$$r_H = -k_9 r_x \quad 2.18$$

$$F_{pH} = \frac{1 + k_7 H + k_8 H^2}{1 + k_7 H_0 - k_8 H_0^{-2}} \quad 2.19$$

Where P is the product concentration, r_x is the biomass formation rate, r_s is the substrate utilisation rate, r_P is the rate of product formation, r_H is the rate of proton formation, and F is a factor to account for variations in pH. This model does not account for any variation in the temperature. However, others have used Arrhenius-type equations to account for kinetic variations due to temperature changes. An additional energy balance over the system would be required to account for the effect of cooling due to feed addition and heating due to the exothermic reactions occurring (Dai et al., 2014).

Table 2.1: Constants for the macroscopic model from (Starzak et al., 1994). Values valid for time in hours, X, S and P in g/dm^3 and H in mol/ dm^3

Table 2.2: Constants for the macroscopic model of Starzak et al. (1994)

constant	value
k_1	0.3289
k_2	0.9645
k_3	12.93
k_4	5.705
k_5	0.0453
k_6	0.0288
k_7	10830
k_8	$6x10^{-12}$
k_9	0.023

In practice, simple unstructured models that describe the yeast's growth, substrate consumption and product formation are adequate to describe systems for many applications. However, the models may not adequately describe the transition between zero-order growth kinetics and substate limited growth that can occur in fed-batch fermentations (Esener et al., 1983).

Several unstructured models have been developed for yeast growth to account for various limiting and inhibitory effects such as substrate limitation, product inhibition and limitations due to cell concentration. Modifications to the Monod Model include the Contois equation, given in Equation 2.20, which allows for mass transfer limitations related to the cell concentration (Contois, 1959). This modification is appropriate for modelling the growth at high cell concentrations, while the Monod model is more suitable at lower cell concentrations(Oliveira et al., 2017).

$$\mu = \frac{\mu_{max} S}{X k_s + S} \quad 2.20$$

Where μ is the specific growth rate of the yeast.

Further modifications can be made to the Monod Model such as the Andrews Equation which accounts for decreases in the growth rate caused by substrate inhibition shown in Equation 2.21 (Andrews, 1968). As the concentration of reducing sugars increases various factors such as reactions with components of the cell, formation of complexes with the enzyme or other participants of the reaction, modification of the properties of the conditions of the fermentation medium and interference with control functions of the cell (Edwards, 1970), can reduce the rate at which the biochemical reaction occurs.

$$\mu = \frac{\mu_{max} S}{k_s + S + S^2/K_I} \quad 2.21$$

Where K_I is the inhibition constant.

Many other forms of kinetics have been derived to describe substrate inhibition, but these are not used as frequently (Oliveira et al., 2017).

The other type of inhibition that must be considered is product inhibition, as the increase in ethanol concentration during fermentation will reach a point at which the product, ethanol, becomes toxic to the cells and prevents further fermentation.

Ghose & Tyagi (Ghose & Tyagi, 1979) developed kinetics for yeast that includes both substrate and product inhibition. The kinetics of product inhibition are shown in Equation 2.22 for the specific rate biomass formation and Equation 2.23 for the specific rate of ethanol production. As the ethanol concentration approached the maximum ethanol concentration (P_m and P_m' for growth and product formation respectively) the rate slowed to zero. For the yeast used, Saccharomyces

cerevisiae NRRL-Y-I32, using consistent nutritional medium and bagasse hydrolysate as a source of reducing sugars, the concentration of ethanol beyond which growth could not occur (P_m) was found to be 87 g/L, and the concentration beyond which product formation could not occur was found to be 114 g/L.

$$\frac{\mu}{\mu_0} = 1 - \frac{P}{P_m} \qquad 2.22$$

$$\frac{v}{v_0} = 1 - \frac{P}{P_m{}'} \qquad 2.23$$

Where μ_0 is the expected specific rate of biomass growth without inhibition v_0 is the expected specific rate of product formation without inhibition, v is the specific rate of product formation.

To include the effect of substrate inhibition Equation 2.24 and 2.25 were developed (Ghose & Tyagi, 1979).

$$\frac{\mu}{\mu_0} = \left(1 - \frac{P}{P_m}\right)\frac{S}{S + K_s + \frac{S^2}{K_s\omega}} \qquad 2.24$$

$$\frac{v}{v_0} = \left(1 - \frac{P}{P_m{}'}\right)\frac{S}{S + K_s{}' + \frac{S^2}{K_s{}'\omega'}} \qquad 2.25$$

Where ω and ω' are variables representing the magnitude of the interference of binding of the substrate on the enzyme for the biomass and product formation respectively, and K_S' is the substrate constant for the production of biomass.

Ghose & Tyagi (1979) found the values for ω and ω' were found to be 427.5 and 455.0 for biomass formation and product formation respectively, but note that the inhibitory effect of the substrate is due to the presence of sugars such as xylose and cellobiose in the hydrolysate and that the use of glucose in the feed would have a value of ω above 1000 indicating a "small inhibitory effect".

Levenspiel (1980) provides a generalised nonlinear inhibition term including Monod kinetics for substrate limitation. Equation 2.26 shows that at low ethanol concentrations, the fermentation rate will be unaffected, with the inhibition caused by the ethanol increasing until the maximum ethanol concentration (P_m) is reached. As the ethanol concentration approaches P_{max} the growth rate approaches zero. The toxic power (n) determines the inhibitory effect's strength. If n>1, the effect of the inhibition is more significant at higher concentrations. If n<1, the effect is greater at lower concentrations; if n=1, the effect is evenly distributed.

$$\mu = \frac{\mu_{max} S}{k_s + S}\left(1 - \frac{P}{P_m}\right)^n \qquad 2.26$$

Where P_m is the maximum ethanol concentration that the yeast can tolerate, and n is the toxic power.

Luong (1985) extended this model, proposing a slightly different form, shown in Equation 2.27 and Equation 2.28 for the effect on the kinetics of biomass formation, and product formation respectively.

$$\frac{\mu}{\mu_0} = 1 - \left(\frac{P}{P_m}\right)^n \qquad 2.27$$

$$\frac{v}{v_0} = 1 - \left(\frac{P}{P_m}\right)^n \qquad 2.28$$

While the kinetics related to the formation of biomass and ethanol are often linked, it has also been noted that the kinetics of product formation continue even once growth of new cells has ceased (Aiba et al., 1968) hence Equation 2.24 will be true for cases where there is limited cell growth.

The effect of temperature on the growth rate can be estimated using a modified form of the Ratkowski equation (Zwietering et al., 1991). The relationship given in Equation 2.29 is better suited for predicting the temperature relationship for microbial kinetics than the Arrhenius law (Ali et al., 2011).

$$\mu_m = \left[a * (T - \theta_1) * (1 - e^{\{b*(T-\theta_2)\}}\right] \quad 2.29$$

Where a, b, θ_1 and θ_2 are empirical constants.

Many other variables can be considered when modelling microbial growth, such as pH, carbon dioxide concentration (Chang et al., 2018) (Jones & Greenfield, 1982) and nutrient concentration (Button, 1978). A plateau characterises the effect of pH on the growth kinetics to a maximum where the growth kinetics are not affected over an optimal range. However, outside the optimal range, growth kinetics are severely affected (Starzak et al., 1994). Carbon dioxide effects are caused by inhibiting enzyme activity and disruption of membrane function CO_2 partial pressures above 0.5 MPa (Thibault et al., 1987).

Nutrient effects on yeast growth kinetics are more challenging to quantify as the yeast requires an extensive range of nutrients to function optimally, with nutritional limitations found to be the main reason yeasts cannot tolerate high ethanol concentrations (Casey et al., 1984). Nutrients that may cause limitations include magnesium, nitrogen, lipids, and lipid-protein complexes (Dombek & Ingram, 1986). These limitations are difficult to model. However, nutrient sources that contain a wide variety of materials and vitamins, such as yeast extract and rice bran, have been found to achieve higher ethanol concentrations during fermentation but are expensive and can contribute a large part of the cost of some fermentations (MochidzukiI et al., 2015).

2.4 Conclusion

Fuel ethanol production using *Saccharomyces cerevisiae* is a global industry with significant potential by supplementing petroleum fuels and producing various other products. The critical factors that affect the fermentation performance of Saccharomyces cerevisiae include substrate concentration, product inhibition, and the kinetics of the yeast strain used. To optimise the production of ethanol through fermentation, it is difficult to predict the kinetics of the system without a large number of experiments and strict control of the fermentation conditions.

3) Optimisation of ethanol production

A reliable model is necessary to determine the mathematical optimal production of ethanol. The factors that limit the potential production and the "levers" or variables that can be changed to affect the process must be known. Due to the multi-dimensional, nonlinear nature of bioprocesses, it is attractive to use machine learning techniques to use historical data to develop a data-driven model (Mowbray et al., 2021a). A fed-batch process adds additional complexity due to the changes in volume and inconsistent feed rates. Hence, Artificial Neural Networks have been used in the development of data-driven models for fed-batch ethanol fermentations by *Saccharomyces cerevisiae* to optimize the feed rate profile (Xiong & Zhang, 2005) (Arpornwichanop & Shomchoam, 2009) (Z. Li & Dewan, 2012). Fed-batch fermentations allow for the addition of feed during the batch, giving some control over the substrate and product concentrations present in the fermenter, which allows for the reduction of inhibitions that can affect both the formation of biomass and the formation of product. In this case, ethanol (Hong, 1986). Another issue with the control of fermenters is the lack of online measurements of essential process parameters. Using machine learning to estimate the values for these parameters allows for greater control and increases the potential for optimisation of the system (Rani & Rao, 1999).

Modern data-driven modelling techniques, such as Artificial Neural Networks, promise to optimise and control fermentations due to their ability to model non-linear biological reactions (Sewsynker-Sukai et al., 2017). When developing the neural network, it is crucial to consider the stability and reliability of the predictions and the amount of data required to train the network. Overfitting the network to the data can lead to instabilities in the predictions, leading to inadequate optimisation of the problem. Another critical aspect of the neural network model in terms of optimisation is that the optimisation must be able to be done online, and change based on the measured feedback from the

fermentation system and plant model mismatches should also be accounted for (Xiong & Zhang, 2005).

3.1 Factors Affecting Ethanol Yield

Many factors stress the yeast cells during industrial fermentations and can affect the fermentation performance. Lopes et al. (2016) list the stresses affecting fermentation as biological, chemical and physical. The biological stressors are due to contamination by unwanted organisms such as wild yeasts and bacteria. This contamination is a particular issue in processes where the yeast cells are recycled, such as in Brazilian distilleries. Wild yeast strains, such as those of genus Dekkera, Schizosaccharomyces and Candida, as well as undesirable Saccharomyces strains, can lower the ethanol yield through the production of unwanted byproducts and the introduction of traits such as flocculation and excessive foaming. The primary bacterial contaminants are strains of Lactobacillus or Bacillus, and while the bacterial population can be controlled using antibiotics, acid washes, and chemical biocides, cases where the bacterial population has reached a concentration of 10^{-8} per millilitre can cause losses of up to 30 kL of ethanol per day in a plant producing 1 million litres per day.

Chemical stressors include acidic products from biological contamination, such as lactic acid, salts and ions in the fermentation broth and high ethanol concentrations. These stressors can lead to stuck fermentations and reduce the viability of cells when recycled. Physical stressors such as temperature must also be considered, as high temperatures can affect the fermentation performance. Understanding these stressors is of utmost importance. However, it is difficult to reproduce the stressful conditions of a distillery at a laboratory scale, and few laboratories are able to do so (Amorim et al., 2011).

3.2 Optimisation of fermentations

Most work on optimising the production of ethanol in fed-batch fermentations has focused on adjusting the feed to account for substrate and product inhibition (Hong, 1986), (Chaudhuri & Modak, 1998), (Na et al., 2002) (Zihin et al., 2018). Hong (1986) showed that Pontryagin's maximum principle can be used to determine the optimal feeding policy for 2 cases where the initial substrate concentration in the fermenter is equal to the feed concentration and where the feed concentration is not the same as the initial concentration. Pontryagin's maximum principle is a method that allows the optimal path between two states of a process to be determined. A limitation of the optimisation is that the parameters of the differential equations must be known.

Na et al. (2002) overcame this limitation by using genetic algorithms to estimate the model parameters used to optimise the feeding profile. However, This research was performed at low substrate concentrations and focussed on biomass production. Therefore, biomass formation was optimised rather than ethanol production.

Petersen & Jorgensen (2014) showed that an analytical solution to the optimal feed profile could be determined using economic nonlinear model predictive control. However, a simple model for biomass formation included substrate inhibition but not product inhibition. Ryde et al. (2021) extended this to demonstrate that the optimal feed trajectories for microbial fed-batch fermentations with substrate inhibition are non-unique and further show that on-off control is optimal in terms of the sensitivity of the system.

3.3 The use of soft sensors in fermentations

Soft sensors combine physical measurements with a software model to infer measurements that are not otherwise available. Using soft sensors allows for the measurement of variables that cannot be measured using the measurement of

variables that can (Kadlec et al., 2009). Furthermore, offline measurements can provide delayed information that is of little use in dynamic optimisation. Hence, soft sensors can provide values for variables such as the composition of the fermentation broth far faster than offline analysis by using higher frequency online measurements from the process. (Zhu et al., 2020).

The model for the soft sensor can be a simple linear model, a more complex mechanistic model derived from first principles, or a data-driven model.

The method used to develop a soft sensor is given by Zhu et al. (2020). Firstly, the data must be collected and cleaned to remove data that may not be meaningful due to hardware issues, communication failures, or unusual process conditions which would not provide realistic data. Secondly, the variables of interest must be selected. While statistical methods can be used, this is often based on the practitioner's expertise. Thirdly, the model must be selected, trained, and validated. Models generally fall into two categories, namely mechanistic and data-driven models. Mechanistic models rely on the knowledge of the physical and chemical balances of the process.

3.4 Neural networks in modelling and optimisation of ethanol production by *Saccharomyces cerevisiae*

Artificial neural networks have been used in biochemical engineering since the 1990s in applications ranging from the characterization of amino acid sequences to process simulation and prediction of fermentation variables, among others (Mowbray et al., 2021b). Specifically for fermentations of *Saccharomyces cerevisiae,* ANN models have been used for the prediction of the specific growth rate (Petrova et al., 1998), cell mass and ethanol concentration (Pramanik, 2004), and models for use in Nonlinear Model predictive control (NMPC) (Nagy, 2007).

Many studies show similar multilayer feedforward networks using measured variables at time t=t as inputs to determine an unknown variable at time t=t (Pajcin et al., 2017). Another approach is to use known inputs at t=t to predict the value of the variables at t=t+1 (Chaudhuri & Modak, 1998), although this was used for fed-batch production of invertase and secreted protein rather than ethanol fermentation. This approach has the added benefit of using the predicted values at t=t+1 to predict the values at t=t+2 and so on to predict the values over the whole fermentation.

Another network architecture that has succeeded in predicting fermentation kinetics is the recurrent neural network (Barrera-Cortes & Baruch, 2000). Nagy (2007) uses a network that uses a sequence of inputs and previous output values, with reactor temperature and coolant flow from the four previous time steps used to predict the reactor temperature at any time.

Nagy (2007) used an ANN model as the basis of an NMPC system to control the bioreactor's cooling system. While the ANN model performed well, the training data was created using a simulation, and the ethanol concentration was low, as the highest concentration was 12.5 g/L; hence, ethanol inhibition was not likely a significant factor in the dataset. Ławryńczuk (2008) used the same underlying model in their controller; hence, it suffers many of the same issues.

Eslamloueyan & Setoodeh (Eslamloueyan & Setoodeh, 2011) used hybrid-neuro modelling for optimising fed-batch fermentation of ethanol by recombinant *Saccharomyces cerevisiae*, using several decision variables such as initial liquid in the reactor, the feed flow rates, the switching time from aerobic to anaerobic operation and the final batch time. An issue with the approach used is that the hybrid model is compared to a simulation; hence, the approach was not proven to work under real conditions.

Hybrid model strategies have also been adopted in the control and optimisation of baker's yeast fermentations where biomass is the product (Yuan et al., 1999)(Tian et al., 2002) (Karakuzu et al., 2006). In these cases, the biomass was maximised, and ethanol production minimised or prevented as much as was possible. Yuan et al. (1999) used artificial neural networks combined with a fuzzy logic controller to optimise the biomass formed and were able to double the density of the yeast formed compared to PID control, and it is unclear in this case how the controller would be able to deal with changes in the process that result in a plant/model mismatch as the process is assumed to be unchanged. Tian et al. (Tian et al., 2002)used augmented recurrent neural networks to optimise the same process, but again, the controller developed is not adaptive.

3.5 Robust optimisation

Robust optimisation is a method of optimisation that allows an optimisation problem to be solved for a model with uncertain parameters (Ben-tal & Nemirovski, 2002). The uncertainty does not need to be known; however, it needs to be part of a postulated uncertainty set, and robust optimisation will seek a feasible solution from within the stated set (N. H. Lappas & Gounaris, 2018). A consequence of this approach is that the result is inherently conservative, with the solution often taking the form of the best possible solution in a worst-case scenario. Robust optimisation is similar to stochastic programming (SP); however, for SP, probability distribution functions of the underlying stochastic parameters must be determined, whereas, in robust optimisation, the uncertain parameters are assumed to belong to a deterministic probability set (Maggioni & Potra, 2014). Robust optimisation has been used widely in the optimisation of power networks (Kazemzadeh et al., 2019) (Wang et al., 2016), distribution networks (Xu et al., 2021) and other applications (Beyer & Sendhoff, 2007).

Dynamic optimisation, which takes place over more than a single span, has been used extensively in process engineering. However, few examples of dynamic optimisation consider parametric uncertainty(Nolasco et al., 2021). Several methods have been applied to optimisation under uncertainties, including semi-infinite programming, the multi-scenario method, the back-off method, linearization promoted robust optimisation and measurement-based re-optimisation (Liang & Yuan, 2022). The solution to a robust optimisation problem may be overly conservative. Hence, methods such as adjustable robust optimisation have been developed to reduce the conservatism of the solution by introducing variables that can be adjusted as data is collected (N. Lappas & Gounaris, 2016). There are few examples of this application for dynamic optimisation. However, Liang & Yuan(2022) demonstrated that the approach works for nonlinear chemical processes.

3.6 Conclusion

The optimisation of fermentation processes requires an accurate model and accurate measurement of process variables, neither of which are often available. Machine learning algorithms such as Artificial Neural Networks hold promise in estimating model parameters that can change between batches and would otherwise not be known until after the fermentation is complete. Such a hybrid strategy can be used as an adaptive model for a process where the model parameters are unknown or changing.

Due to the uncertainty caused by noisy or unknown measurements and the lack of an accurate process model, optimisation of the process can lead to sub-optimal solutions that cause issues in the process. Robust control can be used to develop an optimal solution that considers the uncertainty, preventing sub-optimal solutions.

4) Development of fed-batch bioreactor system

4.1 Introduction

A 100 L fed-batch bioreactor system was developed to collect fermentation data. The variables that must be controlled during fermentation depend primarily on the fermentation performed. Some bioprocesses require careful control of many variables, including DO, pH, and redox potential. The production of ethanol from sugar feedstock through fermentation by *Saccharomyces cerevisiae,* only required control of the temperature of the liquid in the fermenter (Lisci et al., 2021). To monitor the sugar and ethanol concentrations in the liquid the density of the solution was measured and used to estimate the substrate and product concentrations. Control and data collection for the system was performed by a Programmable Logic Controller (PLC) with data stored remotely using Thingspeak.

4.2 Experimental progression

A mathematical model was required to determine the optimal feed profile required to maximise ethanol production, which required experimental data; hence, the progression of the work was as follows.

1) A fed-batch bioreactor system was developed to provide the datasets used in the optimisation.
2) A method was developed to provide an online estimation of the ethanol and sugar concentration during fermentation.
3) The data collected was used to model the system.
4) The developed models were used to determine the optimal feeding strategy
5) The optimal strategy was implemented online by developing a method to estimate the model parameters online.

4.3 Fed-batch bioreactor system and data collection

4.3.1 Bioreactor Equipment

The Bioreactor system used, similar to that described by Higginson & Brooks (Higginson & Brooks, 2022), is shown in Figure 4.1. The fermentation vessel comprised a 100 L jacketed cylindroconical vessel fabricated from stainless steel by Falcon Engineering. During fermentation, the top of the fermenter was covered using a stainless-steel plate to prevent evaporation and contamination. However, gasses were able to vent freely. TT1 is the PT100 temperature probe, TT2 is a DS18B20 temperature probe, and AT1 is the iSpindle floating sensor used for the measurement of the density of the liquid.

A Grothen G328 peristaltic pump P1 was used to feed additional substrate during the fermentation. The feeding rate of the pump was controlled by using an L298N H-Bridge driver controlled by an Arduino Uno. The feeding rate could be adjusted by cycling the pump on and off to maintain 100% flow (always on), 50% (1 minute on, 1 minute off), 33.33% 1 minute on, 2 minutes off or 25% flow (1 minute on 3 minutes off). The fluid was pumped from a 25 L vessel into the fermenter.

The mass of feed added to the fermenter was recorded using a Nagy floor scale, on which the vessel was placed throughout the fermentation. The readings from the scale were recorded manually during feeding to determine the feeding rate in terms of mass.

The pump could also be controlled automatically using the PLC, where the feed was controlled by either the estimated ethanol concentration or the estimated sugar concentration in the fermenter.

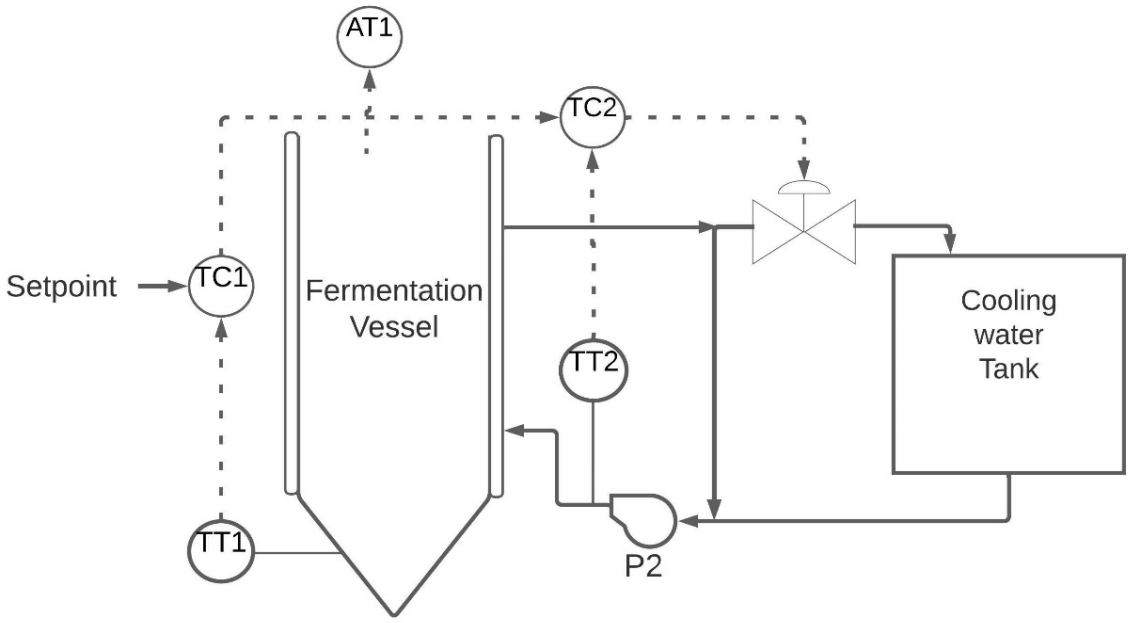

Figure 4.1: Bioreactor temperature control system.

The temperature control system consisted of a Lowara CEA 70/3 centrifugal pump, P2, that circulated water in the reactor jacket. The pump speed was controlled by a Siemens Micromaster 440 variable frequency drive connected to the PLC. A cascade control system was implemented in the PLC and used to control the fermenter temperature. The primary controller, TC1, consisted of an integral controller, while the secondary controller, TC2, was proportional-only.

Due to constraints on the number of inputs that could be used with the PLC, the DS18B20 temperature probe was connected to an Arduino Uno development board with a W5100 ethernet shield. The ethernet shield allowed the Arduino Uno to publish the values of the jacket temperature via MQTT, with an MQTT server running on a Raspberry Pi single-board computer. The MQTT values received from the Arduino were then written to the memory of the PLC using a Python script running snap 7 (Molenaar & Preeker, 2022). The Python script allowed the Raspberry Pi to send the values over the Profinet network. The temperature values were updated every 10 seconds.

Figure 4.2: iSpindle device for measurement of density

The density during the fermentation was measured using an iSpindle, shown in Figure 4.2. The device uses the tilt of the cylinder in which it is housed to determine the specific gravity of the liquid (Violino et al., 2020). The device works by measuring the angle at which it is floating using a 3-axis accelerometer. The lower the density of the liquid, the lower the device will float in the liquid, meaning an angle closer to vertical. The measured angle is then used to calculate the

specific gravity based on Equation 4.1, where the calibration determines g_1, g_2, g_3 and C constants.

$$SG = g_1(tilt)^3 * 10^{-6} + g_2(tilt)^2 * 10^{-4} + g_3(tilt) + C \qquad (4.1)$$

The iSpindle device required calibration before each batch. The device was placed in water, and the density was measured. If the measured density deviated from the known density of water (1.00 kg/L), the calibration in the device was updated using a supplied calculation that determined the values for g_1, g_2, g_3 and C.

The measurements from the iSpindle device were published to the MQTT server over WI-FI and written to the PLC memory in the same way as the temperature readings. The SG value measured by the iSpindle was updated every 10 minutes. The device can also measure the temperature of the liquid. However, this was not used, as there was already a higher frequency temperature reading from TT1.

Various values such as the fermentation temperature, ambient temperature, the SG, the mass of feed added, and jacket temperature were read from the PLC once per minute by the Raspberry Pi running a Python script. These values were then sent to the Thingspeak cloud service. The data is stored on the Thingspeak service as a public channel and can be accessed from MATLAB using the API keys.

The fermenter was not mixed, as the turbulence from an impeller would have affected the density measurement. However, mixing was not required as the bubbles formed have been shown to have a significant mixing effect during fermentation. Internal mixing is only required if solids are present in the fermentation, such as when performing simultaneous saccharification and fermentation (H. L. Zhang et al., 2012).

4.3.2 Experimental conditions

The fermentation medium comprised a mixture of sucrose, yeast extract and water. The initial medium for the fermentations was produced by mixing 5 kg of sucrose sugar, 40 kg of water, and varying amounts of yeast extract. The feed

added during the fermentation comprised a concentrated sugar solution composed of 10 kg sugar and 10 kg water. Yeast extract was used as a nutrient source, providing a wide range of nutrients required for yeast growth, such as amino acids, peptides, vitamins and other trace elements (J. Zhang et al., 2003).

.

In each case, water was heated to approximately 80°C, and the amount required was measured using a Nagy floor scale. Similarly, the amount of sugar was measured. The amount of yeast extract was measured using a balance. The components were thoroughly mixed until all the sugar was dissolved.

The initial medium was added to the fermenter and allowed to cool. When it had reduced to 40°C, the yeast was added. The yeast used was Angel Thermal Tolerance Alcohol Active Dry Yeast; the yeast characteristics are given in Table 4.1. This yeast was chosen due to its high ethanol tolerance and ability to ferment in a wide pH range. As the yeast is not sensitive to pH, pH was not controlled.

Table 4.1: Angel Thermal Tolerance Alcohol Active Dry Yeast characteristics (Angel Yeast, 2023)

Temperature tolerance	28°C -42°C
Ethanol Tollerance	≤17% (v/v)
Acid Tolerance	high resistance to acid, produce gas when PH is 2.5, which is favourable for controlling prevent bacteria contamination and improving alcohol productivity.
Osmotic tolerance	60% glucose max
Reproductive ability	Strong reproductive ability, small consumption.

The amount of yeast added to each fed-batch experiment was measured using a balance, as shown in Table 4.2. The yeast was rehydrated by removing approximately 10 L of the medium, adding the yeast, and mixing the lyophilised yeast for 10 minutes. The rehydrated yeast was added to the fermenter, and the temperature control system started. The density was monitored during the initial phase, and the feed was started once the density was measured at a specific value, which varied between the experiments. For Experiment 1 to Experiment 4, the variable investigated was the feed flow rate. The flow rate for each experiment was determined based on the results of the previous experiment to try to reduce the sugar concentration in the fermenter, as shown in

Table 4.3. The effect of the added mass of yeast was then tested in experiment 5 by doubling the amount added. Experiments 6, 7 and 8 were then performed to test the effect of increasing the mass of yeast extract added by doubling, tripling and quadrupling the amount of yeast extract added. The amount of yeast added varied at 150, 300 g and 200 g for the three experiments. The final experiments, Experiment 9 and Experiment 10, were performed with feedback control based on the SG measurement. The conditions for each of the experiments were selected to provide a broad range of input data for the models, however the conditions were not chosen to provide the optimal training dataset, but rather to provide a realistic example of a dataset, hence missing data, equipment failures and other issues that caused problems in the datasets were included.

Table 4.2: Initial conditions for the experiments

Experiment	Sugar (kg)	Yeast extract (g)	Water (kg)	Yeast added (g)
1	5	100	40	100
2	5	100	40	100
3	5	100	40	100

4	5	100	40	100
5	5	100	40	200
6	5	200	40	150
7	5	300	40	300
8	5	400	40	200
9	5	200	40	200
10	15	100	50	100

The feed rates used in the experiments are shown in Table 4.3.

During Experiment 9 and Experiment 10, in addition to the substrate-containing feed, dilution water at 35°C was added to dilute the ethanol in the fermenter. The effect of this dilution will be discussed further in Chapter 5.

Table 4.3: Feed rate during experiments

Experiment	Reaction type
1	Constant feed at 0.985 kg/h
2	Constant feed at 0.713 kg/h
3	Constant feed at 0.283 kg/h
4	Constant feed at 0.385 kg/h
5	Varied feed
6	Varied feed
7	Constant feed at 3.333 kg/h
8	Feed added to maintain SG at setpoint.
9	Feed was added to maintain sugar concentration at the setpoint with water addition.
10	Batch reaction with water addition

Details of the experimental conditions and the data from these experiments can be found in Appendix A.

4.4 Conclusion

This Chapter has described the development of the bioreactor system that allowed for data collection using various initial conditions and feeding profiles. The data collected was then used in the development of a soft sensor that allowed for online estimation of ethanol and sugar concentrations during the fermentations. The online measurements were then used to model ethanol production during fermentation, allowing for optimisation of the process based on the model and the conditions during the fermentation.

5) Online monitoring of ethanol concentration

5.1 Introduction

The online monitoring of the ethanol concentration during a fed-batch fermentation allows for effective modelling and online optimisation of the fermentation (Polakovi & Manflenius, 1994). A thorough review of available sensors for measuring ethanol concentrations is shown by Memon et al. (Memon et al., 2022). Methods previously used include enzymatic, spectroscopic, chromatographic, refractive index, densimetry, pyncometry capillary electrophoresis and calorimetric methods. These methods have various advantages and disadvantages; however, there are few options for online monitoring of ethanol concentrations. Recent research has shown that ultrasonic measurements with machine learning (Bowler et al., 2021), an electronic nose composed of an array of gas sensors (Feng et al., 2021) and fibre optic ethanol sensors (Memon et al., 2022) may be used in the online measurement of ethanol; however, these methods are not yet widely available.

One of the oldest methods for determining the ethanol concentration in fermentation is by using density measurements at the start and during the fermentation, with reports of the relationship between density measurements and the degree of fermentation dating to as early as 1784 (Cutaia et al., 2012). Most methods, however, derive from the work of Balling (Balling, 1846), which was based on experiments in the beer brewing industry. While these equations have been used in the brewing industry and are effective in predicting the ethanol concentration during batch fermentation, the use of this method in fed-batch fermentations has not been explored previously. This chapter will compare the results of using online density measurement to monitor the ethanol concentration during a fed-batch fermentation and the off-line analysis of samples by High-Performance Liquid Chromatography (HPLC).

5.2 Calculation of ethanol concentration based on density measurements.

The calculations to determine the ethanol concentration use the extract in terms of °Plato. °Plato is a standard measurement in brewing, and 1°P is equivalent to 1 g of sugar in 100 g of solution as per Equation 5.1.

$$°Plato = \frac{mass\ sugar}{mass\ sugar + mass\ water} * 100 \qquad 5.1$$

The conversion from specific gravity to °Plato is based on the data provided in tables produced by the American Society of Brewing Chemists, reproduced as Table 5.1 (Siebert, 1980). The predicted values were produced using Equation 5.2, and the coefficients were found using Excel. The third-order polynomial showed a good fit with low residuals.

Table 5.1: °Plato and SG conversion data showing fit and error

°Plato	SG	Predicted °Plato	error
0.0000	1.0000	-0.0060	0.0060
0.0130	1.0001	0.0069	0.0061
0.6420	1.0025	0.6375	0.0045
1.2830	1.0050	1.2785	0.0045
3.8260	1.0150	3.8171	0.0089
5.0600	1.0200	5.0712	-0.0112
6.3250	1.0250	6.3152	0.0098
7.5580	1.0300	7.5490	0.0090
8.7810	1.0350	8.7727	0.0083
9.9930	1.0400	9.9861	0.0069
11.1950	1.0450	11.1893	0.0057
12.3870	1.0500	12.3822	0.0048
13.5690	1.0550	13.5649	0.0041
14.7410	1.0600	14.7373	0.0037
15.9030	1.0650	15.8994	0.0036
17.0550	1.0700	17.0511	0.0039
18.1970	1.0750	18.1925	0.0045
19.3310	1.0800	19.3236	0.0074

$$°Plato = -25.766 * SG^3 - 124.17 * SG^2 + 583.54 * SG - 433.61 \qquad 5.2$$

The calculated extract value at the start of the fermentation is known as the original extract (OE). The calculated extract value is known as the apparent extract (AE) during fermentation. Due to the presence of ethanol during the fermentation, the conversion from SG to °Plato must be corrected, as the ethanol reduces the overall density. Balling (Balling, 1846) provides an empirical relationship between the apparent extract and the real extract (RE), given in Equations 5.3 and 5.4.

$$q = 0.22 + 0.001 * OE \tag{5.3}$$

$$RE = \frac{q * OE + AE}{1 + q} \tag{5.4}$$

Where: q is the attenuation coefficient.

The real extract indicates the amount of sugar present in the medium during fermentation, and the substrate concentration can be calculated using Equation 5.5.

$$S = \frac{RE}{100} * SG * 1000 \tag{5.5}$$

Where S is the sugar concentration in g/L.

The alcohol percentage can be calculated using a correlation from Balling (de Clerck, 1992), shown in Equation 5.6.

$$A_{w\%} = \frac{OE - RE}{2.0665 - 0.010665 * OE} \tag{5.6}$$

Where $A_{w\%}$ is the percentage of ethanol by mass in the solution

This can then be converted into the ethanol concentration using Equation 5.7

$$P = \frac{A_{w\%}}{100} * SG * 100 \qquad 5.7$$

Where P is the ethanol concentration in g/L.

These correlations were developed explicitly for batch fermentations; however, adding feed would not affect the balances on which they are based. A modification of these correlations was developed so that the equations can be applied to a fed-batch reaction by adjusting the original extract value as the feed is added.

$$OE = \frac{initial\ mass\ of\ sugar + mass\ of\ sugar\ in\ feed}{initial\ mass\ of\ solution + mass\ of\ feed} \qquad 5.8$$

The total sugar consumed was calculated using Equation 5.9, derived from Equation 5.1.

$$S_t = OE * m_f - \frac{RE}{100}\left(\frac{m_w}{1 - \frac{RE}{100} - \frac{A_{w\%}}{100}}\right) \qquad 5.9$$

Where: m_f is the total feed (sugar and water combined) to the system in kg, m_w is the mass of water fed to the system in kg.

5.3 Determination of ethanol concentration by HPLC analysis.

During the fermentations described in Chapter 4, in addition to the density measurements, samples were taken for later analysis by high-performance liquid chromatography (HPLC) for comparison.

The HPLC analysis was performed using an Agilent 1200 series HPLC, including a degasser, quaternary pump, autosampler, and refractive index detector (RID). The column used was a Biorad fermentation monitoring column. 0.001 M H_2SO_4 solution in ultrapure water was used as the mobile phase.

For the analysis, the RID was maintained at 40°C and the column at 65°C. The flow rate of the mobile phase was maintained at 0.8 ml/min for 14 minutes.

The chromatographs were processed using Chemstation software. The calibration was performed using ethanol samples in water at 50 g/L, 75 g/L and 100 g/L. Each sample was analysed using the HPLC three times, and the average of the three analyses was taken as the value. The average standard deviation over all the samples was less than 0.7 g/L.

5.4 Results and Discussion

5.4.1 Comparison of measured and predicted ethanol concentration.

The comparison between the values determined using Equation 5.7 and those measured using HPLC is shown in Figure 5.1, Figure 5.2 and Figure 5.3. The predicted values shown are the moving average of 30 samples to reduce the noise. The moving average was found using the movmean function in MATLAB. The data for experiment 4 is not shown as the HPLC samples were not taken for this experiment. As can be seen from the figures, there is good agreement between the predicted values based on the online SG measurement. The average difference between the HPLC measurement and the predicted online value was 7.23 g/L, or, in terms of percentage, 14.79%. The percentage variation was, however, somewhat skewed due to readings that deviated by over 200% at very low ethanol concentrations. The large deviations at low ethanol concentrations were exacerbated due to the negative values predicted by the equation, as the SG reading was higher than the actual starting SG due to the vigorous fermentation at the start of the fermentation. Once these values were removed from the dataset, the average difference between the measured and predicted values was a more reasonable 10.16%.

A histogram of the difference between the predicted and measured values is shown in Figure 5.4. The distribution shows that the majority of the values were predicted within ±7.0 g/L. However, there were several outlying values with deviations of more than -14 g/L

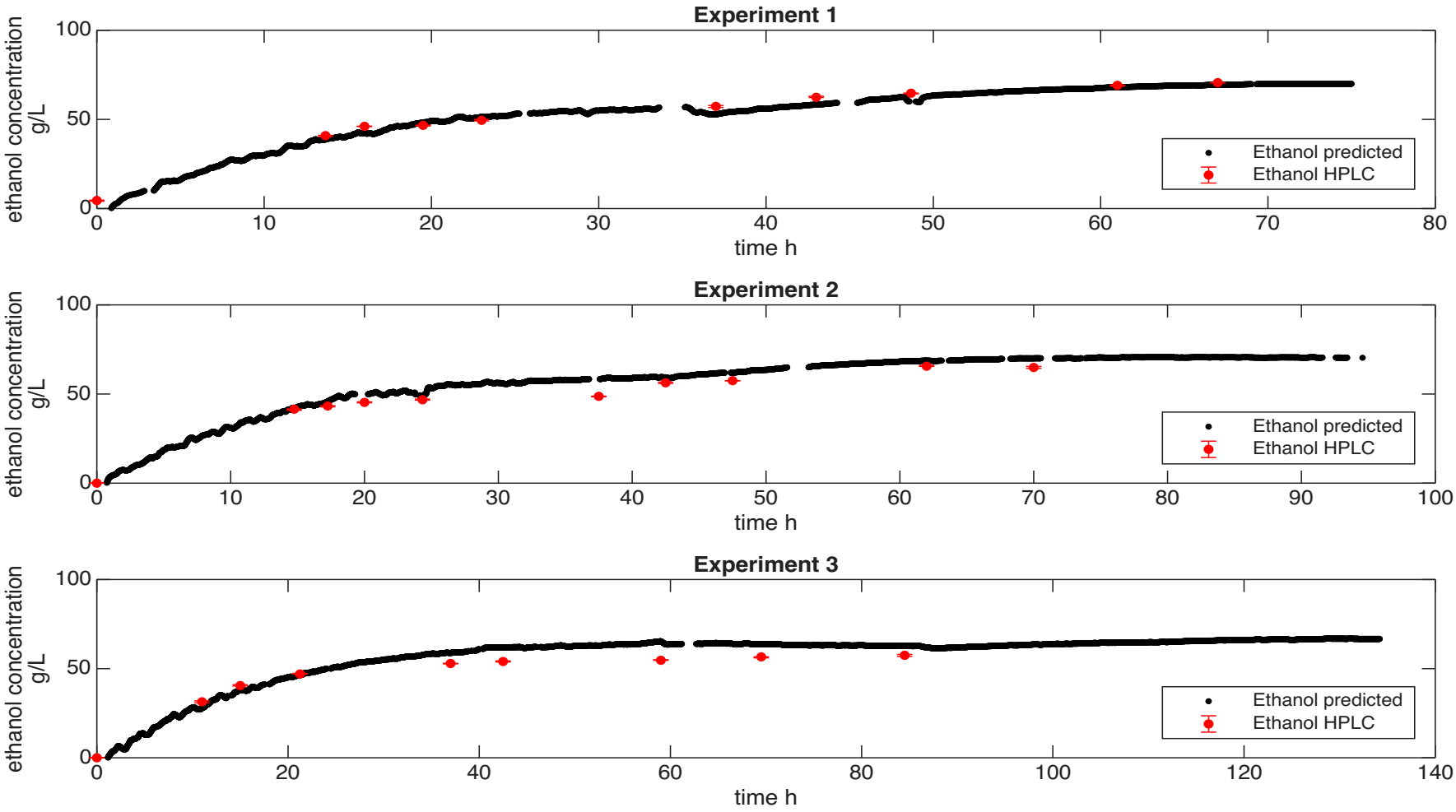

Figure 5.1: Predicted ethanol concentration with measured values for Experiments 1,2 & 3

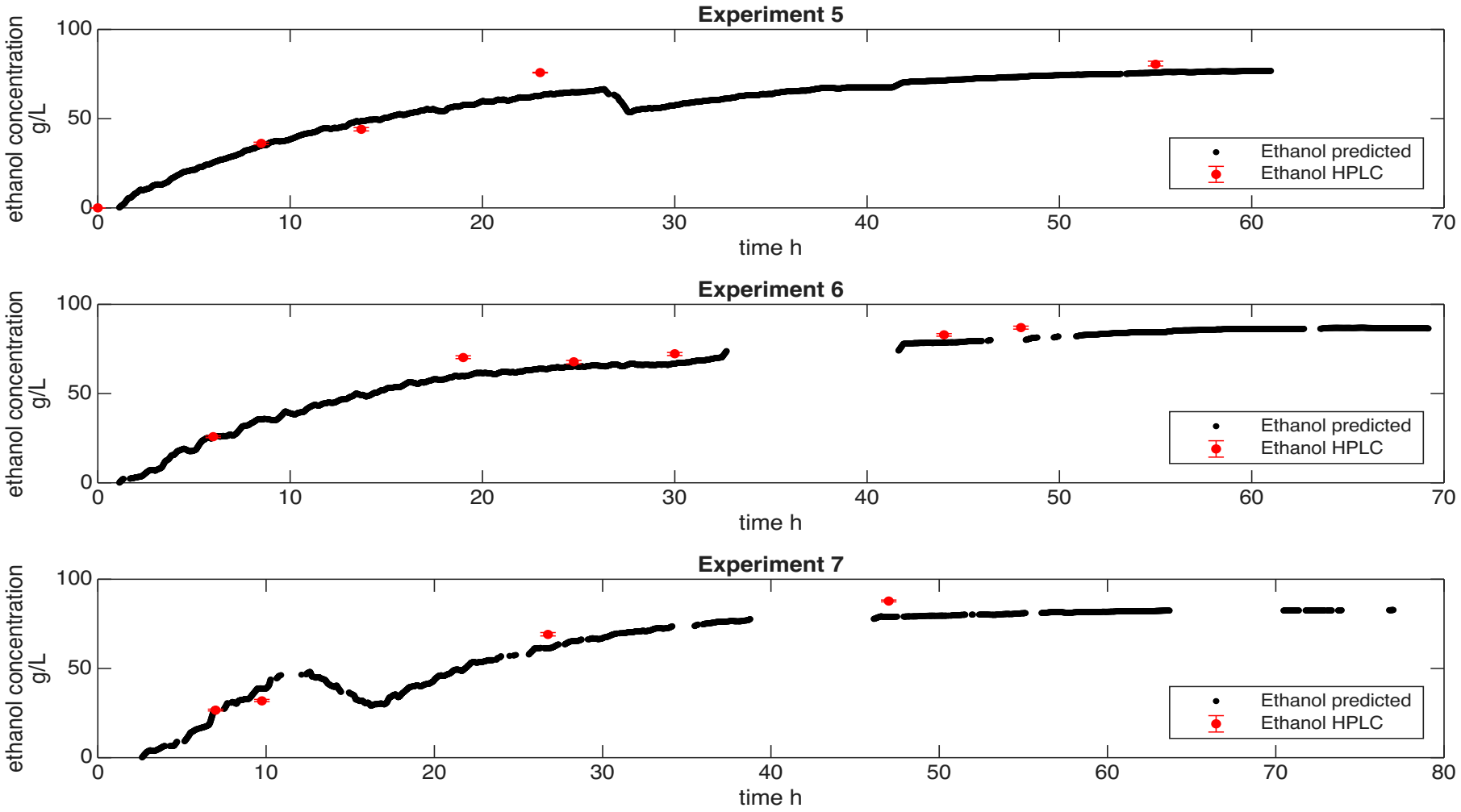

Figure 5.2: Predicted ethanol concentrations with measured values for Experiment 5, 6 & 7

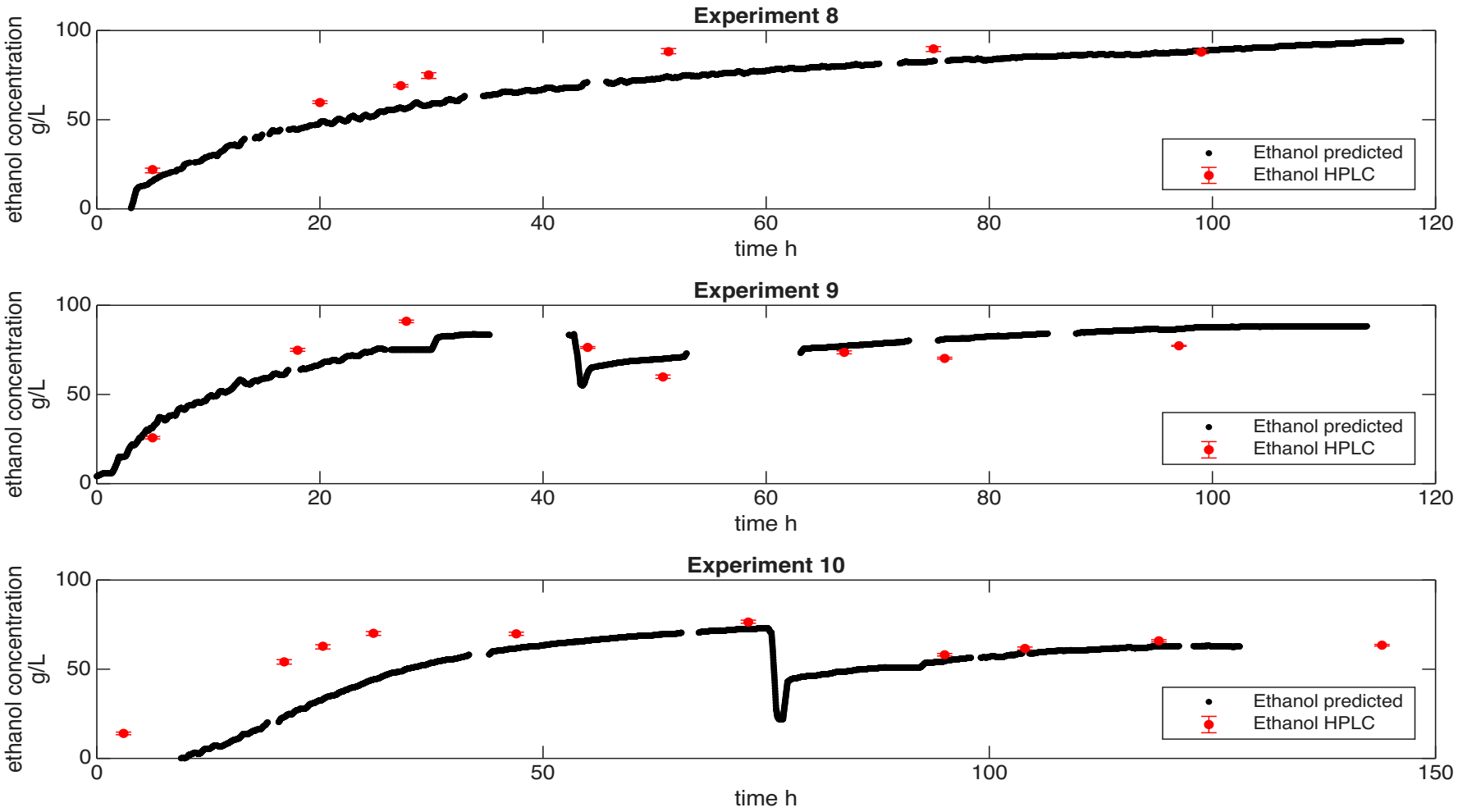

Figure 5.3: Predicted ethanol concentration and measured values for Experiments 8, 9 & 10

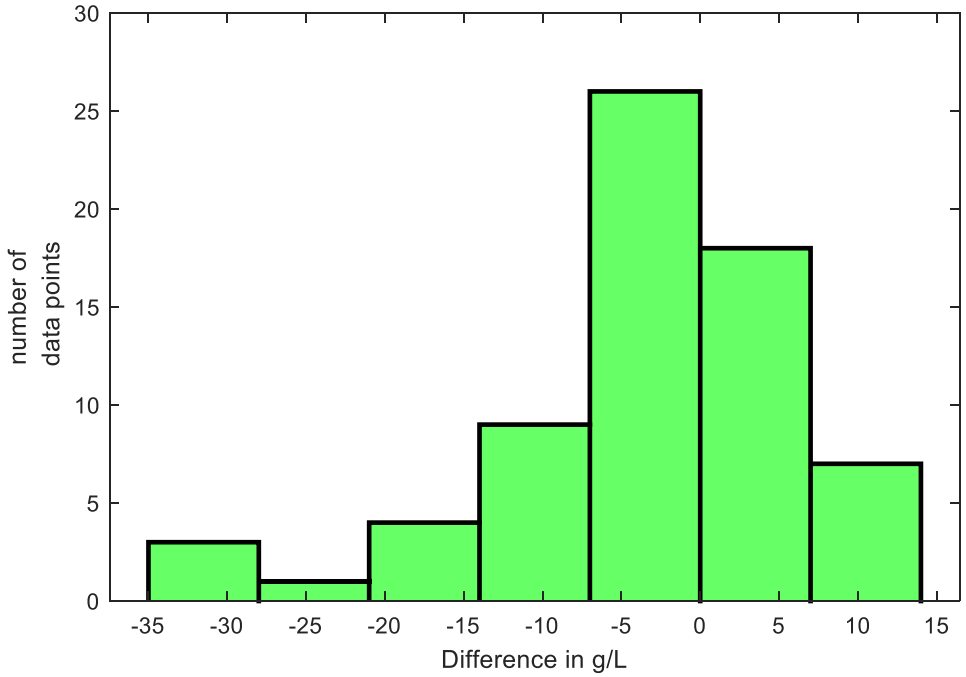

Figure 5.4: Distribution of differences between the predicted and measured ethanol concentration

The most significant deviations were found in Experiment 10 at the fermentation stage, where the SG was higher than in the other experiments, as shown in Figure 5.3. Due to the cubic nature of the calibration curve of the iSpindle device, the effect of the tilt on the SG measured becomes greater. Hence, the iSpindle becomes far less accurate at these high SG values. It should be noted that the readings from the iSpindle device should be treated with caution at high SG values. The predicted ethanol concentrations for experiment 10 do, however, show good agreement after the fermentation has progressed and the density of the fermentation medium has decreased due to the consumption of sugar and production of ethanol. The relationship between °Plato values determined based on the mass of sugar and water, compared to values calculated based on the measurement made by the ISpindle device, is shown in Figure 5.5. The measurement made by the device was accurate below 30°P however, it overestimated the gravity between 10°P and 30°P by an average of 2.49°P, with the most significant deviation from the known value being 4.61°P at 20°P. as all of

the experiments except for Experiment 10, used concentrations that meant the gravity was below 12°P, this is not an issue. However, the large deviations at 20°P do account for the significant errors between the ethanol concentrations measured using the HPLC and those calculated using Equation 5.7 for the initial 30 hours of Experiment 10. After 40 hours, the gravity dropped below 10°P, and the HPLC measurements and the predicted ethanol concentration were more closely aligned.

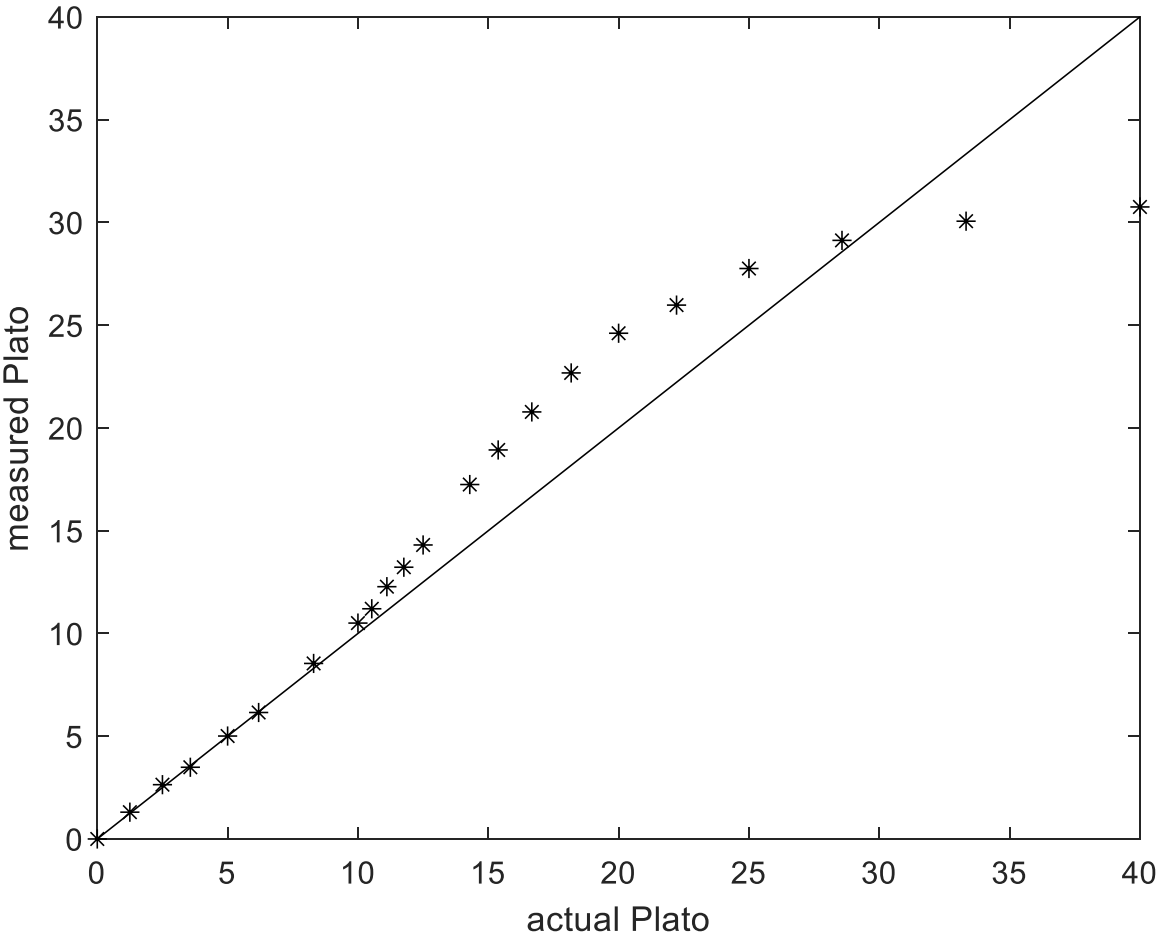

Figure 5.5: Comparison of measured Plato values with known values

An integral aspect of the accuracy of the predicted values calculated using Equation 5.7 is the amount of feed in terms of both sugar and water added. Errors in the measurement or, as was the case in the Experiments performed, estimation

of the feed added to the fermenter can cause errors in predicting the ethanol concentration. Several experiments, such as Experiment 1, show a significant dip in the ethanol concentration when the feeding stopped, as shown in Figure 5.1, at approximately 50 hours. While this decline is possibly due to mixing effects, it is more likely that the point at which the feeding was stopped, estimated based on the rate of addition and the remaining mass of the vessel, was incorrectly estimated.

The overall comparison between the predicted and measured ethanol concentrations is shown in Figure 5.6. The negative ethanol concentrations calculated at the start of the fermentation, before any ethanol formation, have been excluded due to the issues with the measurement of the SG that was experienced at the start of the fermentations. The parity plot shows that the

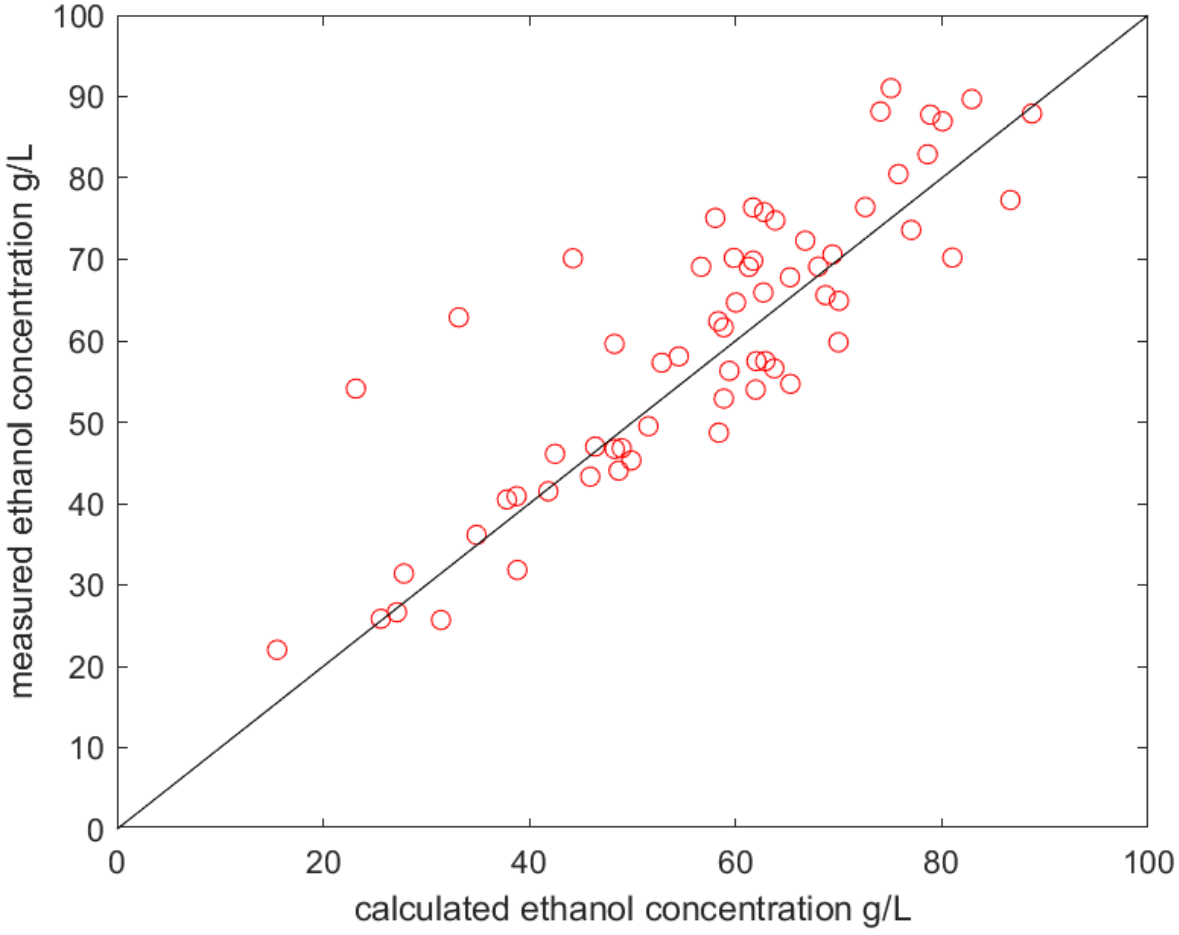

Figure 5.6: Parity plot of predicted and calculated ethanol concentrations. Negative predicted ethanol concentrations have been excluded.

prediction provided by the SG measurement provides a reasonable estimate for the ethanol concentration during fermentation.

5.4.2 Prediction of total sugar consumption

For the predicted values of the ethanol concentration described in the previous section, the assumption integral to the calculation is that ethanol yield is consistent in terms of g of ethanol produced per g of sugar consumed. Hence, the calculations can be used to determine the total amount of sugar consumed using Equation 5.9. The total sugar consumed is also a valuable variable to track, as the value is independent of the volume. Hence, it provides a more consistent

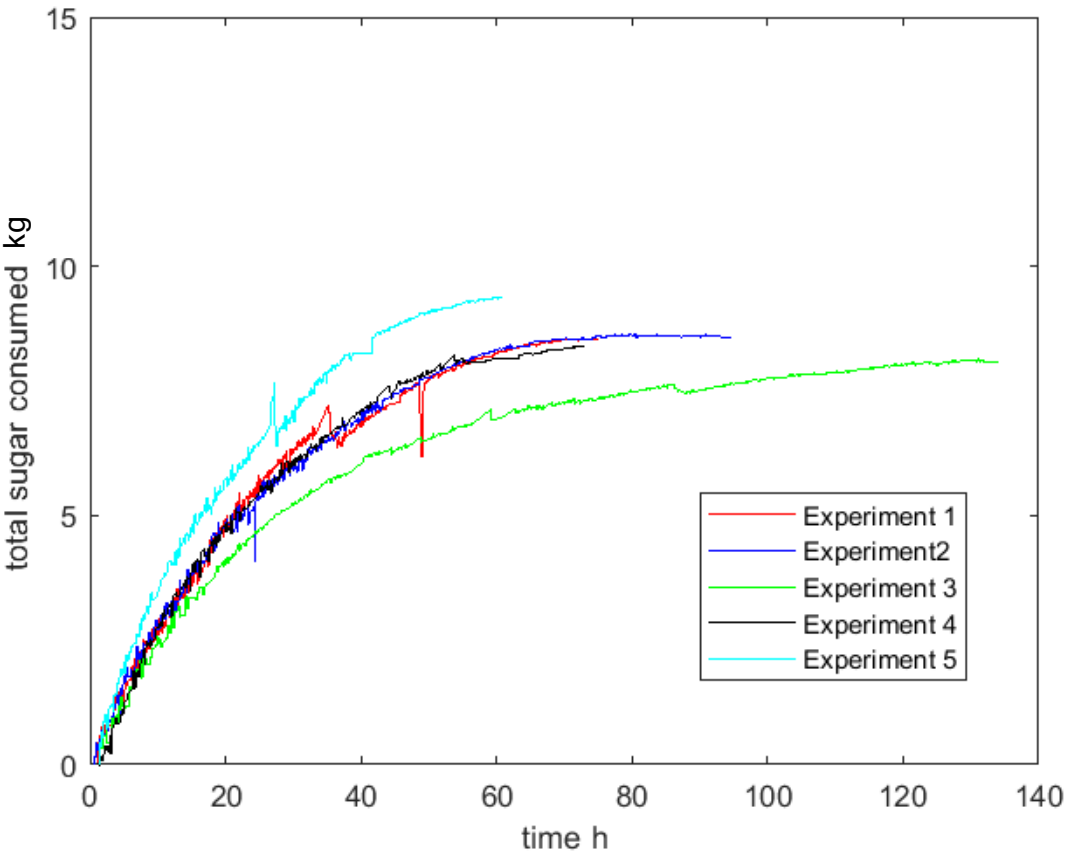

Figure 5.7: total sugar consumed for Experiment 1 to 5

indication of the fermentation's effectiveness. As the ethanol produced per gram of sugar was consistent, and the total amount added to each fermentation was

15 kg, the total amount consumed is effectively proportional to the ethanol yield for each fermentation. As the calculation of the total sugar consumption is based on essentially the same balance as the calculation for the ethanol concentration, it can be assumed that this calculation would have similar errors to the predicted ethanol concentration.

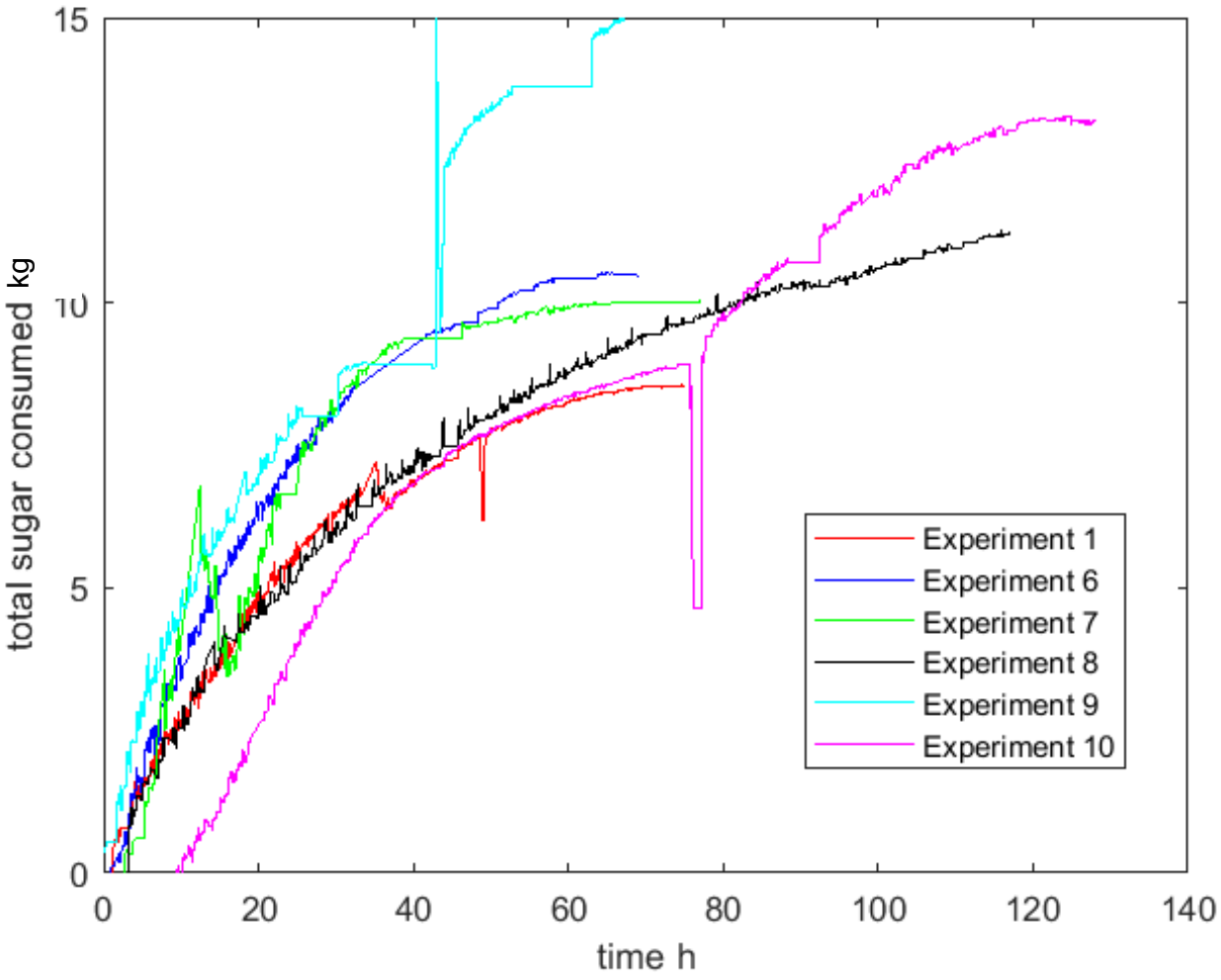

Figure 5.8: Total sugar consumed in Experiments 6, 7, 8, 9 and 10. The results for experiment 1 added for comparison.

The trajectory for the total sugar consumed in Experiments 1 to 5 is shown in Figure 5.7. Notably, the total sugar consumed in Experiment 1, Experiment 2, and Experiment 4 follow nearly identical trajectories. Experiment 3 was slower; however, the total amount of sugar consumed by the end of the fermentation

reached a similar value to the others. The total sugar consumed during experiment 5 was greater than the first four and was faster. All experiments, however, show a similar shape to the total amount of sugar consumed.

The amount of sugar consumed during the remaining experiments is shown in Figure 5.8. The later experiments consumed far more total sugar than Experiment 1, with Experiments 9 and 10 consuming 14.43 kg and 13.27 kg of the initial 15 kg of sugar, respectively. The experiments show a similar trajectory of total sugar consumption, with the consumption rate being fast initially and slowing dramatically by the end of the fermentation. Experiments 9 and 10 also show significant changes in the readings at the point where large additions of feed or water were made. The instability in the measurements at this point is expected as the fermenter took some time to stabilise after the large additions.

5.5 Conclusion

Online density measurements have been shown to allow the online monitoring of key fermentation parameters during the fermentation. While there were some outliers in the data caused by process conditions, the majority of calculated values for the ethanol concentration were within 10% of the values determined using HPLC analysis.

While this has been done for batch fermentations, based on the initial and final densities, this work showed that the technique can be extended to fed-batch fermentations with minor modifications.

A further extension of the equations allowed for calculating the total sugar consumed during the fermentation. The total sugar consumption provides better comparisons between the fermentations as the variable is independent of the volume, which varied as feed was added and sugar consumed and converted to ethanol by the yeast.

6) Modelling of fed-batch ethanol fermentations

6.1 Introduction

Mathematical models are invaluable tools in the control and optimisation of processes, allowing for determining optimal operating points and proving predictions for the effects of process changes. Hence, the modelling of biochemical processes has become one of the main areas of biochemical engineering research (Mowbray et al., 2021a).

The production of ethanol from sugar by *Saccharomyces cerevisiae* has been extensively studied; however, a universal model that accounts for all systems that cover the entire range of values or situations possible has not yet been developed. This can be seen by the wide range of modelling approaches that have been developed, such as the macroscopic models developed by Starzak et al. (Starzak et al., 1994), the bottleneck effect of Sonnleitner and Käppeli (Sonnleitner & Käppeli, 1986) as well as machine learning models such as those developed by Dewasme et al. (Dewasme et al., 2015).

Many analytical models use the rate of biomass formation as a basis for the calculation of other state variables, with the amount of ethanol produced and sugar consumed assumed to be proportional to this amount. The foundation for these models is usually the Monod model, which provides for substrate-limited growth that exhibits growth that is similar to zero-order kinetics at high substrate concentrations and can be approximated by first-order kinetics at lower substrate concentrations. Extensions to this model can predict the effect of the ethanol concentration, the pH and other process variables on the rate of biomass formation and, thus, the rate of product formation. It must, however, be remembered that the model is a simplistic representation of numerous complex reactions occurring within the cell. Hence, it can be not easy to obtain a model that is accurate under all conditions. Models such as Flux Balance Analysis (FBA) models do incorporate many more reactions into the kinetic model; however, they also increase the mathematical complexity of the model (Scheiblauer et al., 2018).

An additional issue with many models is that the measurements required are difficult to obtain, or can be inaccurate, or missing in a certain dataset. Data-driven modelling approaches allow for the creation of black box models or grey box hybrid models based on the data that is available (Charef et al., 2009).

The models presented in this chapter were created with two goals in mind. Firstly, the model was required to predict the ethanol concentration at which the yeast would no longer be able to ferment, essentially predicting the concentration of ethanol that could be in a certain batch. The second goal was to enable the simulation of fermentations so that methods of optimisation could be tested. To be able to predict the behaviour of the system, the model must be able to incorporate the factors that affect the ethanol concentration at which the yeast can no longer ferment.

6.2 Analytical model of fermentations

As mentioned previously, most mechanistic models of yeast fermentation are based on the Monod model, which is described in detail in Chapter 2. This model cannot, however, be used for this case, as there is little to no cell growth during the fermentation due to the lack of aeration.

In all cases, at the end of the fermentation, there was a substantial amount of sugar substrate remaining. Hence, the limiting factor in the production of ethanol does not appear to be the substrate concentration. Furthermore, Experiment 1, Experiment 2 and Experiment 4 exhibit almost identical amounts of total sugar consumed at all points during the fermentation, while the Experiments had vastly different feed rates that caused the sugar concentration to vary greatly between the Experiments with no effect on the kinetics. A limitation on this is that Experiment 3 experienced greatly diminished rates of fermentation once the substrate concentration dropped to approximately 30 g/L, so the assumption that the kinetics are not substrate-limited is restricted to situations where the substrate concentration remains above that value.

Hence, a model was developed based on the ethanol inhibition described by Levenspiel (Levenspiel, 1980). As the biomass concentration is assumed to not change significantly during the fermentation due to the lack of aeration, the inhibitory effects of the ethanol concentration are applied to the rate of substrate consumption rather than cell growth in a similar manner to Luong (Luong, 1985). The model of the substrate concentration during batch fermentation is given in Equation 6.1. This model is based on the concentration of the various state variables during fermentation. Hence, it would be difficult to solve in a case where feeding causes changes in these variables.

$$\frac{d(S_0 - S)}{dt} = -v_s * (1 - P/P_m)^n * X_{\square} \qquad 6.1$$

Where: S_0 and S are the initial substrate and substrate concentrations respectively in g/L, *vs* is the specific rate of substrate consumption ($g_{sugar}/g_{biomass}.h$), P_{max} is the maximum ethanol concentration that can be tolerated by the yeast, and n is a constant.

To account for the changing volume due to feeding, Equation 6.1 can be multiplied by the volume V(t), to change the concentrations into amounts of sugar consumed, and the total biomass present in the fermentation. S_0 can be assumed to be constant, and $S*V(t)=S_t$; hence, the rate of change in the total amount of sugar consumed can be given by Equation 6.2.

$$\frac{dS_t}{dt} = v_s * (1 - P/P_m)^n * X_t \quad 6.2$$

This can be further simplified by assuming that, for the purposes of the model, the total biomass X_t is constant during the fermentation due to the lack of aeration. The rate and the biomass can then be combined to form a new constant $v_{max,}$ as shown in Equation 6.3.

$$\frac{dS_t}{dt} = v_{max} * (1 - P/P_m)^n \quad 6.3$$

To fit the models, the solved ODE was compared to the experimental data and the RMSE was minimised. The data was converted to hourly data by taking a 60-minute moving average of values and using the interp1 function in MATLAB to obtain a dataset without any missing values. The parameters were determined by minimising the square of the Euclidian norm of the difference between the data and the model values using the fminsearch function in MATLAB. The model was solved numerically using ode45, and solved simultaneously with the volume, which is given in Equation 6.4.

$$\frac{dV}{dt} = F \quad 6.4$$

$$\mathrm{P} = Y_{P/S}\frac{S_t}{V} \quad 6.5$$

The ethanol concentration could then be determined after solving the total sugar consumed and volume. The amount of sugar consumed was multiplied by $Y_{P/S}$, the yield of g ethanol per kg of sugar consumed, to determine the amount of ethanol produced. The total ethanol produced was then divided by the volume to determine the concentration, which is shown in

Equation 6.5. The value of Y_{PS} was determined for each experiment in a similar manner to the previous parameters by solving the ODEs and using the fminsearch function in MATLAB to minimise the norm of the squared error between the data and the model fitting. The initial parameters v_{max} P_{max} and n were found using the ethanol concentration from the data, which was interpolated from the hourly data. Once the other parameters were determined, the yield coefficient was determined based on the data. The code used for fitting the parameters is given in Appendix B.

The comparison between the model fitting and the data is shown in Figure 6.1. The determined parameters are given in Table 6.1. It can be noted that the model fitting shows good agreement with the data, with low values for the normalised root mean squared error (NRMSE) in all cases except for Experiment 8 and Experiment 10. It would be expected that Experiment 10 would not show good agreement due to the measurement issues, as discussed in Chapter 5.

Table 6.1: parameters determined for model fitting. The maximum ethanol concentration achieved during the batch was included for comparison.

batch	v_{max} g/h	P_{max} g/l	n	NRMSE	R^2	maximum ethanol concentration g/l
Exp1	0.443	69.240	1.459	0.038	0.994	70.175
Exp2	0.327	61.337	0.695	0.014	0.999	70.623
Exp3	0.428	57.983	1.301	0.040	0.988	65.551
Exp4	0.366	64.076	1.027	0.044	0.992	68.852
Exp5	0.494	66.359	0.949	0.028	0.998	76.785
Exp6	0.457	69.301	0.694	0.037	0.995	86.930
Exp7	0.497	66.461	0.936	0.085	0.973	83.144
Exp8	0.526	69.384	1.191	0.075	0.993	86.960
Exp9	0.502	90.833	1.128	0.079	0.973	90.364
Exp10	0.353	92.260	1.275	0.168	0.966	73.032

While the volume was determined by solving the system of ODEs in MATLAB, the volume did not affect the total amount of sugar consumed. Initial fits for v_{max} and P_{max} were performed using volume values from the data. Once the yield coefficient was determined, the ethanol concentration in the ODE was determined based on Equation 6.5 and then used in the calculation of the ethanol concentration.

The concentration of ethanol was calculated in terms of g/L while the units of the total sugar consumption were in kg. This was done to maintain the scale of the data with the ethanol concentration in a range up to approximately 100 g/L and the maximum sugar consumed at 15 kg rather than 0.1 kg/L or 15000 g, respectively. This was not an issue as the yield coefficient acted as a unit conversion. However, the units should be noted.

Experiment 8 and Experiment 10 did not show good fits for the parameters determined by the fminsearch function, so the parameters for those experiments were determined using genetic algorithms to obtain a better fit. The ga function in MATLAB was used with the limits for the parameter estimation limited to v_{max} between 0.1 and 2, P_{max} between 50 g/L and 150 g/L and n between 0.5 and 1.5. These fits showed better agreement with the data, indicating that there are local minima in the determination of the parameters for these experiments. Hence, for these cases, the initial values used when determining the parameters using the simplex algorithm determine the values of the parameters obtained. The ga algorithm demonstrated no significant differences when applied to the remaining datasets.

In most cases, the theoretical maximum ethanol tolerance for the yeast predicted by the model fitting for each experiment was higher than that at which the fermentation stalled, with the P_{max} value obtained from the fitting giving, for example, the model fit for Experiment 4 gives a maximum theoretical ethanol concentration that is 27.3 g/L higher than the actual maximum ethanol centration found during the Experiment. While all experiments reached the point at which the yeast could no longer ferment, data collection continued for longer for some experiments, such as Experiment 2 and Experiment 3 and in such cases, it can be seen that the theoretical maximum ethanol concentration, P_{max} is predicted as much closer to the value that was obtained during the fermentation.

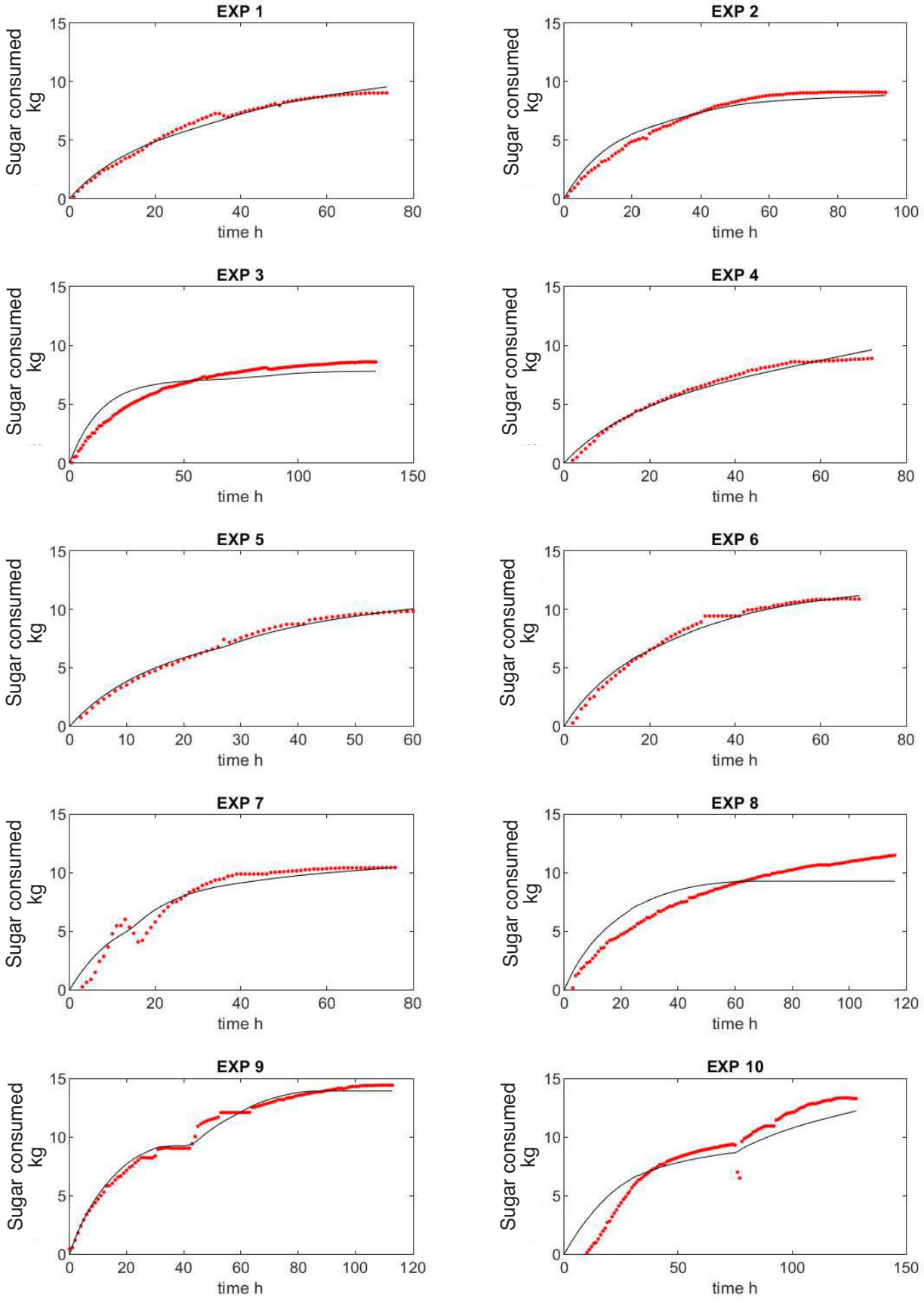

Figure 6.1: Model fitting compared to data, data shown as red points, model as black line

In Figure 6.1 the model for each Experiment was solved for the same timespan as the data, which obscures some deviations between the data and the model from being clearly seen on the plots. Many of the model plots have not reached a static value for the total sugar consumption, which was the case for all the experimental batches. Hence if the model was solved for a longer period, the Normalised Root Mean Squared Error (NRMSE) would increase as the total sugar consumption predicted by the model increased. Examples of this would be Experiment 5 and Experiment 8, where the total sugar consumption would continue to increase due to the high P_{max} value in comparison to the maximum ethanol achieved, which was 88.92 g/L and 76.79 g/L, respectively.

To increase the accuracy of the predicted maximum ethanol concentration, the dataset for each experiment was adjusted to increase the number of data points after the fermentation had stopped. This was achieved by increasing the length of each experiment to 150 hours, with the final ethanol concentration, and the total sugar consumption unchanged at the final value for the additional data points. It is reasonable to assume that the fermentation had ceased completely in all cases, and in cases where the static phase was maintained for a longer period, there was no additional sugar consumed.

As can be seen from Figure 6.2, the additional data allowed for the theoretical maximum ethanol concentration for each experiment to be predicted with more accuracy, with P_{max} values within 10 g/L of the measured value in all cases with the exception of Experiment 10, for which the previously discussed issues with measurement make the fits unreliable.
The parameters were then used to determine the yield of ethanol per gram of substrate, $Y_{P/S,}$ by minimising the norm of the squared error between the values determined using Equation 6.5. The yield was determined to be 438.69 g of ethanol per kg of sugar, which is slightly less than the stoichiometric value of 538.4 g/kg determined from Equation 6.6. This is expected as some of the sucrose is consumed by the cells for the production of by-products of fermentation, such as glycerol, or in endogenous metabolism during the fermentation.

$$C_{12}H_{22}O_{11+}H_2O \rightarrow 4C_2H_5OH + 4CO_2 \qquad 6.6$$

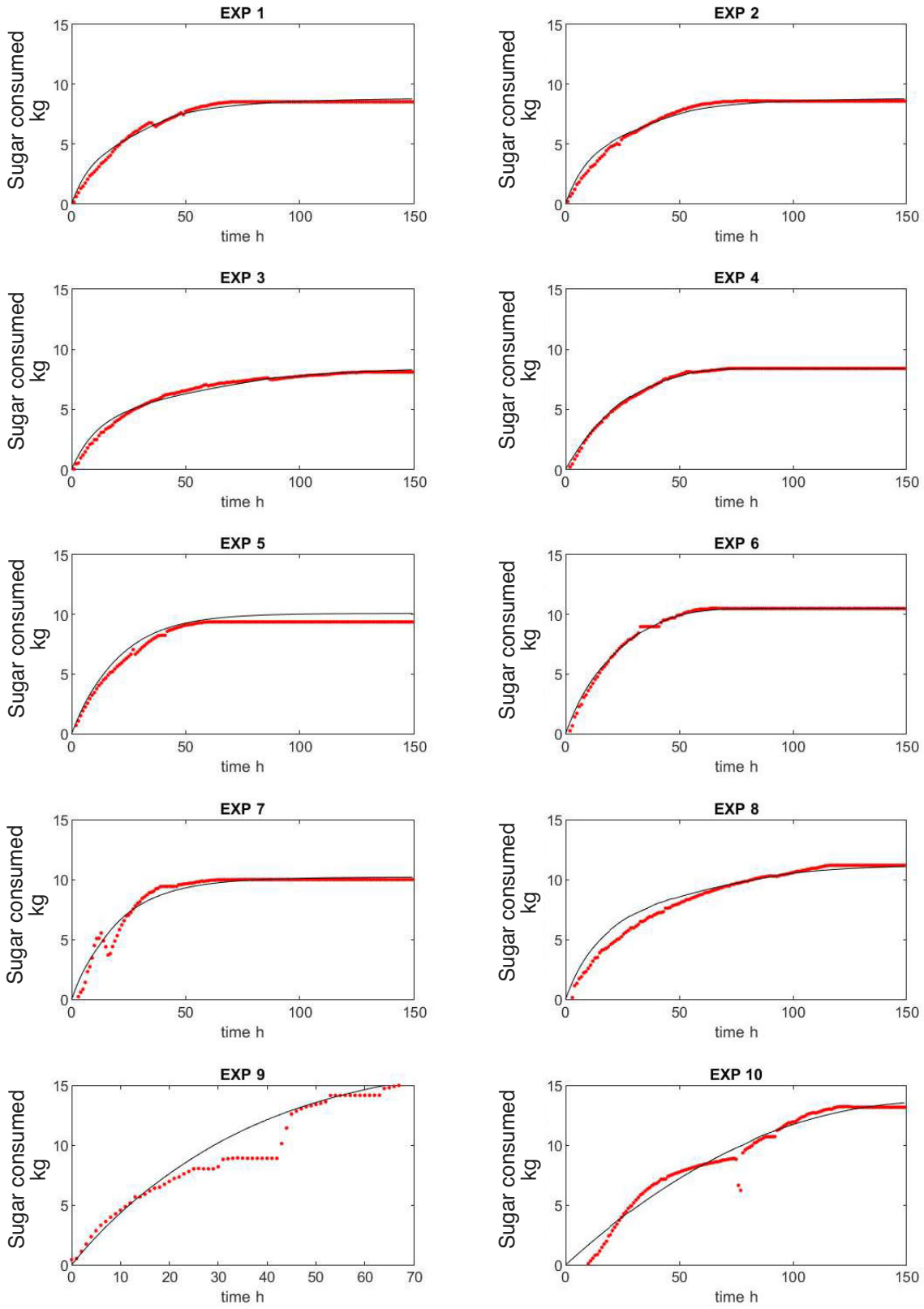

Figure 6.2: Model fits obtained using longer datasets. data shown by red stars, model shown as black line.

Table 6.2: Parameter values determined based on 150-hour fermentation time

batch	v_{max} g/h	P_{max} g/l	n	NRMSE	R^2	maximum ethanol concentration g/l
Exp1	0.542	58.045	1.305	0.278	0.988	70.175
Exp2	0.545	61.564	1.247	0.301	0.990	70.623
Exp3	0.445	56.795	1.268	0.256	0.988	65.551
Exp4	0.333	54.562	0.572	0.134	0.999	68.852
Exp5	0.513	81.172	0.992	0.568	0.994	76.785
Exp6	0.533	68.629	0.816	0.224	0.997	86.930
Exp7	0.555	67.877	1.073	0.515	0.972	83.144
Exp8	0.536	72.180	1.141	0.615	0.991	86.960
Exp9	0.507	129.483	0.918	0.906	0.969	90.364
Exp10	0.173	121.371	0.526	0.894	0.969	73.032

The relationship between the variables, such as the initial yeast concentration and initial biomass concentration, was then determined based on the values in Table 6.3. The relationship between P_{max} and yeast extract can be seen in Figure 6.3. For the linear fit, the result for Experiment 10 was omitted as it is clearly an outlier. The linear fit is given in Equation 6.7. the parameters of the linear fit were determined using the curve fitting tool in MATLAB. The RMSE for the fit was calculated by the tool to be 4.416, with an R^2 value of 0.86. This shows that the linear fit will be adequate to predict the maximum ethanol concentration for a given amount of yeast extract. This will be useful in simulating the process, but it must be noted that the nutrition available is most often unknown for a given feedstock; hence, the fit is not applicable to general ethanol fermentations.

$$P_{max} = 0.0725Y_x + 67.32 \qquad 6.7$$

Where Y_x is the amount of yeast extract added to the fermentation in g

Table 6.3: Parameters determined based on 150-hour fermentation time compared to the initial yeast added and yeast extract.

batch	v_{max} g/h	Pmax g/l	n	yeast g	added yeast extract g
Exp1	0.489645	71.948	1.157766	100	100
Exp2	0.495306	73.782	1.191711	100	100
Exp3	0.389544	72.421	1.221763	100	100
Exp4	0.490279	72.696	1.207311	100	100
Exp5	0.563057	77.073	0.917352	200	100
Exp6	0.584604	87.442	0.9845	150	200
Exp7	0.525772	85.253	1.095098	300	300
Exp8	0.313524	95.766	0.899548	200	400
Exp9	0.654732	85.467	0.790933	200	200
Exp10	0.231432	187.027	3.014362	100	100

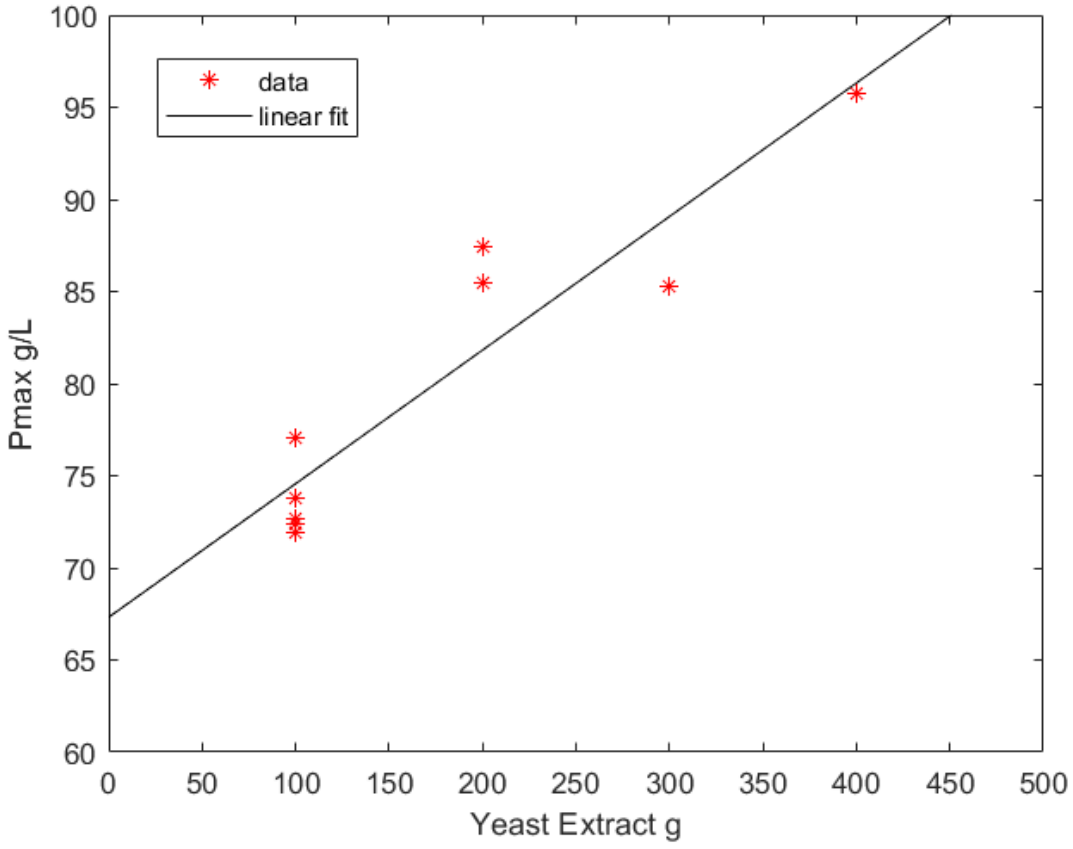

Figure 6.3: Linear fit for maximum ethanol concentration

The relationship between ν_{max} and both the yeast extract and initial biomass concentration was investigated, and using the curve fitting tool, a linear fit was determined as shown in Equation 6.8. the fit for this equation is, however, not as good, with an R^2 value of 0.2583 and an RMSE of 0.08769, or a normalised RMSE of 0.1751. While the lack of fit shows that there are unmeasured variables affecting ν_{max} the model can be used to estimate the ν_{max} value for various initial conditions for simulation purposes

$$\nu_{max} = 0.4528 + 0.00197X_0 - 0.000815Y_x \qquad 6.8$$

No viable fit for the n value could be determined, as only a second-order polynomial could be used with both the yeast extract and initial yeast concentration as inputs. There is not enough data to enable the calculation of the parameters for such a fit, as it results in overfitting. Hence, for simulation, the range of n values will be limited to 0.8 to 1.2.

6.3 Modelling of fermentations using neural networks.

In order to optimise the ethanol produced during the fermentation, a reliable method of predicting the maximum theoretical ethanol concentration is required. Due to the issues with using the mechanistic model for prediction where the initial yeast and nutrition are unknown, neural networks were used to model the fermentation.

A similar approach to that used in Chapter 3 was attempted. However, as variables such as biomass concentration could not be measured online, several changes to the approach were required.

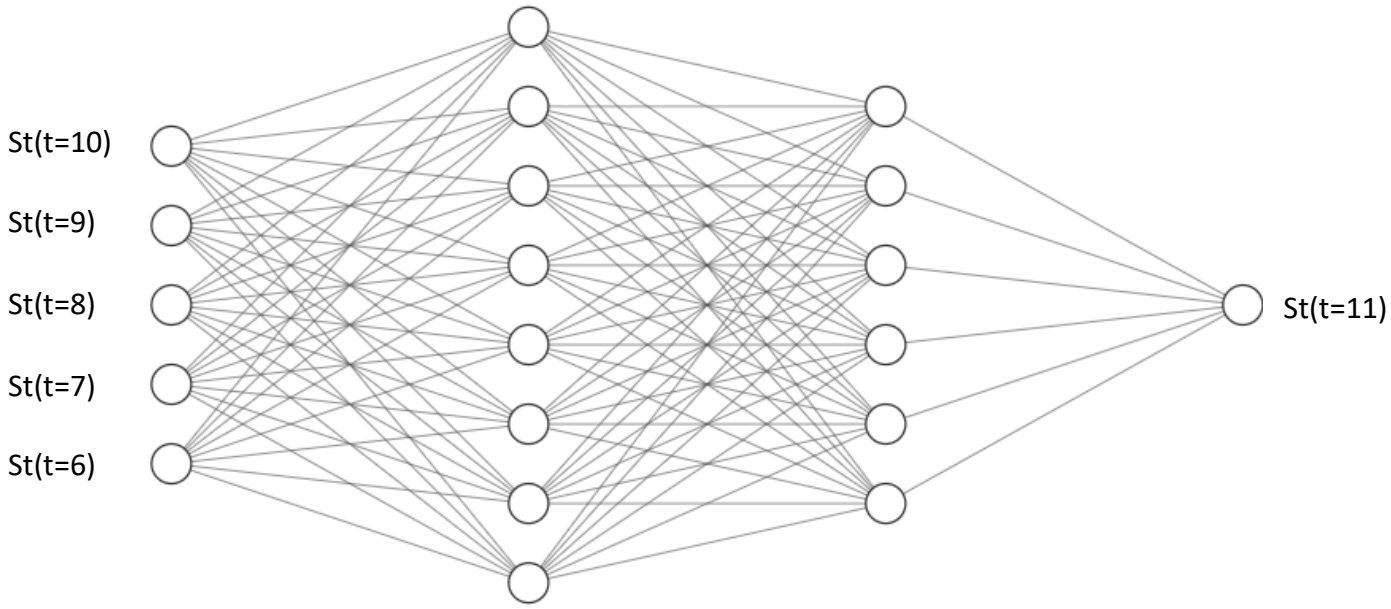

Figure 6.4: Neural network structure used for prediction of total sugar consumption

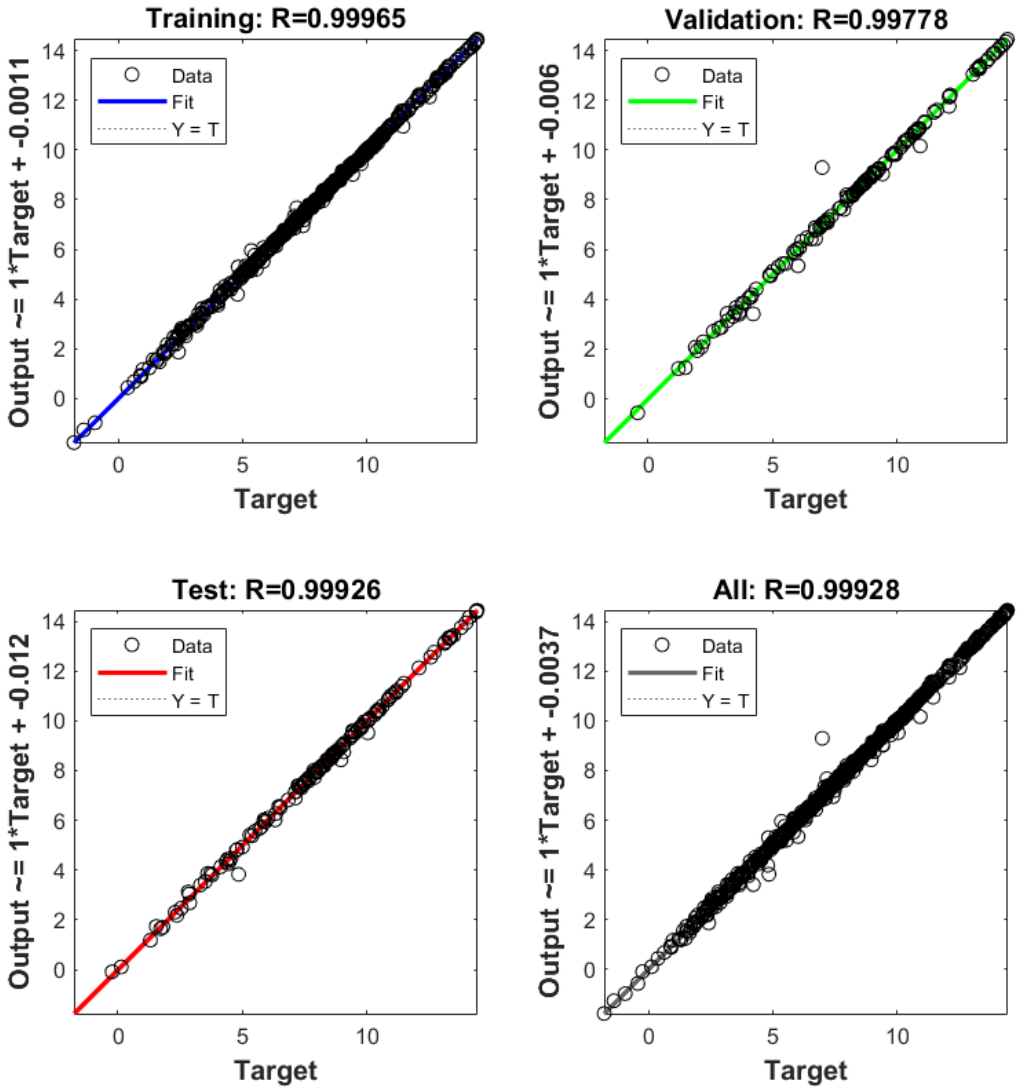

Figure 6.5: Parity plot generated by the MATLAB neural network toolbox

For the inputs, there needed to be inputs that would allow the net to determine at what ethanol concentration the fermentation would reach the maximum value and stop fermenting. As the nutrition available is assumed to be unknown, this could not be used as an input, and since this was the major cause of the changes in the maximum ethanol concentration, a proxy variable that could stand in for this variable was required. To achieve this, rather than using various input variables at time t to predict outputs at time t+1, 5 sequential inputs at hourly intervals of the total sugar consumption were used to predict the next value for the sugar consumed. The structure of the neural network is shown in Figure 6.4 for a network with 2 hidden layers of 8 and 6 neurons, respectively. The network was trained

on all data using the Levenberg-Marquart training algorithm. The dataset was split to consist of a training set, which comprised 70% of the data, and validation and testing datasets, which each consisted of 15% of the data.

While there were variations in the outputs from the network architecture, the trained network was always able to predict the data very well, and the predicted values matched well with the training, validation and testing datasets, as shown in Figure 6.5. The trained network could be used as a predictive modelling tool by using known values of the total sugar consumed from an experiment at times t=10, t=9, t=8, t=7 and t=6 to predict the value at t=11. The predicted output was then used as an input, along with the known values from t=10, t=9, t=8, and t=7, to determine the total sugar consumed at t=12 and so on. To predict the total sugar concentration at t=16 and beyond, only values that were predicted were used. It is important to note that the training of the network was based only on the ability of the network to predict the next value based on the previous 5 known values, not on the ability of the model to match the data for the overall experiment. Hence, although the whole dataset is used to train the network, the comparison between the neural network model and the data uses inputs that are generated by the previous iterations of the model rather than by the data. The fit provided by the neural network model varied greatly, not only in terms of the different experiments but importantly, the model varied significantly between attempts at training due to the random seed used to train the network. Figure 6.6 shows that the results of the neural network model could be very close to the data; however, they could also deviate significantly from the data randomly. Hence, using this approach to predict the maximum ethanol concentration is not adequate for the optimisation required due to the instability of the ANN model.

As the speed of the reaction is largely inconsequential to the optimisation of the ethanol production, an approach was chosen where inputs were used to predict only the final ethanol concentration. The goal of the network was to be able to use any 10 hourly data points for the total amount of sugar consumed to predict the maximum theoretical concentration of ethanol that could be achieved in each fermentation. Many architectures were considered. However, to capture the rate of change of the fermentation, 9 sequential values for the hourly change in the total sugar consumption were calculated using Equation 6.9.

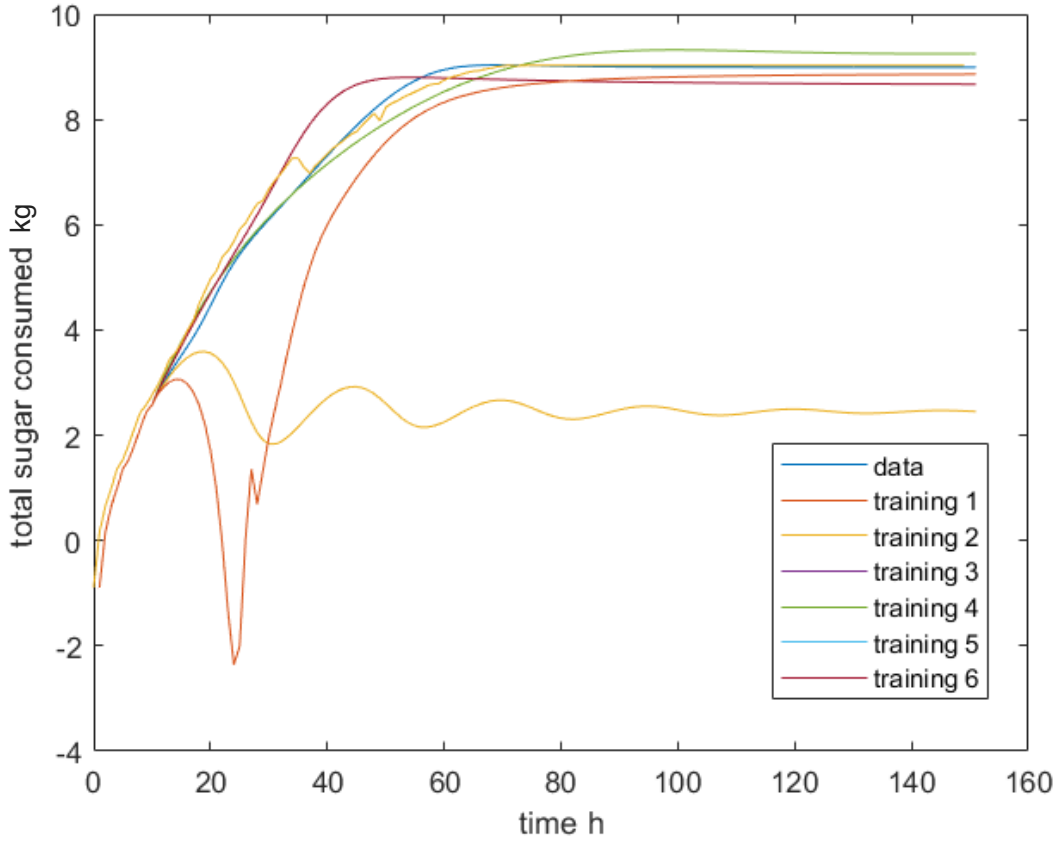

Figure 6.6: Model results after training the network 6 times using different seeds

$$\Delta S_{t(t=k)} = S_{t(t=k)} - S_{t(t=k-1)} \qquad 6.9$$

Where $\Delta S_{t(n)}$ is the change in total substrate consumed in the hour prior to t=n,

Eleven inputs were used in the network. Nine sequential values for $\Delta S_{t(k)}$ measurements of the total sugar consumption during the fermentation(from k=t to k=t-8), the volume (feed) added at k=t (in litres per hour) and the ethanol concentration at k=t. The inputs were used

to determine the maximum theoretical ethanol concentration. The training data was constructed by using the maximum ethanol concentration attained by each run as the output for the data from that run. This allows for the prediction of the ethanol concentration at any point during the fermentation after t=10.

To determine the number of neurons required in the network several tests were done using varying numbers of neurons in the hidden layer. A network was trained using the MATLAB neural network toolbox, using a 70% training 15% testing and 15% validation split in the dataset. The network was trained using the Levenberg-Marquardt algorithm using a constant seed. The activation function for the neurons in all cases was a logarithmic sigmoid. The Neural network model is given in Appendix B. The root mean squared error between the predictions over the whole dataset does not decrease as the number of neurons increases, as shown in Figure 6.7. There is a minimum at 18 neurons, with an RMSE value of 4.047, however, this minimum does not seem to be part of a larger trend and the RMSE values vary greatly. There are several cases where the RMSE is large even with 47 neurons in the hidden layer, however it is possible that as more neurons are added the RMSE could decrease. This, however would increase the possibility of overfitting the network to the data.

To reduce the errors in the prediction, a second hidden layer of neurons was added, The effect of adding neurons on the prediction was explored. Networks were trained in a similar manner as previously described and compared to the actual values to determine the RMSE for each configuration. While the RMSE value increases for networks where the number of neurons in either the first or second hidden layer is 1, there is no obvious trend, and the RMSE obtained seems distributed randomly, with the best configuration being 21 neurons in the first hidden layer and 6 in the second hidden layer, which had an RMSE value of 3.7855.

The results of the training, validation, and testing of the network are shown in Figure 6.8. The consistency of the R^2 value between the training and testing data shows that the network performed similarly in training, and the overall value of 0.908 shows that the prediction is reliable.

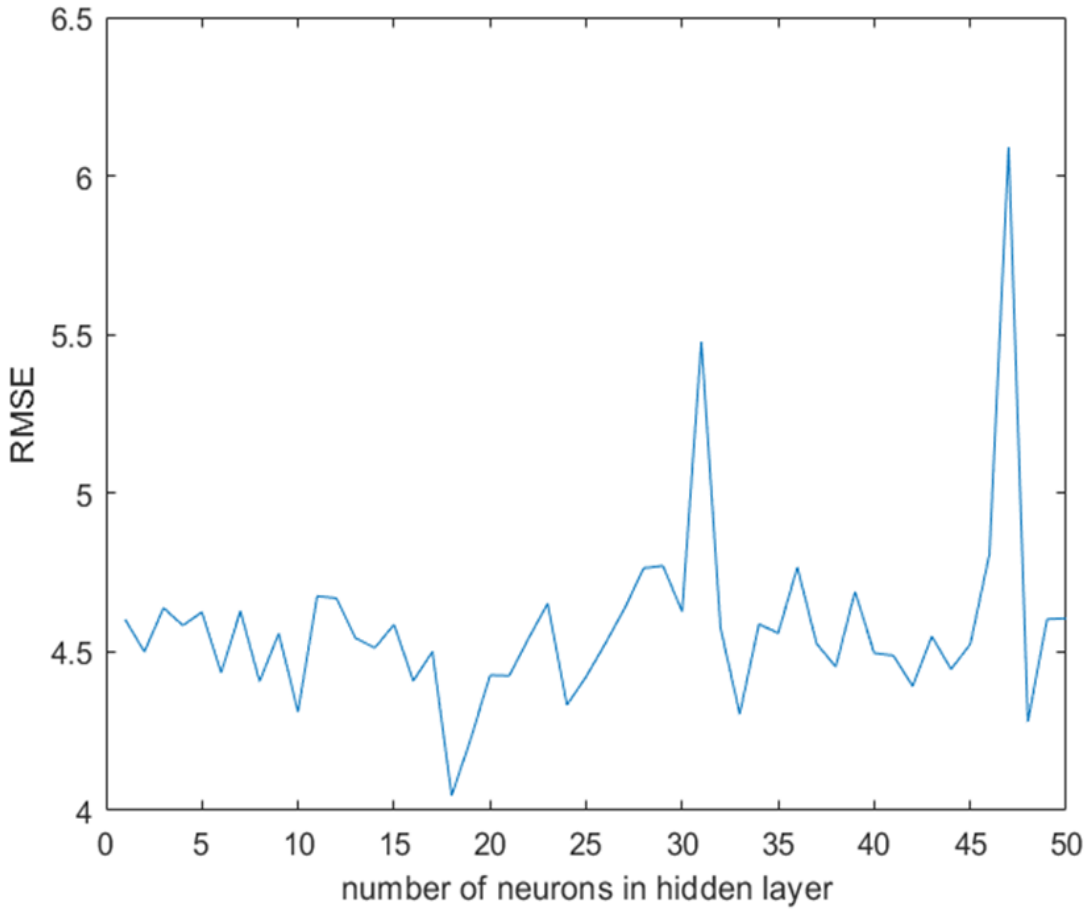

Figure 6.7: Sum of squared error for predictions over the entire dataset compared to the number of neurons in the hidden layer.

For comparison the dataset was also used to train models using the Regression Learner App in Matlab. This allows for multiple regression algorithms to be trained simultaneously, including linear regression, Regression Trees, Gaussian Process Regression, Ensemble Trees, Neural Networks and Support Vector Machines. When trained the best fit was provided by Bagged Ensemble trees with an R^2 of 0.8 on the test data, and a RMSE of 4.0905, followed by Rational Quadratic Gaussian Process Regression with an R^2 of 0.8 and a RMSE of 4.1047. This shows that the custom Neural Network Model developed was superior to alternative algorithms and could be more easily customised.

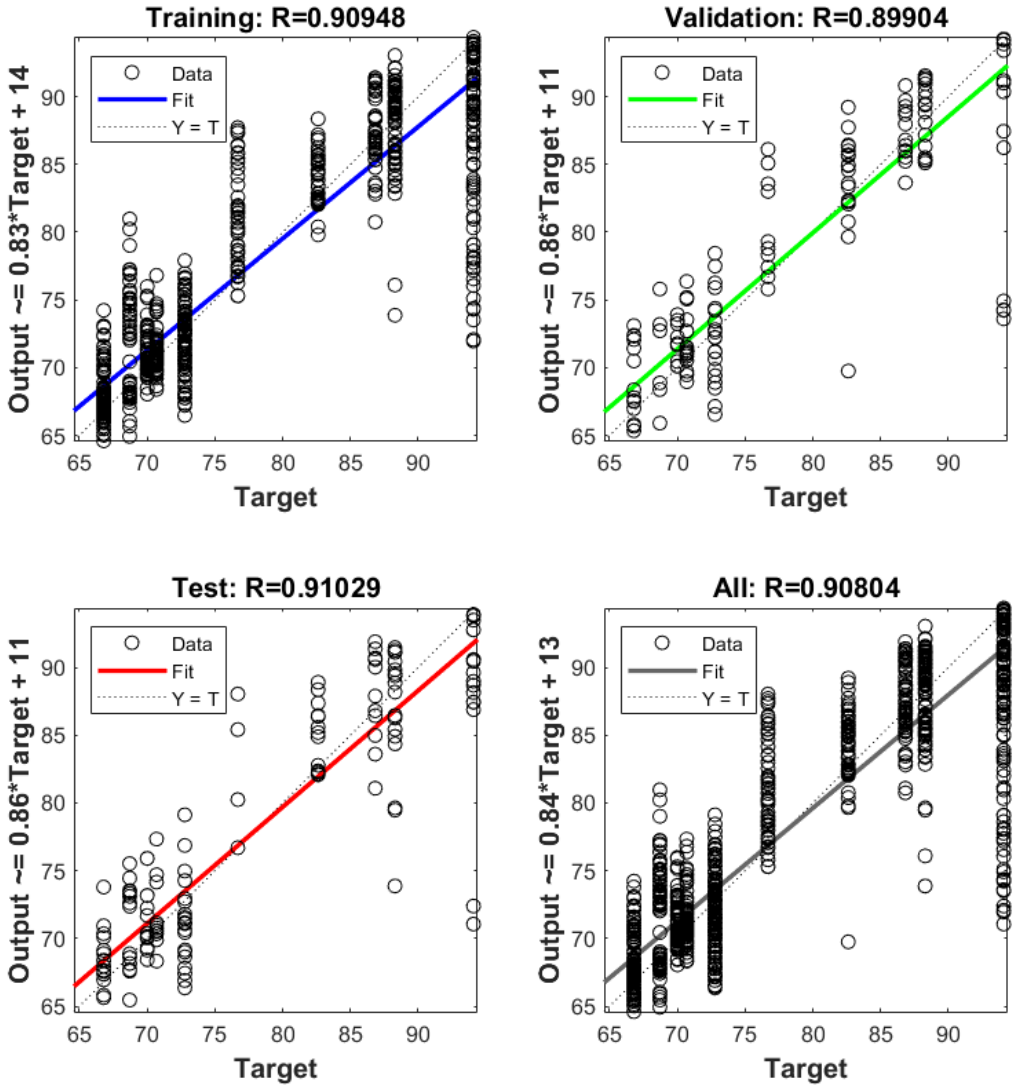

Figure 6.8: parity plots showing the training of the network

The comparison between the predicted maximum ethanol concentration and the actual ethanol concentration as the fermentations progressed is shown in Figure 6.9. In most cases, the prediction was able to converge to the final ethanol concentration, with the exception of Experiment 10, where the ethanol concentration at the end of the experiment was slightly lower than the ethanol concentration prior to the addition of water.

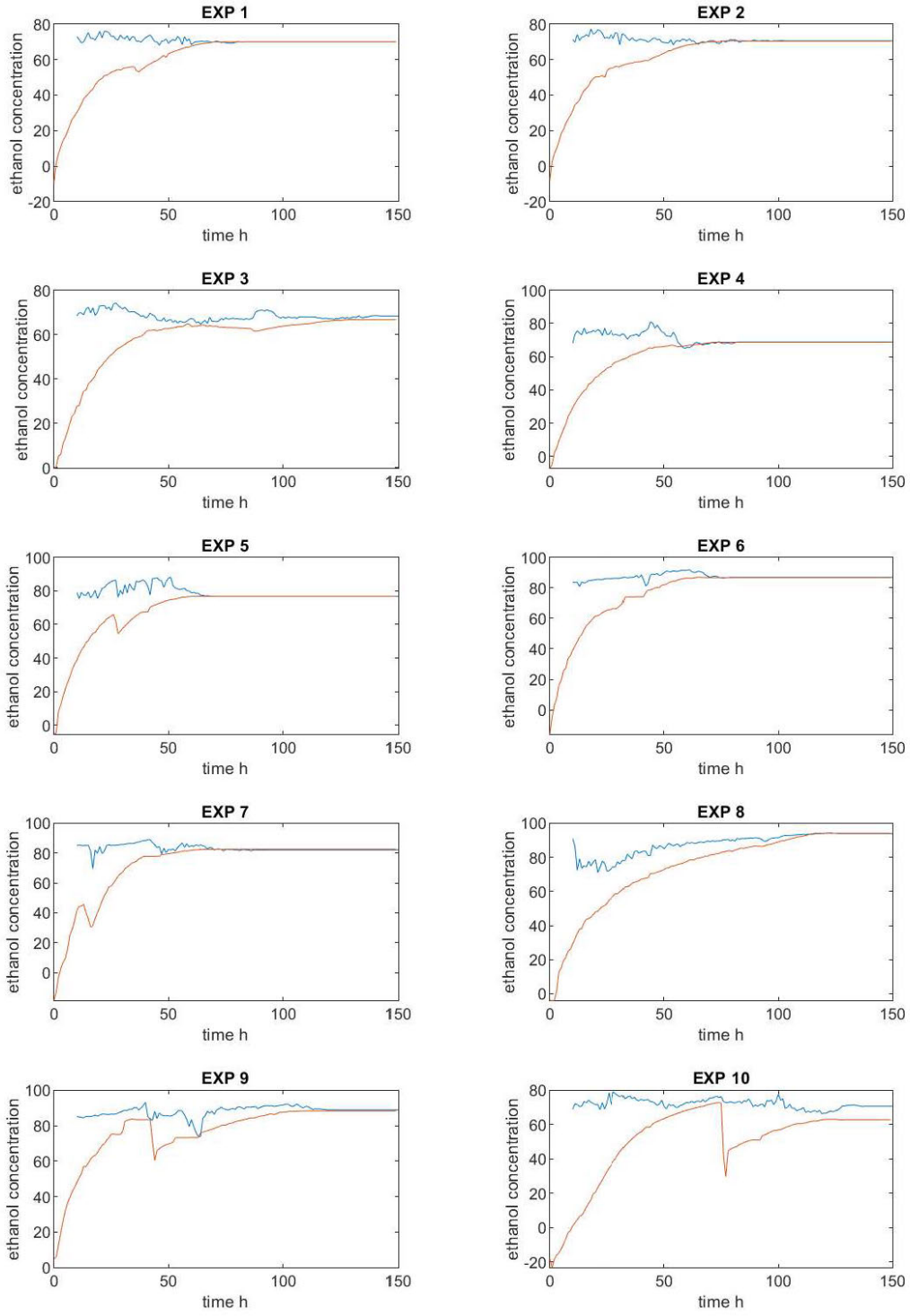

Figure 6.9: theoretical maximum ethanol concentration in g/L compared to the ethanol concentration as the fermentation progresses, fermentation data given in orange, prediction in blue

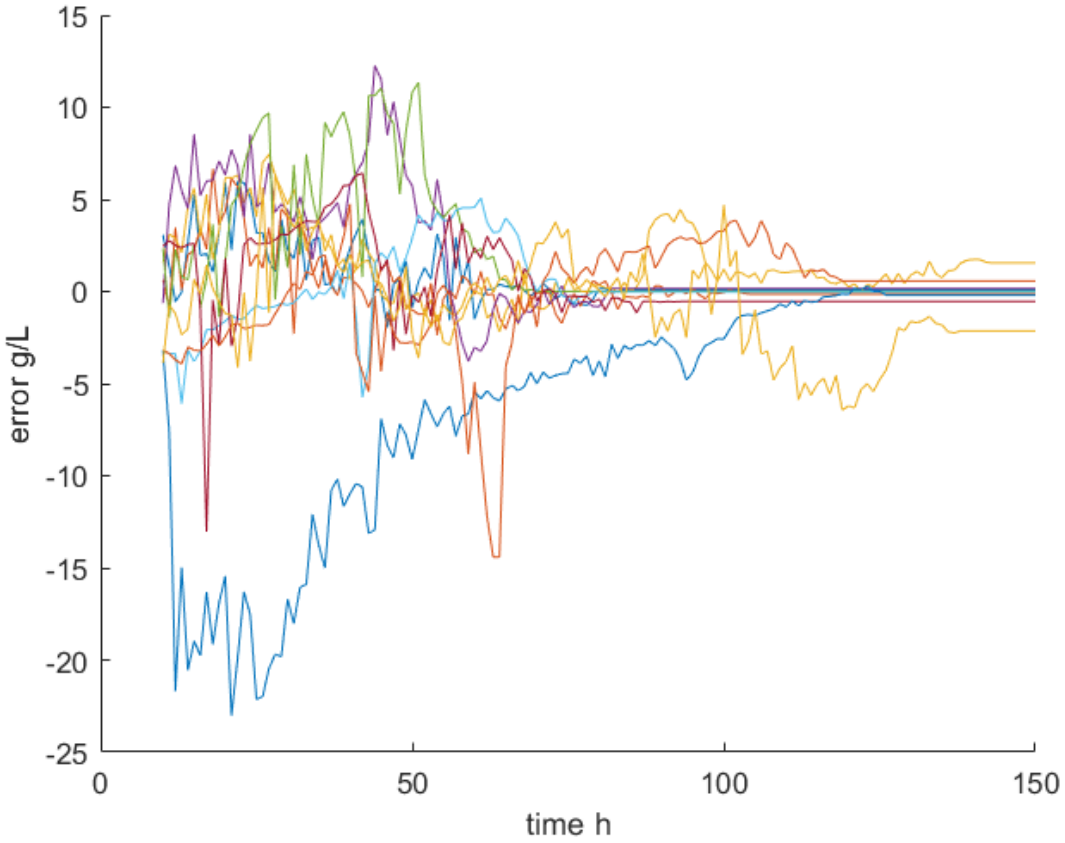

Figure 6.10: comparison of the error between the actual and predicted maximum ethanol concentration for the 10 experimental datasets.

The difference between the predicted and actual maximum ethanol concentration is shown in Figure 6.10. In all cases, the error converges towards zero as the fermentation completes, showing that the uncertainty in the prediction decreases with fermentation time.

6.4 Neural network performance on simulated datasets

As the dataset used in training is the same dataset that was used in testing, there is a potential that the network that was developed would not perform well on new datasets that were not part of the training set.

New data was produced from simulations to test the performance of the predictions from the network. The simulations were performed in Simulink, using Equation 6.3, Equation 6.4 and Equation 6.5. the relationships determined from the data to determine v_{max} and P_{max} based on the initial yeast extract, and yeast concentrations were used to determine the

fermentation profiles for fermentation where X_0 ranged between 100 g and 400 g, and Y_x ranged between 100 g and 400 g both in increments of 10 g. The initial conditions for the simulation were chosen to be similar to those of the experimental datasets, with an initial volume of 42.5. The feed was added at a constant rate of 0.5 L/h, starting at 10 hours and continuing until the maximum volume of 57.5 L was achieved. The dataset was interpolated to make it hourly data, and the ANN was used to predict the maximum ethanol concentration over the course of the fermentation. The simulated dataset was composed of 960 fermentations with varying yeast and yeast extract at the start.

The error in the prediction for the whole dataset is shown in Figure 6.11. The error between the predicted and actual maximum ethanol concentration converges towards 0 as the fermentations progress, showing that the network trained on the experimental data is able to predict the maximum ethanol concentration of the simulated data, showing that the network is able to predict the maximum ethanol concentration for fermentations not included in the original dataset. Importantly, the largest errors are negative errors, with the largest error in absolute terms being approximately -25 g/L. As an erroneously low prediction for the maximum ethanol concentration can result in the addition of too much water to dilute the batch, this will need to be taken into account when determining the uncertainty of the prediction.

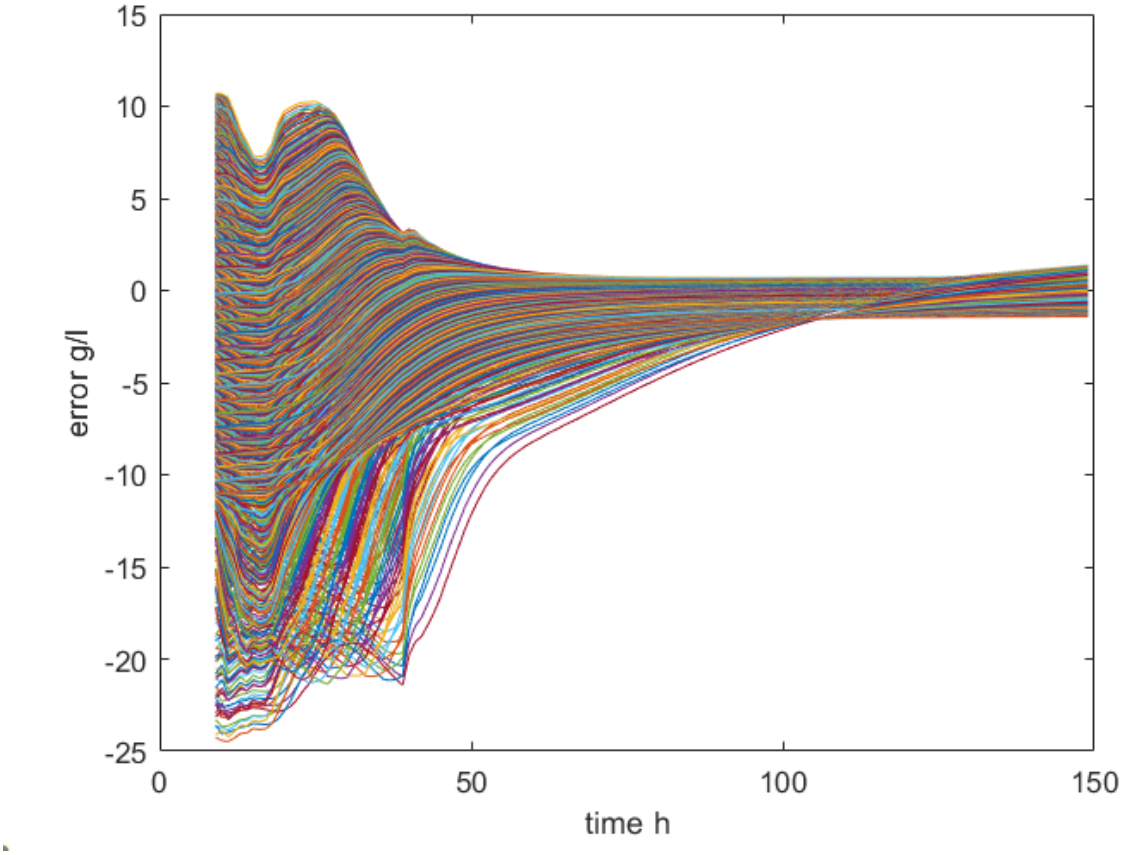

Figure 6.11: error between predicted and actual maximum ethanol concentration over 960 simulated fermentations

6.5 Conclusion

A model was developed to describe the consumption of sugar by *Saccharomyces cerevisiae* in a fed-batch fermentation by modelling the total amount of sugar consumed and relating this to the amount of ethanol produced. The model can be used for simulation purposes, but due to the unknowns of the process, especially in terms of the nutrition available, the model can only be used after the fermentation is complete to determine the parameters.

For the prediction of the theoretical maximum ethanol concentration, an Artificial Neural Network was developed and trained to be able to predict this value using only known values from the fermentation. As the network used only sequential values of the total sugar consumed, the ethanol concentration and the feed at any point during the fermentation, this prediction can be made using simple measurements and calculations.

The uncertainty of the prediction can also be estimated. Hence, the network can be used in the robust optimisation of the ethanol fermentation process.

7) Robust optimisation of ethanol production

7.1 Introduction

The main objective of this research is to determine an approach that can be used to determine the optimal ethanol yield of a fed-batch fermentation by *Saccharomyces cerevisiae*. Based on the model and data in Chapter 6, substrate inhibition was not observed. Thus, manipulating the feed to control the sugar concentration during the batch was not a viable optimisation strategy. Substrate limitations were only observed at low substrate concentrations of less than 30 g/L; hence, substrate limitation did not affect the majority of fermentations as, in most cases, the sugar concentration at the end of the fermentation was high. The ethanol concentration was the main factor that affected the fermentation rate and the variable that caused the fermentation activity to cease.

As the ethanol concentration increased, the rate of fermentation slowed until the maximum ethanol concentration was reached. The maximum ethanol concentration was not constant over all the batches and was affected by various factors, such as the nutrition available in the fermentation. Thus, the maximum ethanol concentration for a batch is unknown at the start of the batch.

Neural networks were used to predict the maximum ethanol concentration during the batch. Ten sequential measurements for the total sugar consumption, the ethanol concentration, and the feed rate were used as inputs to a network that was able to predict the final ethanol concentration. The error between this predicted value and the actual final ethanol concentration reduces as the fermentation continues and the ethanol concentration nears the final value. Hence, the uncertainty of this parameter reduces as the fermentation progresses. As the uncertainty decreases, the accuracy with which the maximum ethanol concentration can be estimated increases, so as the fermentation progresses, the accuracy of the estimate increases.

Optimising the batch based on this uncertain value could lead to optimal solutions that are infeasible or suboptimal. Hence, robust optimisation was used as a method to determine the optimal solution.

7.2 Optimisation strategy

7.2.1 calculation of optimal solution

Two optimisation strategies were investigated to maximise ethanol yield. The ethanol yield was defined as per Equation 7.1 as the ratio of ethanol produced per batch and the amount of sugar fed to the batch. It should be noted that this does not relate to the yield $Y_{X/S}$ which was assumed to be constant for calculation purposes.

$$yield = \frac{P_t}{S_{tf}} \tag{7.1}$$

Where P_t is the total ethanol formed during the fermentation in g. S_{tf} is the total sugar added to the fermenter in kg.

Hence, the optimisation problem can be written as shown in Equation 7.2 to determine the maximum ethanol yield per batch:

$$\max \frac{PV}{S_0 V_0 + S_f V_f} \tag{7.2}$$

S_0 is the initial substrate concentration in the fermenter in g/L, V_0 is the initial volume in L, S_f is the substrate concentration in the feed in g/L, and V_f is the volume of feed added.

As each batch's product concentration was limited to a maximum theoretical ethanol concentration, two potential methods can be used to optimise the process

by either decreasing the amount of sugar added to the fermenter for a fixed volume of water, or increasing the water added to the fermenter for a fixed mass of sugar, so that the ethanol concentration would ideally be equal to P_{max} and the sugar concentration at the end of the fermentation would be zero.

The total feed added to the fermentation was optimised by assuming the total product formed could be calculated using Equation 7.3, which is obtained by multiplying the product concentration from Equation 6.5 by the fermentation volume.

$$P_t = Y_{P/S} S_t \tag{7.3}$$

Where S_t is the total mass of sugar consumed during the fermentation.

The optimal yield is achieved when the amount of sugar added to the fermenter in the feed is equal to the total sugar consumed during the fermentation $S_{ft}=S_t$. Equation 7.1 is then reduced to the yield=$Y_{P/S,}$ which would be the theoretically highest achievable yield. To determine the amount of feed required, Equation 7.4 can be used to determine the optimal feed.

$$S_0 V_0 + S_f V_f = \int_0^{\infty} \nu_{max} * \left(1 - \frac{P}{P_{max}}\right)^n X_t \tag{7.4}$$

S_0 is the initial substrate concentration in the fermenter in g/L, V_0 is the initial volume in L, S_f is the substrate concentration in the feed in g/L, and V_f is the volume of feed added.

As the optimisation is based on the final conditions of the fermentation, the integral can be replaced with S_t= V *P/$Y_{P/S}$. The product concentration at the end of the fermentation can be assumed to be $P_{max,}$ and the volume is the sum of the

initial volume, and the volume of the feed added to the fermenter. The balance then becomes Equation 7.5.

$$S_0V_0 + S_fV_f = \frac{P_{max}(V_0 + V_f)}{Y_{P/S}} \quad 7.5$$

Hence, the optimal feed volume can be determined by Equation 7.6.

$$V_f = \frac{V_0\left(P_{max} - Y_{P/S}S_0\right)}{(Y_{P/S}S_{f-}P_{max})} \quad 7.6$$

7.2.2 Comparison of optimisation strategies

The system described in Chapter 5 was used as the basis for optimisation, in which the constants are given in Table 7.1. The resulting optimal feed rate required for a range of P_{max} values is shown in Figure 7.1.

Table 7.1: Parameters used to determine optimal feed volume

Parameter	Value	Unit
V_0	43.1	L
$Y_{P/S}$	438.69	g/kg
S_0	0.116	kg/L
S_f	0.625	kg/L

The optimal feed volume increases as the value of P_{max} increases. It would reach an asymptote at P_{max} values greater than 274.18 g/L, which is the P value which corresponds to the total conversion of all sugar in the feed to ethanol, without the product inhibition affecting the final ethanol concentration. The total ethanol produced also increases linearly, which indicates that at low P_{max} values, limiting the feed volume can result in lower ethanol production. For example, a P_{max} of 70 g/L will produce less than 4000 g of ethanol, while a P_{max} of 130 g/L will produce more than double the amount at 8029.4 g

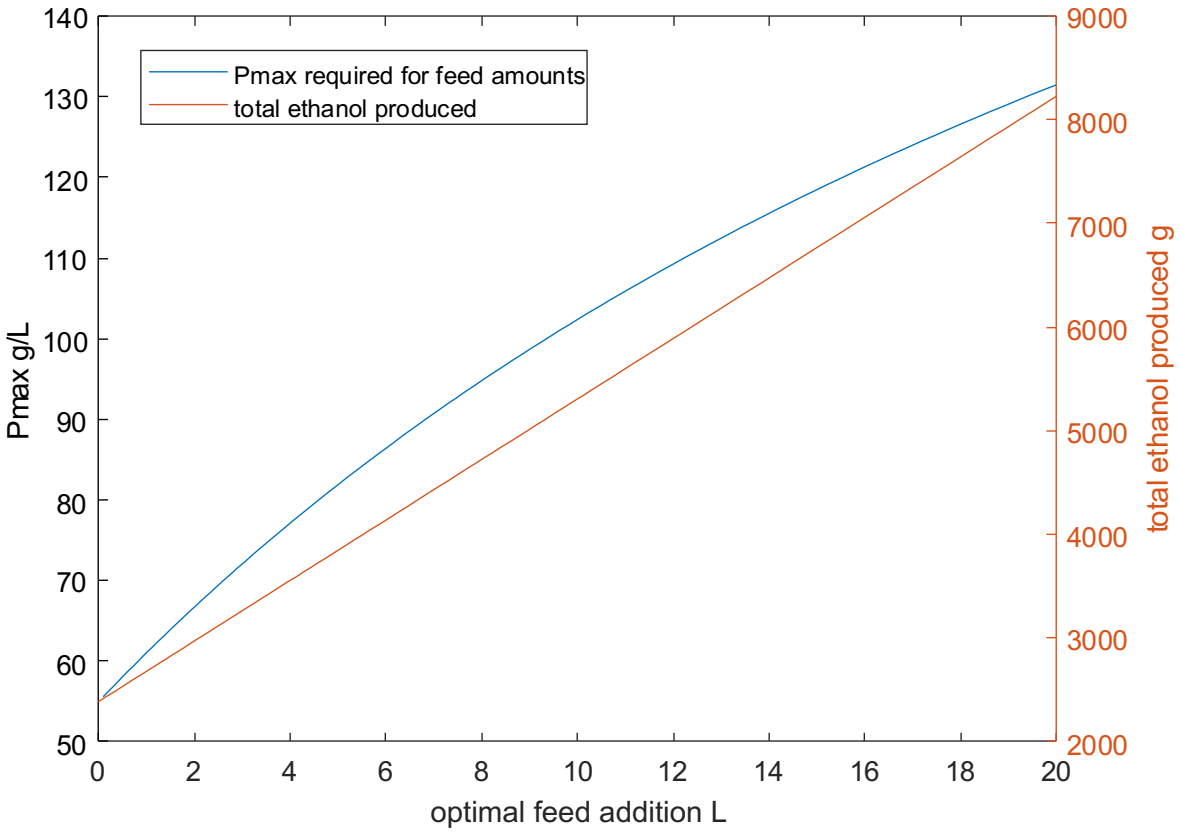

Figure 7.1: Optimal feed volume and total ethanol production

The lower total production at low P_{max} values demonstrates the limitation of this optimisation method. While this method will minimise excess sugar, the sugar that will not be fermented will not be added to the fermentation. However, the ethanol produced in the batch will not be optimised. The optimisation can ensure higher ethanol production rates by changing how the yield is defined, as shown in Equation 7.1. The optimisation strategy can be amended by assuming the feed volume is fixed. Hence, the total amount of sugar added to the fermentation is constant. As the volume of feed added is constant, an additional variable must be added to manipulate the system and reduce the ethanol concentration. For this purpose, additional water is added to the fermentation to dilute the ethanol. In this case, the balance will become a function of the volume of dilution water added, V_{dw}, as shown in Equation 7.7.

$$P_{max} = \frac{Y_{P/S}(S_0V_0 + S_fV_f)}{(V_0 + V_f + V_{dw})} \quad 7.7$$

The parameters shown in Table 7.1 were used, and V_f was constant as 16 L, containing 10 kg of water and 10 kg of sugar. The optimal value for V_{dw} was determined using Equation 7.8 for a range of P_{max} values between 10 g/L and 150 g/L.

$$V_{dw} = \frac{Y_{P/S}(S_0V_0 + S_fV_f)}{P_{max}} - (V_0 + V_f) \quad 7.8$$

Figure 7.2 shows that the amount of dilution water required increases as the P_{max} value decreases since more water is needed to dilute the ethanol produced from the sugar. As the amount of sugar added is constant, the total mass of ethanol produced is constant at 6575.1 g, as all sugar is consumed in all cases. The practical considerations of the system would prevent this at P_{max} values, where the dilution water required would cause the total volume to exceed the maximum volume of the fermenter.

For P_{max} values greater than 112 g/L, the calculated volume of dilution water was negative, indicating that at these values, the sugar would be able to ferment completely without the ethanol concentration reaching the P_{max} limit.

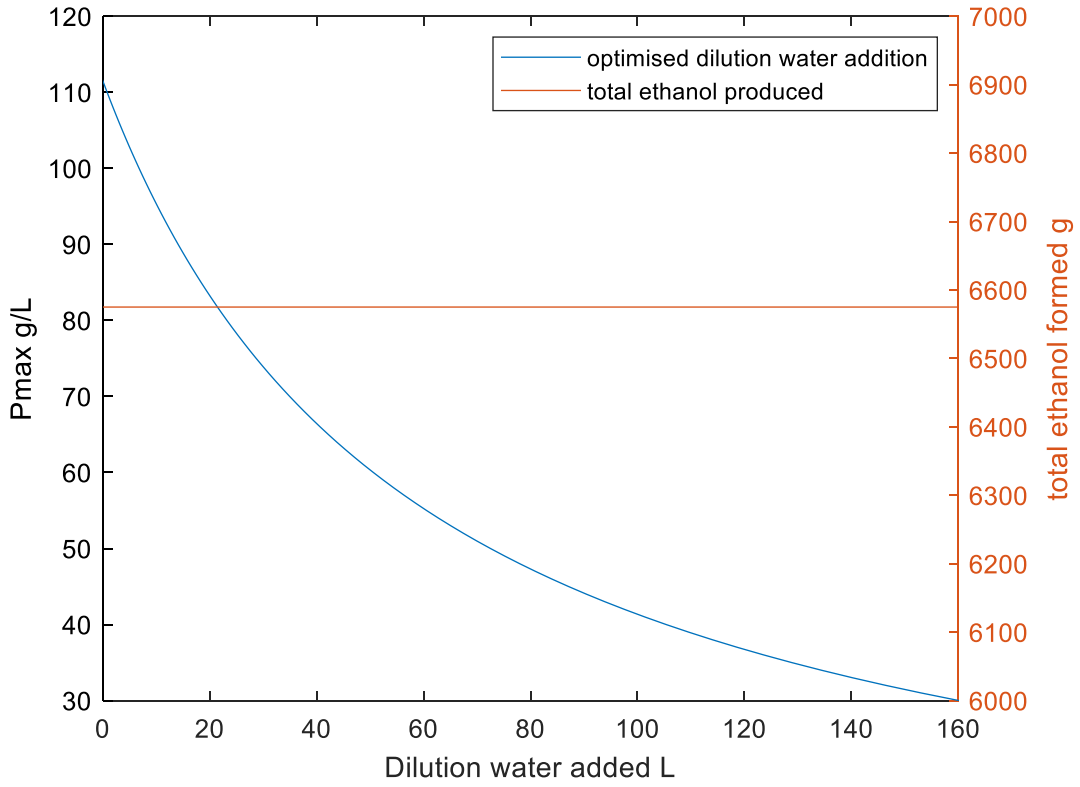

Figure 7.2: Optimised dilution water addition and ethanol produced

7.2.3 Economic analysis

The dilution increases the energy required during distillation. Hence, the effect of dilution on the process's profitability was determined. The ethanol sales price was assumed to be 91 US cents per kilogram of ethanol, while the cost of the sugar was 29 US cents per kilogram (Kohler, 2016). The cost of distillation was determined based on the energy required. The relationship between the energy required and the ethanol concentration of the feed to the distillation column was determined based on data from Kvaalen et al. (Kvaalen et al., 1984). The energy usage and the fit given by Equation 7.9 is shown in Figure 7.8. The fit for Equation 7.8 was found using the curve fitting toolbox in MATLAB. The fit to the data has an RMSE of 316.7 kJ/Kg and an R^2 value of 0.9988.

$$E = 330600P^{-1.018} \quad 7.9$$

Where E is the energy required to purify 1 kg of ethanol to 90% (w/w) in kJ.

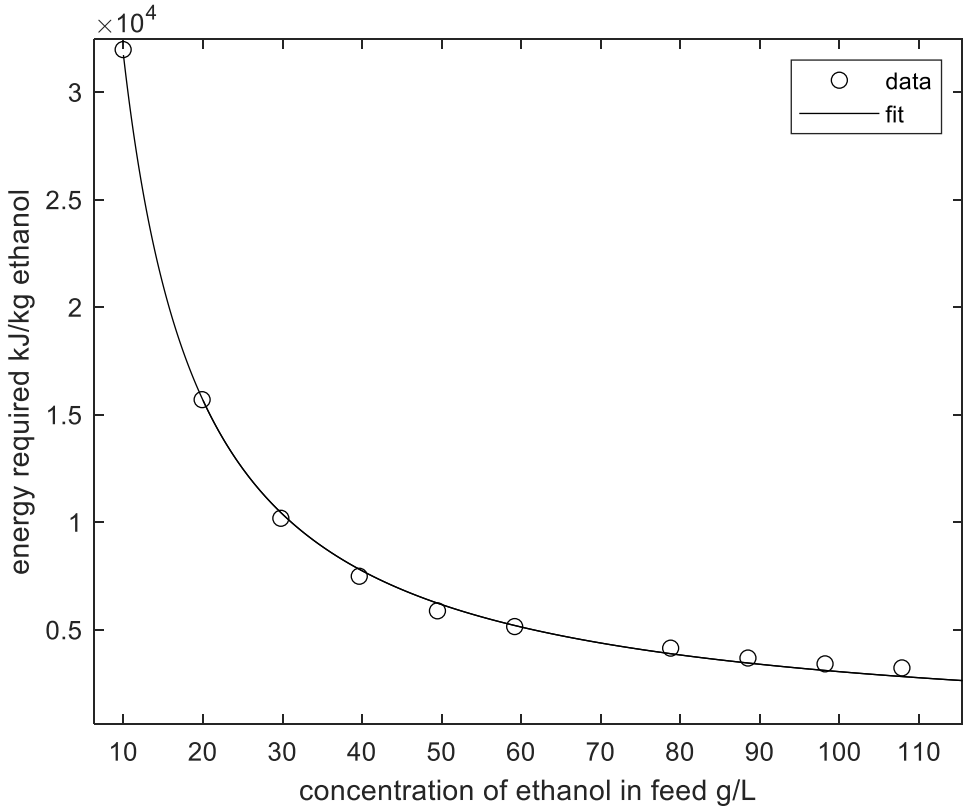

Figure 7.3: Energy requirement for distillation for a range of feed concentrations

The cost of the energy required for distillation was calculated based on the price of steam, which is $12.29 per 1000 lbs (Peters et al., 2023) , giving a cost of 0.00135 US cents per kJ. The potential profit for fermentations where the optimal amount of dilution water has been added is shown in Figure 7.4. For the range of P_{max} values ranging from 30 g/L to 130 g/L, the costs of distillation increase as P_{max} decreases, with a P_{max} of 30 g/L resulting in 149.33 c in profit and 130 g/L resulting in 160.61 c of profit per batch. While the difference is not large at the lab scale used, it would become significant for large industrial fermentations.

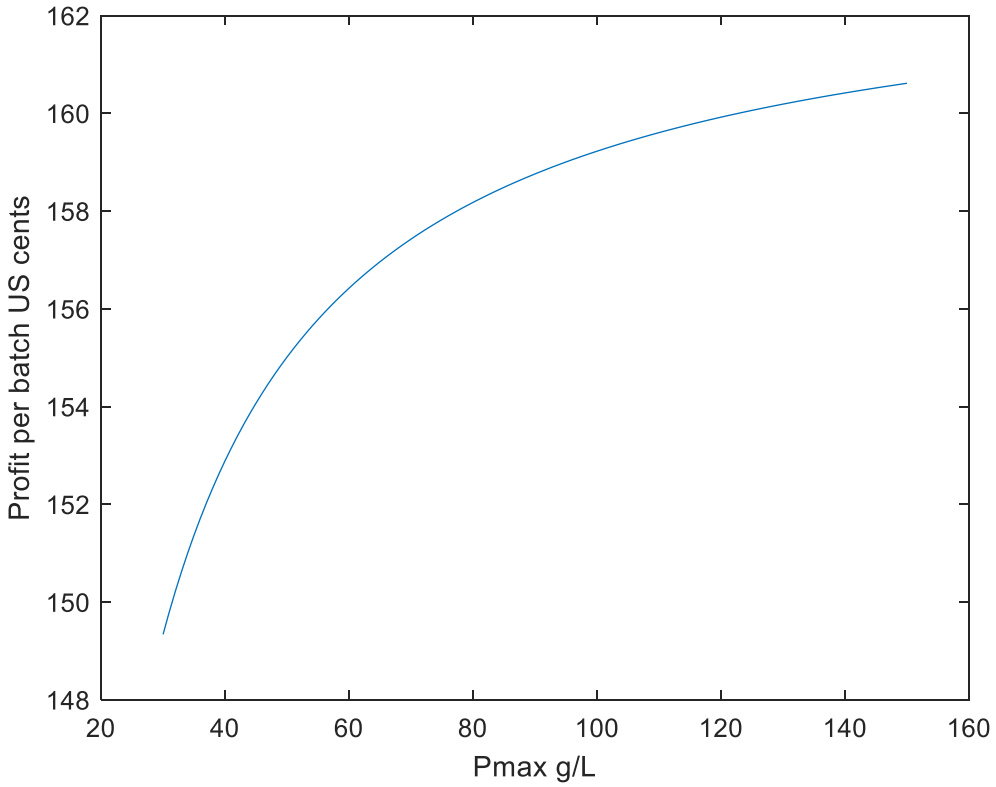

Figure 7.4: Profit per batch assuming total conversion of sugar.

If P_{max} is known, the optimal volume of dilution water can be easily calculated. However, unless the conditions of the fermentation and the feed can be duplicated precisely, the value of P_{max} is not known until the end of the fermentation.

This solution, however, neglects the opportunity cost that long fermentations could cause due to the extended length of fermentations.

7.3 Robust Optimisation

As mentioned previously, the calculation of the amount of water required to complete the fermentation is trivial if P_{max} is known. However, the uncertainty in the parameter makes optimisation difficult. The neural network prediction described in the previous chapter provides an estimate for P_{max}. However, again, there is uncertainty in this estimate. The estimate for the first optimisation test is shown in Figure 7.5

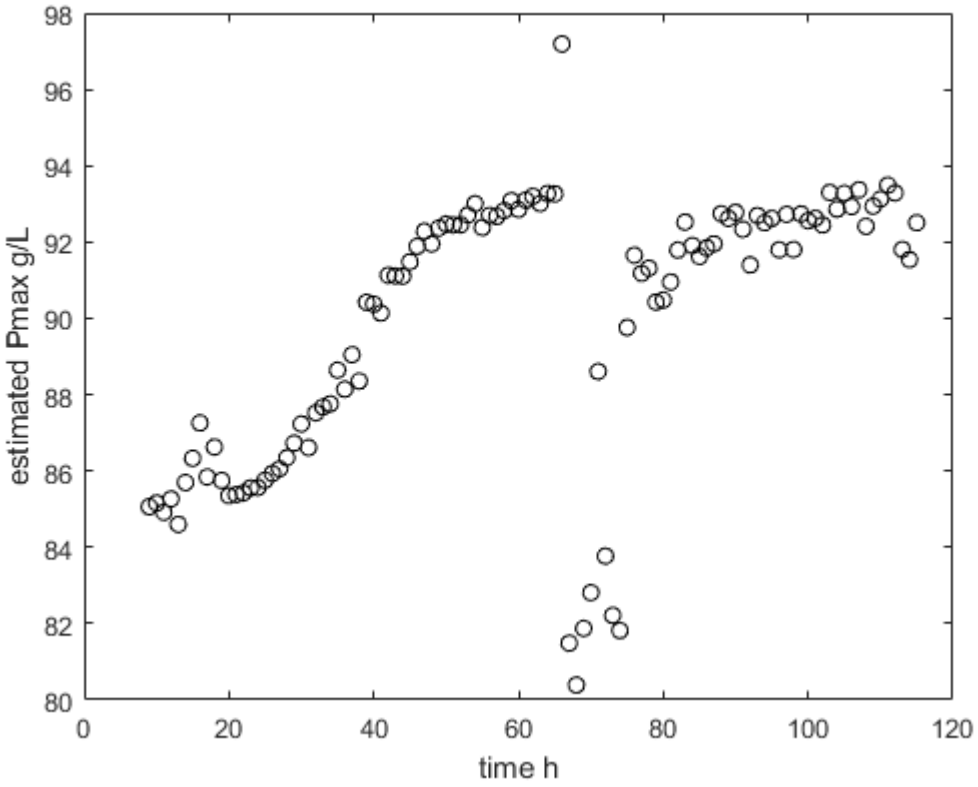

Figure 7.5: Estimated Pmax based on NN model for first optimisation test

The estimated values for P_{max} range from 85 g/L at the start of the fermentation up to a maximum of 97 g/L. The second optimisation test can be considered the optimal profile, so the real P_{max} value is 96.73 g/L. As the NN model underpredicts the ethanol concentration, if the dilution water were added based on this estimate, more water than needed would have been added, increasing the costs

associated with distillation. After 40 hours, the estimate increases to above 90 g/L, but this is the stage of the batch where the fermentation has begun to slow dramatically. Hence, the optimal strategy at this stage would be to add a conservative amount of dilution water during the initial stages of the fermentation so that the fermentation can continue and more sugar can be consumed. However, the algorithm would need to prevent overfeeding of water, as once the water is added, it cannot be removed. Figure 7.6 shows the optimal dilution predicted at hourly intervals. The predictions that calculated a volume larger than the optimal dilution, calculated after the fermentation had stalled, would cause too much dilution water to be added to the fermentation, increasing distillation costs.

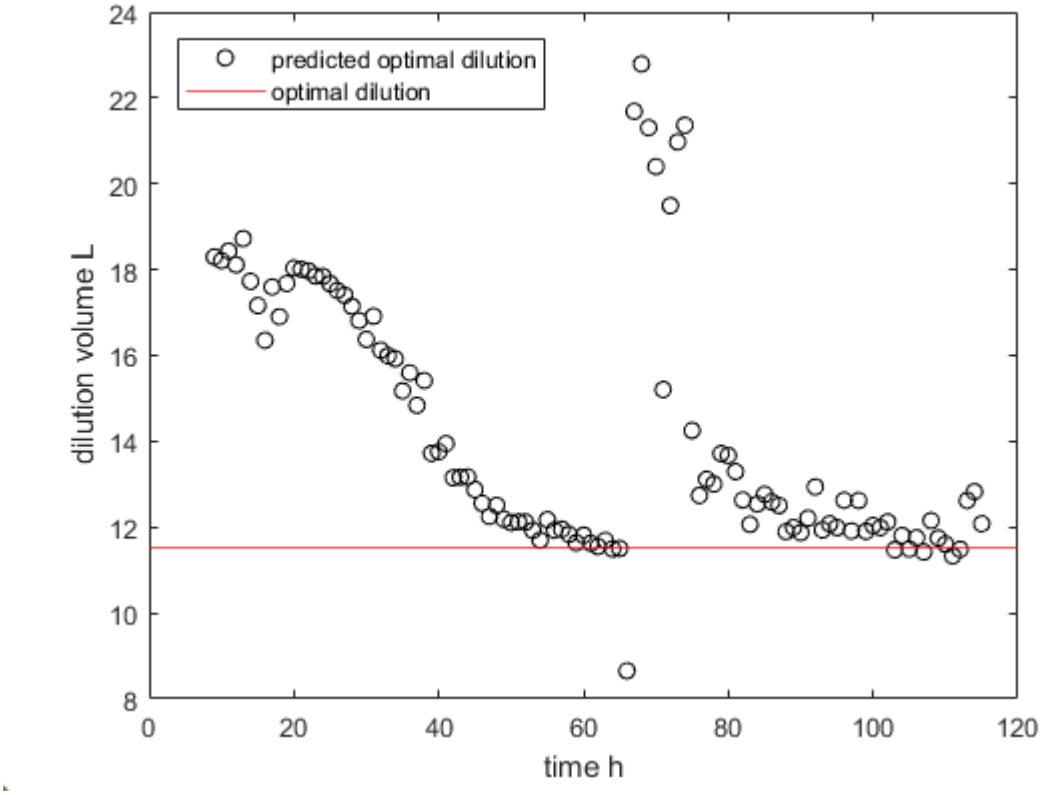

Figure 7.6: Predicted dilution required based on density measurements

Robust optimisation provides a framework for finding a solution for an optimisation problem where there is an uncertain parameter. The solution can be

found even if the uncertainty distribution of the parameter is unknown. The solution is based on an uncertainty set, and the solution must be feasible for all values in the set.

For the optimisation of the ethanol yield, the correct volume of water needs to be determined, and solutions that add too much water must be rejected as infeasible. For this purpose, the bounds of the parameter P_{max} were specified and changed with time. Additionally, as shown in the optimisation test, adding the dilution water too late in the fermentation can limit the benefit. Hence, all additions should occur before 50 h. The upper limit for the value of $P_{max,opt}$ was chosen to be 50% higher than the predicted P_{max} value at t=0 h and decreases linearly, as shown in Equation 7.10. the first prediction can only be made at t=10 due to the required data points for the neural network.

$$P_{max,opt} = \left(1.5 - \frac{0.5 * t}{50}\right) P_{max} \qquad 7.10$$

The lower bound of the parameter does not need to be defined, as the optimal dilution volume calculated at the upper bound is feasible for all lower $P_{max,opt}$ values, as it will be the lowest volume for the set. The upper bound of $P_{max,opt}$ is shown in Figure 7.7.

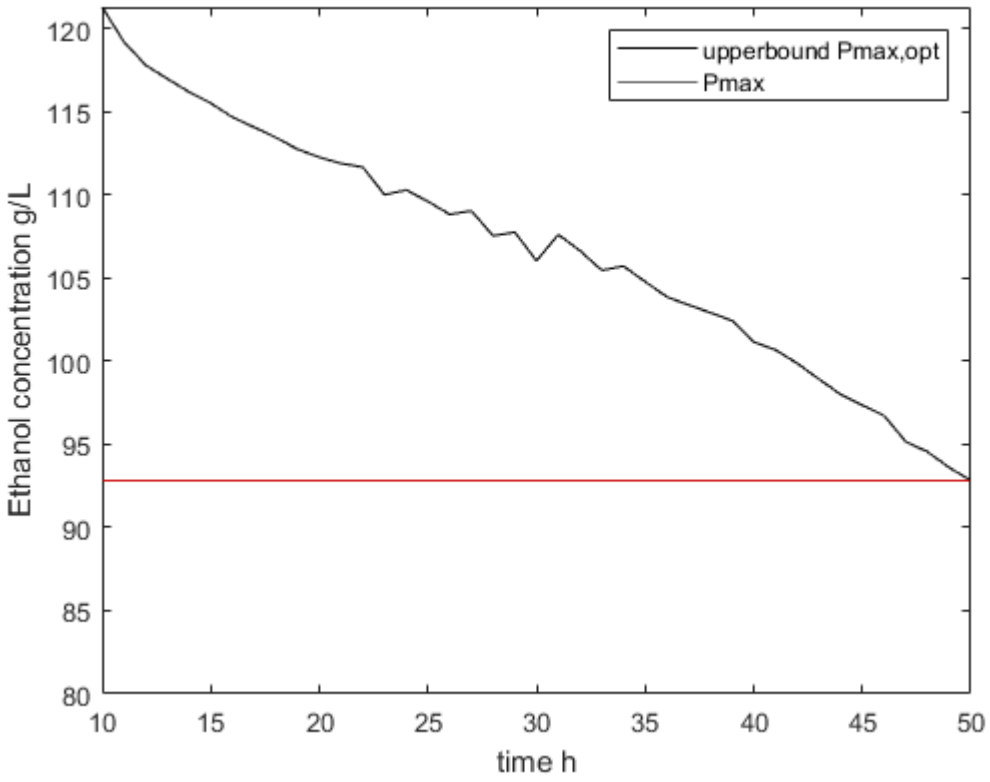

Figure 7.7: upper bound of $P_{max,opt}$

The dilution required to completely ferment the sugar given the maximum ethanol concentration at the upper bound of $P_{max,opt}$ was solved at each time interval, as shown in Figure 7.8. Initially, the optimal dilution volume is negative due to the large values of $P_{max,opt}$, for all negative values, the volume was set to zero. The profile of volume addition that was obtained is shown in Figure 7.9.

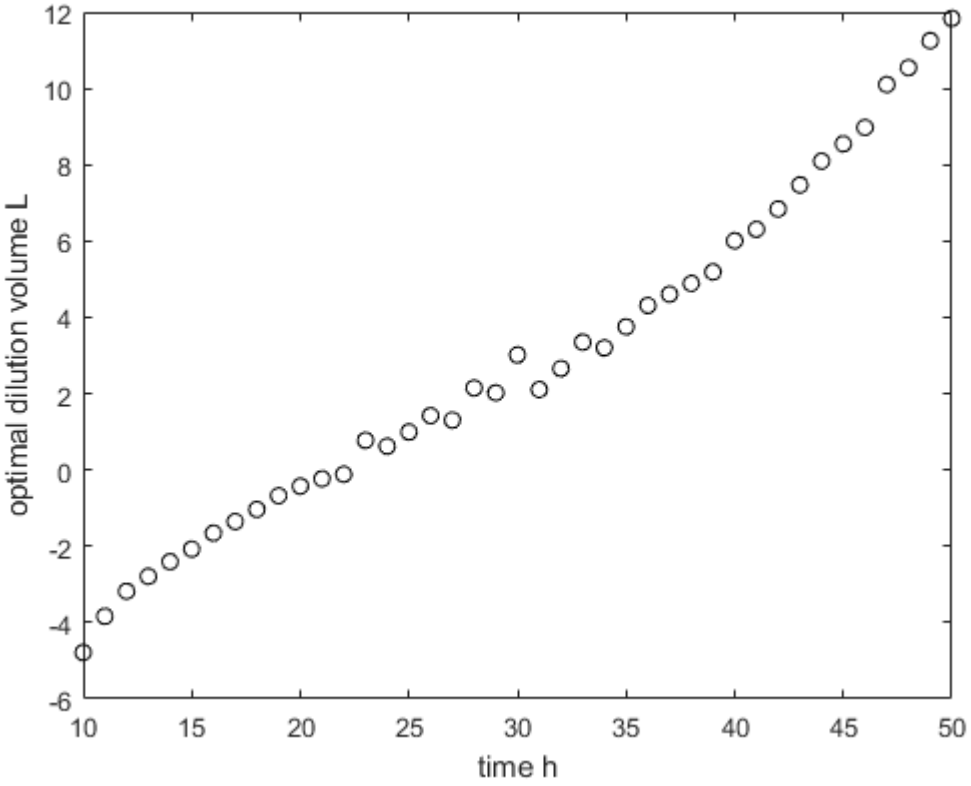

Figure 7.8: optimal dilution volume solved at each time step

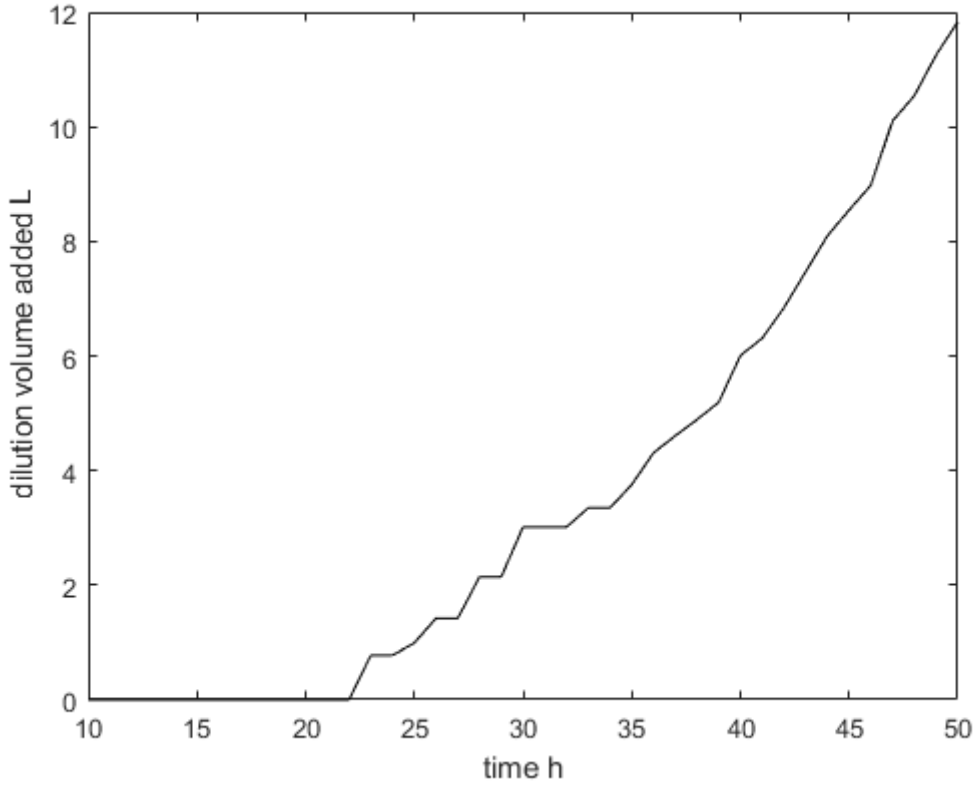

Figure 7.9: volume of dilution water added

The optimal dilution volume profile was then determined for Experiments 1, 2, 3 and 4. These experiments used the same initial conditions, had similar fermentation profiles, and stalled at approximately the same value of $P_{max.}$ The determined dilution volume addition profiles are shown in Figure 7.10

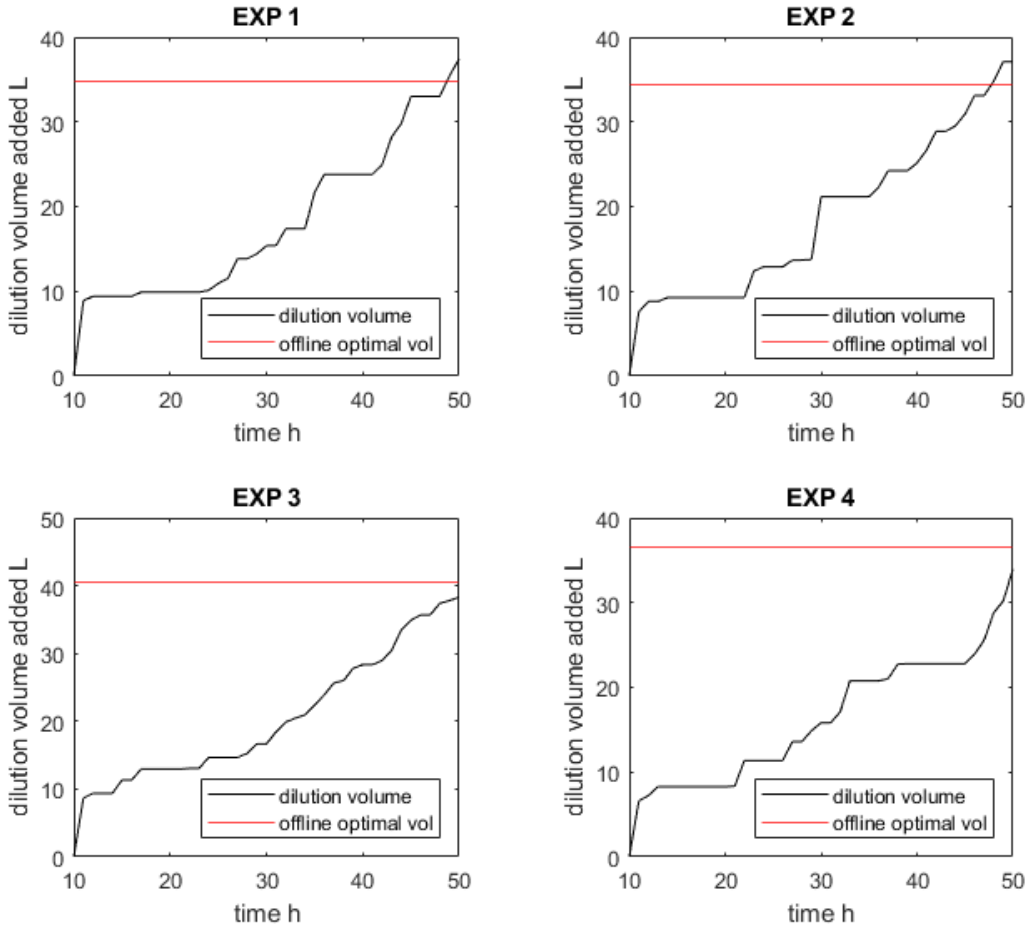

Figure 7.10: dilution volume addition determined using RO

The volumes determined for these experiments were higher than those for the optimisation trials as the P_{max} values were lower due to lower levels of nutrition available. The values for the volume determined using the robust optimisation and neural network model, compared to the values based on the ethanol concentration at which the fermentation stalled, are shown in Table 7.2. The predicted optimal volumes are within 3 litres of the calculated optimal volume.

Table 7.2: volume of dilution water determined using RO and neural network model and calculated optimal dilution volume

batch	dilution volume from RO (L)	calculated optimal dilution volume (L)
exp 1	34.86	37.45
exp 2	34.48	37.10
exp 3	40.62	38.33
exp 4	36.50	33.95

For these experiments, the sugar conversion was only 56% or less, so the volume addition has the potential to almost double the amount of sugar converted and, thus, double the ethanol produced in the batch. As the sugar for fermentation can contribute up to 60% of the cost of the ethanol, this shows that the ability to determine the optimal volume addition before the end of the fermentation could result in a significant increase in revenue due to increased ethanol production, but also decrease the costs associated with the production, while minimising the potential for increasing the costs of distillation.

7.5 Conclusion

The ethanol yield, in terms of the total ethanol formed from the total sugar available, was optimised in two ways: firstly, the amount of feed was controlled to prevent the addition of excess sugar that would not ferment, and secondly, through the addition of water to dilute the ethanol which acts as an inhibitor to further ethanol production. Experimentally, it was demonstrated that this approach could significantly increase the amount of ethanol produced during a batch. To allow this optimisation to be done during fermentation, a neural network model that was able to predict the maximum ethanol concentration for the batch was used. The uncertainty in this prediction made optimisation difficult. However, using robust optimisation and defining the upper bounds of the maximum ethanol concentration, the volume required to optimise the batch could be determined without adding excess water. In theory, the sugar conversion can be increased to 100%, and experimentally, the sugar conversion increased to greater than 90% after the addition of the dilution water.

8) Discussion and recommendations

8.1) Discussion

The optimisation shown in Chapter 7 showed that by manipulating either the feed of sugar or water, the amount of potentially wasted sugar can be reduced, which would reduce vinasse volumes, reduce costs, and increase the potential profitability of the ethanol production process at high gravity.

The limitations of the optimisation should also be noted, as the experiment was limited by conditions that could be recreated in the laboratory setting; hence some conditions would differ from those found in industry.

Firstly the maximum possible ethanol concentrations found were low, well below the ethanol tolerance stated by the manufacturer. As nutritional availability was found to be the major factor affecting the maximum potential ethanol concentration, the conditions could differ where excess nutrition is available, and the modelling could deliver different results.

Secondly, several parameters such as yield, $Y_{X/S}$, and total biomass, X_t, were assumed to be constant. Assuming a constant yield of ethanol formation from sugar is consistent with the majority of work in literature for calculation purposes (Ghose & Tyagi, 1979) (Hong, 1986) (Amillastre et al., 2012). Where this work differs is that the total biomass was assumed to be constant. This corresponds with the data, in that the rate of ethanol formation was greatest at the start, where if the biomass concentration increased, an acceleration of ethanol production and sugar utilisation would be expected. This potentially explains another deviation from the majority of literature, in that the optimal feeding strategy is usually defined by a slow rate of sugar addition to avoid substrate inhibition of biomass formation, rather than being limited by the maximum ethanol concentration. This is also the case where biomass production is optimised as the sugar concentration must be kept as low as possible to prevent the formation of byproducts such as ethanol, and also to prevent substrate inhibition of biomass growth. The use of

substrate concentration minimisation as the optimising criteria is due to the majority of models, such as those used by Hong (1986), including large effects due to substrate inhibition, especially in the formation of biomass. Hence at high sugar concentrations, which inhibit growth of the biomass, ethanol production and sugar utilisation are both severely inhibited. This is supported by the conjunction and batch curves shown in Hong (1986) which show that for the model used, there is no product formation for a substrate concentration higher than 150 g/L. For the high gravity fermentations it is then not unreasonable to assume that the growth of new yeast cells was negligible.

It should also be noted that the maximum ethanol concentration varies between the experiments performed, where commonly it would be assumed that the kinetics of a particular strain is constant. There is remarkably little literature exploring the effect of the fermentation conditions on the kinetic parameters. The nutrients available to the yeast are known to vary between fermentations, and affect yeast performance, however it is not possible, based on currently available information, to predict the effect the variation of fermentation conditions will have on each fermentation. Hence a method was developed to predict the kinetics of the yeast and allow for prediction of the end point of the fermentation. This allowed for the optimisation strategies described in Chapter 7 to be developed.

While it was shown that implementing the changes as early as possible was beneficial what was not investigated was the effect of lengthening the fermentation. This was due to the main optimisation objective being the reduction of residual sugar, however if the profitability of each fermenter was taken into account, both the rate of sugar utilisation and the end point of the fermentation would need to be determined. If the additional ethanol production is sub-optimal, economically, it may be preferable to end a fermentation prior to the end point of the fermentation and allow a new fermentation to begin.

8.2) Conclusion

A bioreactor system was developed to perform the fermentations, and it was shown that by monitoring the density of the liquid in the fermenter the most important process variables, the substrate and ethanol concentration, could be determined based on existing correlations to within 10% of values determined offline using high-performance liquid chromatography. The error found was mainly due to the errors introduced by the measurement device,

A novel model was developed to simulate the fed-batch fermentation for a range of conditions. It was determined that the variable that affected the maximum ethanol concentration was the concentration of the nutrient, yeast extract, that was present in each fermentation. A linear relationship was determined between the maximum ethanol concentration P_{max} and yeast extract added to the start of the fermentation.

It was found that the artificial neural network models were not effective in predicting the progression of the fermentation. The models could not be used as the required inputs were not available to determine the maximum ethanol concentration, as the available nutrients were considered an unknown. The neural network prediction for the ethanol concentration during the fermentation was also unstable, and the seed used in training the network had a significant effect on the results of the model.

After analysing the analytical model, it was determined that the only parameter required to be known to optimise the ethanol concentration was the final ethanol concentration, P_{max}. A neural network model was trained to predict the final ethanol concentration. The neural network model was able to predict the final ethanol concentration with increasing accuracy as the fermentation progressed. However, the largest error in absolute terms was -24.48 g/L, which demonstrates that there is a significant degree of uncertainty in the model.

The main objective of the research was to develop an optimisation strategy for fed-batch ethanol fermentations, increasing the yield of ethanol. This was initially

proposed to use artificial neural networks to assist with the computation of the optimal trajectory for the feed rate, however, due to the kinetics of the system, this optimisation strategy was not feasible. Two strategies were developed in place of the initial proposal, firstly using the neural network prediction of the final ethanol concentration to limit the feed to the amount of sugar that could theoretically be consumed to achieve the maximum ethanol concentration, and secondly, adding dilution water to increase the volume so that all sugar can be consumed and the maximum ethanol concentration, again predicted by the neural network model, can be achieved.

The first optimisation strategy was found to be deficient as it would result in lower production of ethanol, which would decrease revenue, even if the feed costs were reduced. The second strategy, where water was added to the fermentation, was shown to increase the sugar conversion dramatically and based on the results of the experiments, could result in an increase in sugar consumption from 56% to near 100%. The total amount of ethanol produced would also be increased proportionally, while the costs of adding water would be negligible.

8.3) Recommendations for further work

The results and conclusions of this research lead to several recommendations for further work.

1) The estimation of sugar and ethanol concentration using online density measurements should be expanded to look at aerated fermentations. Significant work would need to be done to replicate the correlations for anaerobic fermentations and determine the accuracy of the estimation for these fermentations.
2) The use of a similar optimisation strategy for aerated fermentations should also be investigated. Tests would need to be performed to determine the effect of aeration on sugar consumption and ethanol production. If a similar strategy could be used for aerated fermentations, it would be more applicable to the biofuel industry, while the current research is more applicable to the production of potable ethanol, where anaerobic fermentation is more common.

References

Aiba, S., Shoda, M., & Nagatani, M. (1968). Kinetics of product inhibition in alcohol fermentation. *Biotechnology and Bioengineering*, *10*(6), 845–864. https://doi.org/10.1002/bit.260100610

Ali, S. H., Al-Rashed, O., Azeez, F. A., & Merchant, S. Q. (2011). Potential biofuel additive from renewable sources - Kinetic study of formation of butyl acetate by heterogeneously catalyzed transesterification of ethyl acetate with butanol. *Bioresource Technology*, *102*(21), 10094–10103. https://doi.org/10.1016/j.biortech.2011.08.033

Amillastre, E., Uribelarrea, J., Alfenore, S., & Guillouet, S. E. (2012). Bioresource Technology Dynamic model of temperature impact on cell viability and major product formation during fed-batch and continuous ethanolic fermentation in Saccharomyces cerevisiae. *BIORESOURCE TECHNOLOGY*, *117*, 242–250. https://doi.org/10.1016/j.biortech.2012.04.013

Amorim, H. V., Lopes, M. L., De Castro Oliveira, J. V., Buckeridge, M. S., & Goldman, G. H. (2011). Scientific challenges of bioethanol production in Brazil. In *Applied Microbiology and Biotechnology* (Vol. 91, Issue 5, pp. 1267–1275). https://doi.org/10.1007/s00253-011-3437-6

Andrews, J. F. (1968). A mathematical model for the continuous culture of microorganisms utilizing inhibitory substrates. *Biotechnology and Bioengineering*, *10*(6), 707–723. https://doi.org/10.1002/bit.260100602

Angel Yeast. (2023, November 10). *Brewing & Distilling Yeast*.

Arifeen, N., Kookos, I. K., Wang, R., Koutinas, A. A., & Webb, C. (2009). Development of novel wheat biorefining: Effect of gluten extraction from wheat on bioethanol production. *Biochemical Engineering Journal*, *43*(2), 113–121. https://doi.org/10.1016/j.bej.2008.09.005

Arndt, C., Henley, G., & Hartley, F. (2019). Bioenergy in Southern Africa: An opportunity for regional integration? *Development Southern Africa*, *36*(2), 145–154. https://doi.org/10.1080/0376835X.2018.1447363

Arpornwichanop, A., & Shomchoam, N. (2009). Control of fed-batch bioreactors by a hybrid on-line optimal control strategy and neural network estimator. *Neurocomputing*, *72*(10–12), 2297–2302. https://doi.org/10.1016/j.neucom.2009.01.002

Ayodele, B. V., Alsaffar, M. A., & Mustapa, S. I. (2020). An overview of integration opportunities for sustainable bioethanol production from first- and second-generation sugar-based feedstocks. *Journal of Cleaner Production*, *245*, 118857. https://doi.org/10.1016/j.jclepro.2019.118857

Bai, F. W., Anderson, W. a, & Moo-Young, M. (2008). Ethanol fermentation technologies from sugar and starch feedstocks. *Biotechnology Advances*, *26*(1), 89–105. https://doi.org/10.1016/j.biotechadv.2007.09.002

Balling, C. (1846). *Die Bierbrauerei.* Verlag von Friedrich Temski.

Barrera-Cortes, J., & Baruch, I. (2000). Recurrent neural network model of a fed-batch Saccharomyces cerevisiae fermentation process. *Proceedings of the International Joint Conference on Neural Networks*, *4*, 589–594. https://doi.org/10.1109/ijcnn.2000.860835

Ben-tal, A., & Nemirovski, A. (2002). *Robust optimization – methodology and applications*. *480*, 453–480.

Beyer, H., & Sendhoff, B. (2007). *Robust optimization – A comprehensive survey*. *196*, 3190–3218. https://doi.org/10.1016/j.cma.2007.03.003

Bothast, R. J., & Schlicher, M. A. (2005). Biotechnological processes for conversion of corn into ethanol. *Applied Microbiology and Biotechnology*, *67*(1), 19–25. https://doi.org/10.1007/s00253-004-1819-8

Bowler, A., Escrig, J., Pound, M., & Watson, N. (2021). *Predicting Alcohol Concentration during Beer Fermentation Using Ultrasonic Measurements and Machine Learning*. 1–13.

Button, D. K. (1978). On the theory of control of microbial growth kinetics by limiting nutrient concentrations. *Deep-Sea Research*, *25*(12), 1163–1177. https://doi.org/10.1016/0146-6291(78)90011-5

Cartwright, A. (2007). *Biofuels trade and sustainable development: An analysis of South African bioethanol*. www.dme.gov.za/energy/refso.stm,

Casey, G. P., Magnus, C. A., & Ingledew, W. M. (1984). High-gravity brewing: Effects of nutrition on yeast composition, fermentative ability, and alcohol production. *Applied and Environmental Microbiology*, *48*(3), 639–646. https://doi.org/10.1128/aem.48.3.639-646.1984

Ccopa Rivera, E., Yamakawa, C. K., Saad, M. B. W., Atala, D. I. P., Ambrosio, W. B., Bonomi, A., Junior, J., & Rossell, C. E. V. (2017). Effect of temperature on sugarcane ethanol fermentation: Kinetic modelling and validation under very-high-gravity fermentation conditions. *Biochemical Engineering Journal*, *119*, 42–51. https://doi.org/10.1016/j.bej.2016.12.002

Chang, Y. H., Chang, K. S., Chen, C. Y., Hsu, C. L., Chang, T. C., & Jang, H. Der. (2018). Enhancement of the efficiency of bioethanol production by Saccharomyces cerevisiae via gradually batch-wise and fed-batch increasing the glucose concentration. *Fermentation*, *4*(2). https://doi.org/10.3390/fermentation4020045

Charef, C., Taibi, M., Vincent, N., & Benmahammed, K. (2009). Fuzzy and neuro-fuzzy modelling of a fermentation process. *Int. Arab J. Inf. Technol.*, *6*(4), 378–387. http://citeseerx.ist.psu.edu/viewdoc/download?doi=10.1.1.167.2266&rep=rep1&type=pdf

Chaudhuri, B., & Modak, J. M. (1998). Optimization of fed-batch bioreactor using neural network model. *Bioprocess Engineering*, *19*(1), 71–79. https://doi.org/10.1007/s004490050485

Contois, D. E. (1959). Kinetics of Bacterial Growth: Relationship between Population Density and Specific Growth Rate of Continuous Cultures. *Journal of General Microbiology*, *21*(1), 40–50. https://doi.org/10.1099/00221287-21-1-40

Correa, D. F., Beyer, H. L., Fargione, J. E., Hill, J. D., Possingham, H. P., Thomas-Hall, S. R., & Schenk, P. M. (2019). Towards the implementation of sustainable

biofuel production systems. *Renewable and Sustainable Energy Reviews*, *107*(March), 250–263. https://doi.org/10.1016/j.rser.2019.03.005

Cutaia, A. J., Reid, A., Speers, R. A., & Brew, J. I. (2012). Examination of the Relationships Between Original , Real and Apparent Extracts , and Alcohol in Pilot Plant and Commercially Produced Beers. *Journal of the Institute of Brewing*, *115*(4), 318–327. https://doi.org/https://doi.org/10.1002/j.2050-0416.2009.tb00387.x

Dagle, R. A., Winkelman, A. D., Ramasamy, K. K., Lebarbier Dagle, V., & Weber, R. S. (2020). Ethanol as a Renewable Building Block for Fuels and Chemicals. *Industrial and Engineering Chemistry Research*, *59*(11), 4843–4853. https://doi.org/10.1021/acs.iecr.9b05729

Dai, W., Word, D. P., & Hahn, J. (2014). Modeling and dynamic optimization of fuel-grade ethanol fermentation using fed-batch process. *Control Engineering Practice*, *22*(1), 231–241. https://doi.org/10.1016/j.conengprac.2013.01.005

de Clerck, J. (1992). *A Textbook of brewing*. Chapman.

De Oliva-Neto, P., Dorta, C., Azevedo, F., Gomes, V., & Fernandes, D. (2013). The Brazilian technology of fuel ethanol fermentation – yeast inhibition factors and new perspectives to improve the technology. *Formatex*, 371–379.

Dewasme, L., Vande Wouwer, A., & Samyudia, Y. (2015). Modeling and optimization of bioethanol production process. *2015 19th International Conference on System Theory, Control and Computing, ICSTCC 2015 - Joint Conference SINTES 19, SACCS 15, SIMSIS 19*, 37–42. https://doi.org/10.1109/ICSTCC.2015.7321266

Dombek, K. M., & Ingram, L. O. (1986). Magnesium limitation and its role in apparent toxicity of ethanol during yeast fermentation. *Applied and Environmental Microbiology*, *52*(5), 975–981. https://doi.org/10.1128/aem.52.5.975-981.1986

Edwards, V. H. (1970). The influence of high substrate concentrations on microbial kinetics. *Biotechnology and Bioengineering*, *12*(5), 679–712. https://doi.org/10.1002/bit.260120504

Esener, A. A., Roels, J. A., & Kossen, N. W. F. (1983). Theory and applications of unstructured growth models: Kinetic and energetic aspects. *Biotechnology and Bioengineering*, *25*(12), 2803–2841. https://doi.org/10.1002/bit.260251202

Eslamloueyan, R., & Setoodeh, P. (2011). OPTIMIZATION OF FED-BATCH RECOMBINANT YEAST FERMENTATION FOR ETHANOL PRODUCTION USING A REDUCED DYNAMIC FLUX BALANCE MODEL BASED ON ARTIFICIAL NEURAL NETWORKS. *Chemical Engineering Communications*, *198*, 1309–1338.

Feng, Y., Tian, X., Chen, Y., Wang, Z., Xia, J., Qian, J., Zhuang, Y., & Chu, J. (2021). Real - time and on - line monitoring of ethanol fermentation process by viable cell sensor and electronic nose. *Bioresources and Bioprocessing*. https://doi.org/10.1186/s40643-021-00391-5

Ghose, T. K., & Tyagi, R. D. (1979). Rapid ethanol fermentation of cellulose hydrolysate. II. Product and substrate inhibition and optimization of fermentor design. *Biotechnology and Bioengineering*, *21*(8), 1401–1420. https://doi.org/10.1002/bit.260210808

Gomes, D., Cruz, M., de Resende, M., Ribeiro, E., Teixeira, J., & Domingues, L. (2021). Very high gravity bioethanol revisited: Main challenges and advances. *Fermentation*, *7*(1). https://doi.org/10.3390/fermentation7010038

Hajar, S., Azhar, M., Abdulla, R., Jambo, S. A., Marbawi, H., Azlan, J., Azifa, A., Faik, M., & Francis, K. (2017). *Yeasts in sustainable bioethanol production : A review*. *10*(February), 52–61. https://doi.org/10.1016/j.bbrep.2017.03.003

Higginson, A., & Brooks, K. (2022). A bioreactor system remote laboratory for teaching process control. *IFAC-PapersOnLine*, *55*(17), 350–355. https://doi.org/10.1016/j.ifacol.2022.09.304

Hoang, T. D., & Nghiem, N. (2021). Recent developments and current status of commercial production of fuel ethanol. In *Fermentation* (Vol. 7, Issue 4). MDPI. https://doi.org/10.3390/fermentation7040314

Hong, J. (1986). *Optimal Substrate Feeding Policy for a and Product Inhibition Kinetics*. *1431*, 1421–1431.

Joannis-Cassan, C., Riess, J., Jolibert, F., & Taillandier, P. (2014). Optimization of very high gravity fermentation process for ethanol production from industrial sugar beet syrup. *Biomass and Bioenergy*, *70*, 165–173. https://doi.org/10.1016/j.biombioe.2014.07.027ï

Jones, R. P., & Greenfield, P. F. (1982). Effect of carbon dioxide on yeast growth and fermentation. *Enzyme and Microbial Technology*, *4*(4), 210–223. https://doi.org/10.1016/0141-0229(82)90034-5

Kadlec, P., Gabrys, B., & Strandt, S. (2009). Data-driven Soft Sensors in the process industry. *Computers & Chemical Engineering*, *33*(4), 795–814. https://doi.org/10.1016/j.compchemeng.2008.12.012

Karakuzu, C., Türker, M., & Öztürk, S. (2006). Modelling, on-line state estimation and fuzzy control of production scale fed-batch baker's yeast fermentation. *Control Engineering Practice*, *14*(8), 959–974. https://doi.org/10.1016/j.conengprac.2005.05.007

Kazemzadeh, N., Ryan, S. M., & Hamzeei, M. (2019). Robust optimization vs . stochastic programming incorporating risk measures for unit commitment with uncertain variable renewable generation. *Energy Systems*, *10*(3), 517–541. https://doi.org/10.1007/s12667-017-0265-5

Kohler, M. (2016). An Economic Assessment of Bioethanol Production from Sugar Cane: The Case of South Africa. *Economic Research Southern Africa*, *August*, 14.

Kvaalen, E., Wankat, P., & Mckenzie, B. (1984). *Alcohol Distillation: Basic Principles, Equipment, Performance Relationships, and Safety*. Http:// Www.Ces.Purdue.Edu/Extmedia/Ae/Ae-117.Html.

Lappas, N., & Gounaris, C. (2016). Multi-stage Adjustable Robust Optimization for Process Scheduling under Uncertainty. *AIChE Journal*, *62*, n/a-n/a. https://doi.org/10.1002/aic.15183

Lappas, N. H., & Gounaris, C. E. (2018). Robust optimization for decision-making under endogenous uncertainty. *Computers and Chemical Engineering*, *111*, 252–266. https://doi.org/10.1016/j.compchemeng.2018.01.006

Ławryńczuk, M. (2008). Modelling and nonlinear predictive control of a yeast fermentation biochemical reactor using neural networks. *Chemical Engineering Journal*, *145*(2), 290–307. https://doi.org/10.1016/j.cej.2008.08.005

Levenspiel, O. (1980). The monod equation: A revisit and a generalization to product inhibition situations. *Biotechnology and Bioengineering*, *22*(8), 1671–1687. https://doi.org/10.1002/bit.260220810

Li, J., Zhao, R., Xu, Y., Wu, X., Bean, S. R., & Wang, D. (2022). Fuel ethanol production from starchy grain and other crops: An overview on feedstocks, affecting factors, and technical advances. In *Renewable Energy* (Vol. 188, pp. 223–239). Elsevier Ltd. https://doi.org/10.1016/j.renene.2022.02.038

Li, Z., & Dewan, A. (2012). Optimization of Bioethanol Ethanol Production in Fed-batch Fermentation. In *IFAC Proceedings Volumes* (Vol. 45, Issue 15). IFAC. https://doi.org/10.3182/20120710-4-SG-2026.00092

Liang, E., & Yuan, Z. (2022). Robust dynamic optimization for nonlinear chemical processes under measurable and unmeasurable uncertainties. *AIChE Journal*, *68*(8). https://doi.org/10.1002/aic.17733

Lisci, S., Grosso, M., & Tronci, S. (2021). Different control strategies for a yeast fermentation bioreactor. *IFAC-PapersOnLine*, *54*(3), 306–311. https://doi.org/10.1016/j.ifacol.2021.08.259

Lopes, M. L., Paulillo, S. C. de L., Godoy, A., Cherubin, R. A., Lorenzi, M. S., Giometti, F. H. C., Bernardino, C. D., de Amorim Neto, H. B., & de Amorim, H. V. (2016). Ethanol production in Brazil: a bridge between science and industry. In *Brazilian Journal of Microbiology* (Vol. 47, pp. 64–76). Elsevier Editora Ltda. https://doi.org/10.1016/j.bjm.2016.10.003

Lucio, M., & Fermentec, L. (2008). Continuous and batch fermentation processes: Advantages and disadvantages of these processes in the Brazilian ethanol production Fermentative Performance of Saccharomyces sp. Yeasts for Lager Beer Production View project ALTFERM Project: fermentation with high concentration of ethanol for reduction of vinasses volume View project

Alexandre Godoy Fermentec. In *Article in International Sugar Journal*. https://www.researchgate.net/publication/289874380

Luong, J. H. T. (1985). Ethanol Inhibition in Alcohol Ferment. *Biotechnology and Bioengineering*, *XXVII*, 280–285.

Maggioni, F., & Potra, F. A. (2014). *Stochastic versus Robust Optimization for a Transportation Problem*. 1–35.

McGovern, P. E., Underhill, A. P., Fang, H., Luan, F., Hall, G. R., Yu, H., Wang, C., Cai, F., Zhao, Z., & Feinman, G. M. (2005). Chemical Identification and Cultural Implications of a Mixed Fermented Beverage from Late Prehistoric China. *Asian Perspectives*, *44*(2), 249–275. https://doi.org/10.1353/asi.2005.0026

Memon, S. F., Wang, R., Strunz, B., Chowdhry, B. S., Pembroke, J. T., & Lewis, E. (2022). *A Review of Optical Fibre Ethanol Sensors : Current State and Future Prospects*.

MochidzukiI, K., Kobayashi, S., Wang, H., Hatanaka, R., & Hiride, H. (2015). Effect of Rice Bran as a Nitrogen and Carbohydrate Source on Fed-Batch Simultaneous Saccharification and Fermentation for the Production of Bioethanol from Rice Straw. *Journal of the Japan Institute of Energy*, *94*(1), 151–158. https://doi.org/10.3775/jie.94.151

Modak, J., & Lim, H. (1992). Optimal mode of operation of bioreactor for fermentation processes. *Chemical Engineering Science*, *47*(15), 3869–3884. http://www.sciencedirect.com/science/article/pii/000925099285136Y

Molenaar, G., & Preeker, S. (2022). *python-snap7 Documentation*.

Monod, J. (1949). The Growth of Bacterial Cultures. *Annual Reviews in Microbiology*, *3*(Xl), 371–394.

Morschbacker, A. (2009). Bio-ethanol based ethylene. *Polymer Reviews*, *49*(2), 79–84. https://doi.org/10.1080/15583720902834791

Mowbray, M., Savage, T., Wu, C., Song, Z., Anye, B., Rio-chanona, E. A. Del, & Zhang, D. (2021a). Machine learning for biochemical engineering : A review. *Biochemical Engineering Journal*, *172*(May), 108054. https://doi.org/10.1016/j.bej.2021.108054

Mowbray, M., Savage, T., Wu, C., Song, Z., Anye, B., Rio-chanona, E. A. Del, & Zhang, D. (2021b). Machine learning for biochemical engineering : A review. *Biochemical Engineering Journal*, *172*(May), 108054. https://doi.org/10.1016/j.bej.2021.108054

Mulchandani, A., & Luong, J. H. T. (1989). Microbial inhibition kinetics revisited. *Enzyme and Microbial Technology*, *11*(2), 66–73. https://doi.org/10.1016/0141-0229(89)90062-8

Na, J. G., Chang, Y. K., Chung, B. H., & Lim, H. C. (2002). Adaptive optimization of fed-batch culture of yeast by using genetic algorithms. *Bioprocess and Biosystems Engineering*, *24*(5), 299–308. https://doi.org/10.1007/s004490100251

Nagy, Z. K. (2007). Model based control of a yeast fermentation bioreactor using optimally designed artificial neural networks. *Chemical Engineering Journal*, *127*(1–3), 95–109. https://doi.org/10.1016/j.cej.2006.10.015

Nolasco, E., Vassiliadis, V. S., Kähm, W., Adloor, S. D., Ismaili, R. Al, Conejeros, R., Espaas, T., Gangadharan, N., Mappas, V., Scott, F., & Zhang, Q. (2021). Optimal control in chemical engineering: Past, present and future. *Computers and Chemical Engineering*, *155*, 107528. https://doi.org/10.1016/j.compchemeng.2021.107528

Oliveira, S. C., Stremel, D. P., Dechhechi, E. C. m, & Pereira, F. (2017). Kinetic Modelling of 1-G ethanol Fermentations. In A. F. Jozala (Ed.), *Fermentation Processes*. IntechOpen. https://www.intechopen.com/chapters/52695

Pajcin, I., Grahovac, J., Dodic, J., Jokic, A., Dodic, S., Vucurovic, D., & Milovic, N. (2017). Application of artificial neural networks in modeling and optimization of biofuels production. *Journal on Processing and Energy in Agriculture*, *21*(2), 66–70. https://doi.org/10.5937/jpea1702066p

Palmonari, A., Cavallini, D., Sniffen, C. J., Fernandes, L., Holder, P., Fagioli, L., Fusaro, I., Biagi, G., Formigoni, A., & Mammi, L. (2020). Short communication: Characterization of molasses chemical composition. *Journal of Dairy Science*, *103*(7), 6244–6249. https://doi.org/10.3168/jds.2019-17644

Parapouli, M., Vasileiadis, A., Afendra, A. S., & Hatziloukas, E. (2020). Saccharomyces cerevisiae and its industrial applications. In *AIMS Microbiology* (Vol. 6, Issue 1). https://doi.org/10.3934/microbiol.2020001

Perez-Carrillo, E., Serna-Saldivar, S. O., Chuck-Hernandez, C., & Cortes-Callejas, M. L. (2012). Addition of protease during starch liquefaction affects free amino nitrogen, fusel alcohols and ethanol production of fermented maize and whole and decorticated sorghum mashes. *Biochemical Engineering Journal*, *67*, 1–9. https://doi.org/10.1016/j.bej.2012.04.010

Peters, M., Researcher, P., Savolainen, J., Professor, T., & Luukka, P. (2023). *EXPLORING THE MARKET POTENTIAL FOR SUSTAINABLE STEAM TO ELECTRICITY GENERATION WITHIN THE UNITED STATES LUT School of Business and Management Master's Program in Business Analytics*.

Petersen, L. N., & Jorgensen, J. B. (2014). Real-time economic optimization for a fermentation process using Model Predictive Control. *2014 European Control Conference, ECC 2014*, 1831–1836. https://doi.org/10.1109/ECC.2014.6862270

Petrova, M., Koprinkova, P., Patarinska, T., & Bliznakova, M. (1998). *Specific growth rate model*. *18*.

Polakovi, M., & Manflenius, C. F. (1994). *Evaluation of sensors for the control of a continuous ethanol fermentation*.

Pramanik, K. (2004). Use of artificial neural networks for prediction of cell mass and ethanol concentration in batch fermentation using Saccharomyces cerevisiae yeast. *Journal of the Institution of Engineers (India): Chemical Engineering Division*, *85*(1 SEP.), 31–35.

Puligundla, P., Smogrovicova, D., Sarathi, V., Obulam, R., & Ko, S. (2011). *Very high gravity (VHG) ethanolic brewing and fermentation : a research update*. 1133–1144. https://doi.org/10.1007/s10295-011-0999-3

Rani, K., & Rao, V. (1999). Control of fermenters–a review. *Bioprocess Engineering*, *21*(1), 77.

http://link.springer.de/link/service/journals/00449/bibs/9021001/90210077.htm

Rass-Hansen, J., Falsig, H., Jørgensen, B., & Christensen, C. H. (2007). Bioethanol: Fuel or feedstock? *Journal of Chemical Technology and Biotechnology*, *82*(4), 329–333. https://doi.org/10.1002/jctb.1665

Renewable Fuels Association. (n.d.). *Annual Ethanol Production U.S. and World Ethanol Production*. Retrieved June 19, 2023, from https://ethanolrfa.org/markets-and-statistics/annual-ethanol-production

Roels, J. A. (1981). the Application of Macroscopic Principles To Microbial Metabolism. *Annals of the New York Academy of Sciences*, *369*(1), 113–134. https://doi.org/10.1111/j.1749-6632.1981.tb14182.x

Ryde, T. E., Wahlgreen, M. R., Nielsen, M. K., Hørsholt, S., Jørgensen, S. B., & Jørgensen, J. B. (2021). Optimal feed trajectories for fedbatch fermentation with substrate inhibition kinetics. *IFAC-PapersOnLine*, *54*(3), 318–323. https://doi.org/10.1016/j.ifacol.2021.08.261

Scheiblauer, J., Scheiner, S., Joksch, M., & Kavsek, B. (2018). Fermentation of Saccharomyces cerevisiae – Combining kinetic modeling and optimization techniques points out avenues to effective process design. *Journal of Theoretical Biology*, *453*, 125–135. https://doi.org/10.1016/j.jtbi.2018.05.016

Schuler, M., & Kargi, F. (2002). *Bioprocess Engineering* (2nd ed.). Prentice Hall PTR.

Sewsynker-Sukai, Y., Faloye, F., & Kana, E. B. G. (2017). Artificial neural networks: an efficient tool for modelling and optimization of biofuel production (a mini review). In *Biotechnology and Biotechnological Equipment* (Vol. 31, Issue 2, pp. 221–235). Taylor and Francis Ltd. https://doi.org/10.1080/13102818.2016.1269616

Shugerl, K., & Bellgardt, K.-H. (2000). *Bioreaction Engineering* (1st ed.). Springer Verlag.

Siebert, K. J. (1980). The Science of Beer Routine Use of a Programmable Calculator for Computing Alcohol , Real Extract , Original Gravity , and Calories in Beer.

Journal of the American Society of Brewing Chemists, *38*(1), 27–33. https://doi.org/10.1094/ASBCJ-38-0027

Sonnleitner, B., & Käppeli, O. (1986). Growth of Saccharomyces cerevisiae is controlled by its limited respiratory capacity : Formulation and verification of a hypothesis. *Biotechnology and Bioengineering*, *28*, 927–037.

Starzak, M., Krzystek, L., Nowicki, L., & Michalski, H. (1994). Macroapproach kinetics of ethanol fermentation by Saccharomyces cerevisiae: experimental studies and mathematical modelling. *The Chemical Engineering Journal and The Biochemical Engineering Journal*, *54*(3), 221–240. https://doi.org/10.1016/0923-0467(94)00210-X

Tesfaw, A., & Assefa, F. (2014). Current Trends in Bioethanol Production by Saccharomyces cerevisiae : Substrate, Inhibitor Reduction, Growth Variables, Coculture, and Immobilization . *International Scholarly Research Notices*, *2014*, 1–11. https://doi.org/10.1155/2014/532852

Thibault, J., LeDuy, A., & Côté, F. (1987). Production of ethanol by Saccharomyces cerevisiae under high-pressure conditions. *Biotechnology and Bioengineering*, *30*(1), 74–80. https://doi.org/10.1002/bit.260300111

Tian, Y., Zhang, J., & Morris, J. (2002). Optimal control of a fed-batch bioreactor based upon an augmented recurrent neural network model. *Neurocomputing*, *48*(1–4), 919–936. https://doi.org/10.1016/S0925-2312(01)00680-4

Tse, T. J., & Wiens, D. J. (2021). *Production of Bioethanol — A Review of Factors Affecting Ethanol Yield*. 1–18.

Violino, S., Figorilli, S., Costa, C., & Pallottino, F. (2020). Internet of beer: A review on smart technologies from mash to pint. *Foods*, *9*(7). https://doi.org/10.3390/foods9070950

Wang, L., Li, Q., Sun, M., & Wang, G. (2016). Robust optimisation scheduling of CCHP systems with multi-energy based on minimax regret criterion. *Generation Transmission and Ditribution*, *10*(9), 2194–2201. https://doi.org/10.1049/iet-gtd.2015.1344

Xiong, Z., & Zhang, J. (2005). Neural network model-based on-line re-optimisation control of fed-batch processes using a modified iterative dynamic programming algorithm. *Chemical Engineering and Processing: Process Intensification*, *44*(4), 477–484. https://doi.org/10.1016/j.cep.2004.07.001

Xu, X., Lin, Z., Li, X., Shang, C., & Shen, Q. (2021). Multi-objective robust optimisation model for MDVRPLS in refined oil distribution ABSTRACT. *International Journal of Production Research*, *0*(0), 1–21. https://doi.org/10.1080/00207543.2021.1887534

Yuan, Y., Miao, Z., & Li, S. (1999). FED-BATCH FERMENTATION CONTROLLER IN YEAST FED-BATCH. *Chemical Engineering Communications*, *134*(1), 37–41.

Zabed, H., Faruq, G., Sahu, J. N., Azirun, M. S., Hashim, R., & Nasrulhaq Boyce, A. (2014). Bioethanol production from fermentable sugar juice. In *The Scientific World Journal* (Vol. 2014). ScientificWorld Ltd. https://doi.org/10.1155/2014/957102

Zhang, H. L., Baeyens, J., & Tan, T. W. (2012). Mixing phenomena in a large-scale fermenter of starch to bio-ethanol. *Energy*, *48*(1), 380–391. https://doi.org/10.1016/j.energy.2012.05.015

Zhang, J., Reddy, J., Buckland, B., & Greasham, R. (2003). Toward consistent and productive complex media for industrial fermentations: Studies on yeast extract for a recombinant yeast fermentation process. *Biotechnology and Bioengineering*, *82*(6), 640–652. https://doi.org/10.1002/bit.10608

Zhu, X., Rehman, K. U., Wang, B., & Shahzad, M. (2020). Modern soft-sensing modeling methods for fermentation processes. In *Sensors (Switzerland)* (Vol. 20, Issue 6). MDPI AG. https://doi.org/10.3390/s20061771

Zihin, M., Kanesan, J., Kendall, G., & Huang, J. (2018). *Optimization of fed-batch fermentation processes using the Backtracking Search Algorithm Biomass Substrate feed rate model*. *91*, 286–288.

Zwietering, M. H., Koos, J. T. D. E., Hasenack, B. E., Wit, J. C. D. E., & Riet, K. V. A. N. T. (1991). Modeling of Bacterial Growth Function of Temperature. *Applied*

and Environmental Microbiology, *57*(4), 1094–1101. http://www.ncbi.nlm.nih.gov/pmc/articles/PMC182851/

Appendix A-Experimental Data

A. 1 Results

A.1.1 Experiment 1

The results of Experiment 1 are shown in Table A1. The SG measurements show that the data obtained does not contain significant noise. However, during the fermentation's first two hours, the reading was not reliable when the fermentation was most vigorous. The noise in the initial stage of the fermentation was a feature that was repeated over all the experiments due to the vigorous fermentation that occurred in the first hours of the fermentation. There was a measurement gap between 30 and 40 hours caused by a failure in the data collection system. The disturbance in the data before 50 hours was due to the iSpindle measurement device being removed from the fermenter for testing after the signal was lost. The temperature was maintained near the setpoint of 35°C until after 70 hours when the fermentation had stopped, and the SG values did not change further.

Table A1: Data for Experiment 1

Time h	Vol added /h	SG	Ferm Temp C	total sugar consumed
0	0.00	1.04	38.39	-0.83
1	0.00	1.04	38.78	0.15
2	0.00	1.03	37.98	0.62
3	0.00	1.03	37.46	0.94
4	0.00	1.02	37.18	1.30
5	0.00	1.03	36.97	1.47
6	0.00	1.02	36.76	1.75
7	0.00	1.02	36.60	2.07
8	0.00	1.02	36.33	2.36
9	0.00	1.02	36.11	2.51
10	0.00	1.01	35.91	2.69
11	0.00	1.01	35.72	2.89
12	0.00	1.01	35.52	3.11
13	0.00	1	35.34	3.38
14	0.00	1	35.21	3.51
15	0.71	1.01	34.70	3.67
16	0.72	1.01	34.57	3.89
17	0.72	1.01	34.72	4.05
18	0.72	1.01	34.89	4.36
19	0.72	1.01	35.06	4.59
20	0.72	1.01	34.80	4.81
21	0.72	1.02	34.93	4.94
22	0.72	1.02	35.01	5.19
23	0.72	1.02	34.86	5.28
24	0.72	1.02	35.03	5.44
25	0.72	1.02	34.89	5.65
26	0.72	1.02	35.00	5.75
27	0.72	1.02	34.90	5.92
28	0.72	1.03	34.93	6.06
29	0.72	1.03	35.00	6.10
30	0.72	1.03	35.00	6.29
31	0.72	1.03	34.93	6.43
32	0.72	1.03	34.93	6.53
33	0.72	1.03	35.01	6.66
34	0.72	1.04	34.85	6.78
35	0.72	1.04	34.71	6.78
36	-0.22	1.04	34.58	6.59
37	0.00	1.04	34.85	6.47
38	0.00	1.04	35.01	6.63
39	0.00	1.04	34.83	6.72
40	0.00	1.04	35.06	6.84

41	0.00	1.04	34.86	6.95
42	0.00	1.04	35.03	7.03
43	0.00	1.04	34.82	7.12
44	0.00	1.03	35.08	7.21
45	0.00	1.03	34.90	7.27
46	0.00	1.03	35.02	7.39
47	0.00	1.03	34.90	7.50
48	0.00	1.03	34.98	7.61
49	0.00	1.04	34.86	7.47
50	0.00	1.03	35.02	7.73
51	0.00	1.03	34.90	7.80
52	0.00	1.03	35.02	7.85
53	0.00	1.03	34.90	7.92
54	0.00	1.03	35.04	7.97
55	0.00	1.03	34.90	8.03
56	0.00	1.03	35.01	8.08
57	0.00	1.03	34.91	8.14
58	0.00	1.03	34.93	8.17
59	0.00	1.03	34.84	8.18
60	0.00	1.03	34.76	8.25
61	0.00	1.03	34.89	8.30
62	0.00	1.03	35.05	8.33
63	0.00	1.03	34.90	8.36
64	0.00	1.03	35.04	8.40
65	0.00	1.03	34.91	8.43
66	0.00	1.03	34.89	8.43
67	0.00	1.03	35.06	8.47
68	0.00	1.02	34.83	8.48
69	0.00	1.02	34.90	8.51
70	0.00	1.02	34.90	8.53
71	0.00	1.02	34.68	8.54
72	0.00	1.02	34.55	8.53
73	0.00	1.02	34.42	8.53
74	0.00	1.02	34.32	8.54

A.1.2 Experiment 2

The results of Experiment 2 are shown in Table A.2. Experiment 2 used the same initial conditions as Experiment 1; however, the feed rate was reduced to determine the effect of reducing the sugar concentration on the fermentation rate. The SG measurement follows a similar trend to that seen for Experiment 1, and the temperature was controlled to the setpoint until the fermentation stopped at approximately 70 hours. Once the fermentation had stopped, an additional 50 g of yeast extract, as well as 50 g of additional dried yeast, was added to the fermenter in an attempt to increase the amount of sugar consumed; however, the SG did not change further, and no further fermentation occurred after that point.

Table A2: Data for Experiment 2

Time h	Vol added /h	SG	Ferm Temp C	total sugar consumed kg
0	0.00	1.044735	39.02	-0.72
1	0.00	1.037605	38.89	0.20
2	0.00	1.034804	37.69	0.63
3	0.00	1.032498	36.85	0.88
4	0.00	1.028518	36.27	1.23
5	0.00	1.024077	35.90	1.64
6	0.00	1.023227	35.59	1.82
7	0.00	1.01659	35.32	2.14
8	0.00	1.016399	35.06	2.36
9	0.00	1.016501	34.82	2.54
10	0.00	1.012899	35.04	2.77
11	0.00	1.010697	34.99	3.08
12	0.00	1.006616	34.85	3.17
13	0.00	1.006652	35.01	3.31
14	0.00	1.00341	34.98	3.59
15	0.13	1.001504	34.85	3.80
16	0.43	1.004044	35.07	3.97
17	0.43	1.004493	35.00	4.14
18	0.43	1.003398	34.88	4.44
19	0.43	1.00439	35.09	4.64
20	0.43	1.005361	35.07	4.77
21	0.43	1.006508	34.88	4.83
22	0.43	1.007143	34.81	4.93
23	0.43	1.010377	35.07	5.05
24	0.20	1.011993	34.74	4.96
25	0.37	1.011777	34.51	5.38

26	0.43	1.01136	34.71	5.58
27	0.43	1.014184	34.94	5.66
28	0.43	1.015252	34.89	5.75
29	0.43	1.016211	34.86	5.90
30	0.43	1.017725	35.05	5.95
31	0.43	1.018715	34.88	6.02
32	0.43	1.021026	35.02	6.16
33	0.43	1.021862	34.86	6.30
34	0.43	1.022864	34.91	6.39
35	0.43	1.024514	35.00	6.50
36	0.43	1.026238	34.93	6.58
37	0.43	1.026604	34.94	6.71
38	0.43	1.027846	34.70	6.81
39	0.43	1.02931	34.73	6.87
40	0.43	1.030977	34.97	6.95
41	0.43	1.031624	34.86	7.08
42	0.43	1.032843	34.94	7.17
43	0.43	1.034993	34.99	7.22
44	0.13	1.03394	35.04	7.35
45	0.00	1.033159	34.87	7.44
46	0.00	1.032768	35.05	7.50
47	0.00	1.032172	34.85	7.56
48	0.00	1.031867	34.93	7.61
49	0.00	1.030901	34.94	7.72
50	0.00	1.030638	34.86	7.76
51	0.00	1.029955	35.01	7.85
52	0.00	1.029523	34.98	7.94
53	0.00	1.02898	34.94	7.94
54	0.00	1.02861	34.98	8.04
55	0.00	1.027912	34.93	8.08
56	0.00	1.027826	34.87	8.14
57	0.00	1.027285	34.89	8.19
58	0.00	1.026762	34.96	8.24
59	0.00	1.026425	34.99	8.28
60	0.00	1.02625	35.02	8.32
61	0.00	1.026046	34.93	8.35
62	0.00	1.025665	34.90	8.38
63	0.00	1.025736	34.83	8.38
64	0.00	1.025696	34.75	8.39
65	0.00	1.025147	34.75	8.45
66	0.00	1.025023	34.76	8.48
67	0.00	1.025023	34.83	8.48
68	0.00	1.024774	34.88	8.51
69	0.00	1.024523	34.74	8.54
70	0.00	1.024537	34.51	8.54

71	0.00	1.024549	34.30	8.55
72	0.00	1.024549	34.14	8.54
73	0.00	1.024672	33.84	8.54
74	0.00	1.024465	33.84	8.55
75	0.00	1.024111	33.76	8.60
76	0.00	1.024175	33.58	8.59
77	0.00	1.024174	33.41	8.61
78	0.00	1.024058	33.16	8.61
79	0.00	1.023982	33.04	8.62
80	0.00	1.023943	32.80	8.62
81	0.00	1.024145	32.56	8.60
82	0.00	1.023998	32.37	8.61
83	0.00	1.024126	32.22	8.61
84	0.00	1.024142	32.03	8.61
85	0.00	1.023995	31.99	8.61
86	0.00	1.024139	31.88	8.61
87	0.00	1.024118	31.89	8.59
88	0.00	1.02412	31.89	8.60
89	0.00	1.024064	31.89	8.61
90	0.00	1.024124	31.88	8.60
91	0.00	1.024027	31.90	8.60
92	0.00	1.024146	31.70	8.59
93	0.00	1.024138	31.40	8.59
94	0.00	1.024257	31.06	8.59

A.1.3 Experiment 3

The results from Experiment 3 are shown in Table A3. Experiment 3 used similar conditions to the previous experiments; however, the feed rate was reduced further to reduce the sugar concentration during the fermentation. The SG reached lower values than in Experiment 1 or Experiment 2. The SG showed quite a different profile to that shown in the previous experiments, where the start of the feed can be seen, and the rate of increase seemed approximately constant for the duration of the feeding. In this case, the SG remained constant until approximately 30 hours, when the fermentation slowed. The slowed fermentation rate can be seen in the temperature of the fermenter, where the setpoint could not be maintained after this occurred. The temperature control system required adequate mixing in the fermenter, which would not be the case if the fermentation rate was not fast enough to produce the bubbles necessary for mixing. While the SG increased after the 30-hour mark, the fermentation rate did not increase to the point where the temperature control system could maintain the setpoint temperature.

Table A3: Data for Experiment 3

Time h	Vol added /h	SG	Ferm Temp C	total sugar consumed
0	0.00	1.043189	35.03	-0.04
1	0.00	1.043183	35.55	0.03
2	0.00	1.037361	34.84	0.46
3	0.00	1.0376	34.66	0.53
4	0.00	1.031631	35.06	0.96
5	0.00	1.029609	34.94	1.19
6	0.00	1.02539	34.83	1.47
7	0.00	1.023295	35.18	1.79
8	0.00	1.018781	34.76	2.08
9	0.00	1.019086	34.76	2.17
10	0.00	1.014367	35.01	2.47
11	0.00	1.015442	34.85	2.48
12	0.00	1.009574	34.71	2.81
13	0.00	1.007998	34.85	3.07
14	0.00	1.01	35.00	3.10
15	0.00	1.005876	35.01	3.34

16	0.00	1.004928	34.76	3.44
17	0.03	1.003623	34.83	3.55
18	0.21	1.003424	34.98	3.69
19	0.21	1.001785	35.01	3.94
20	0.21	1.001208	34.74	4.07
21	0.21	1.001521	34.86	4.18
22	0.21	1.000278	35.00	4.34
23	0.21	1.00135	35.01	4.46
24	0.21	1.001128	34.99	4.61
25	0.21	1.000758	34.92	4.71
26	0.21	1.000849	34.87	4.81
27	0.21	1.000762	34.88	4.95
28	0.21	1.00097	34.86	5.05
29	0.21	1.001006	34.76	5.13
30	0.21	1.00136	34.63	5.22
31	0.21	1.001367	34.50	5.30
32	0.21	1.001636	34.34	5.41
33	0.21	1.002033	34.19	5.49
34	0.21	1.00205	34.13	5.58
35	0.21	1.002381	34.03	5.68
36	0.21	1.002518	33.93	5.72
37	0.21	1.003462	33.78	5.79
38	0.21	1.003955	33.70	5.84
39	0.21	1.003955	33.64	5.94
40	0.21	1.003955	33.62	6.08
41	0.21	1.003567	33.61	6.19
42	0.21	1.003969	33.62	6.22
43	0.21	1.004885	33.63	6.26
44	0.21	1.005705	33.43	6.31
45	0.21	1.006588	33.27	6.29
46	0.21	1.007295	32.98	6.37
47	0.21	1.007748	32.80	6.39
48	0.21	1.00791	32.63	6.48
49	0.21	1.008994	32.44	6.51
50	0.21	1.009289	32.28	6.54
51	0.21	1.009946	32.14	6.60
52	0.21	1.010432	31.98	6.64
53	0.21	1.010914	31.86	6.68
54	0.21	1.011458	31.71	6.75
55	0.21	1.011862	31.50	6.79
56	0.21	1.012471	31.42	6.82
57	0.21	1.012798	31.29	6.90
58	0.21	1.012798	31.20	7.00
59	0.21	1.012798	31.20	7.04
60	0.21	1.01517	31.11	6.95

61	0.21	1.015809	30.99	7.01
62	0.21	1.015809	31.03	7.02
63	0.21	1.016567	31.00	7.06
64	0.21	1.017136	31.12	7.12
65	0.21	1.017789	31.28	7.17
66	0.21	1.019039	31.42	7.18
67	0.21	1.01962	31.55	7.17
68	0.21	1.019509	31.67	7.23
69	0.21	1.020458	31.81	7.23
70	0.21	1.02125	31.86	7.26
71	0.21	1.021816	31.91	7.30
72	0.21	1.02245	31.99	7.28
73	0.21	1.023284	31.97	7.30
74	0.21	1.023883	31.99	7.33
75	0.21	1.024485	32.04	7.34
76	0.21	1.025144	31.98	7.37
77	0.21	1.025601	31.92	7.40
78	0.21	1.026474	31.84	7.42
79	0.21	1.026941	31.70	7.45
80	0.21	1.027359	31.63	7.49
81	0.21	1.02802	31.51	7.50
82	0.21	1.028647	31.40	7.53
83	0.21	1.02922	31.36	7.54
84	0.21	1.029985	31.22	7.57
85	0.21	1.030322	31.18	7.59
86	0.17	1.030818	31.19	7.60
87	0.00	1.031631	31.18	7.50
88	0.00	1.032058	31.43	7.46
89	0.00	1.031626	31.58	7.49
90	0.00	1.031692	31.84	7.51
91	0.00	1.031351	32.01	7.54
92	0.00	1.031259	32.17	7.57
93	0.00	1.031106	32.38	7.60
94	0.00	1.030696	32.44	7.62
95	0.00	1.030654	32.58	7.65
96	0.00	1.030484	32.58	7.66
97	0.00	1.030407	32.59	7.68
98	0.00	1.030048	32.58	7.72
99	0.00	1.029932	32.57	7.71
100	0.00	1.029761	32.56	7.75
101	0.00	1.029791	32.54	7.76
102	0.00	1.029488	32.41	7.77
103	0.00	1.029428	32.35	7.79
104	0.00	1.029377	32.23	7.81
105	0.00	1.029066	32.14	7.83

106	0.00	1.029189	32.05	7.83
107	0.00	1.02904	31.96	7.84
108	0.00	1.028971	31.88	7.84
109	0.00	1.02887	31.84	7.86
110	0.00	1.028746	31.77	7.87
111	0.00	1.028722	31.82	7.88
112	0.00	1.028811	31.91	7.89
113	0.00	1.028482	32.00	7.91
114	0.00	1.028247	32.20	7.94
115	0.00	1.028165	32.30	7.95
116	0.00	1.027964	32.44	7.97
117	0.00	1.02787	32.58	7.99
118	0.00	1.027905	32.61	8.00
119	0.00	1.027601	32.73	8.02
120	0.00	1.027615	32.77	8.02
121	0.00	1.027469	32.74	8.05
122	0.00	1.027617	32.76	8.04
123	0.00	1.027289	32.72	8.06
124	0.00	1.027191	32.70	8.06
125	0.00	1.027652	32.67	8.04
126	0.00	1.027176	32.58	8.07
127	0.00	1.02712	32.52	8.08
128	0.00	1.027051	32.44	8.09
129	0.00	1.026948	32.39	8.11
130	0.00	1.026948	32.27	8.11
131	0.00	1.026809	32.24	8.11
132	0.00	1.027033	32.20	8.10
133	0.00	1.027033	32.12	8.09
134	0.00	1.027033	32.17	8.09

A.1.4 Experiment 4

The results of Experiment 4 are shown in Table A4. The conditions for the experiment were similar to the previous three experiments; however, the feed was started earlier and increased slightly to prevent the low sugar concentrations seen in Experiment 3, but to reduce the feed rate in comparison to Experiment 2. The SG followed a similar profile to Experiments 1 & 2. In this case, the temperature controller maintained the setpoint until approximately 55 hours, when the SG ceased to change.

Table A4: Data for Experiment 4

Time h	Vol added /h	SG	Ferm Temp C	total sugar consumed
0	0.00	1.046577	41.52	-0.65
1	0.00	1.048396	40.99	-0.43
2	0.00	1.04129	39.45	0.22
3	0.00	1.035897	38.08	0.45
4	0.25	1.034726	36.92	0.86
5	0.29	1.031567	35.99	1.15
6	0.29	1.030415	35.20	1.50
7	0.29	1.027776	34.60	1.77
8	0.29	1.027305	34.71	2.22
9	0.29	1.025128	35.11	2.45
10	0.29	1.022426	34.48	2.73
11	0.29	1.020206	34.34	2.99
12	0.29	1.020351	34.58	3.23
13	0.29	1.020256	34.89	3.44
14	0.29	1.01863	35.07	3.64
15	0.29	1.018265	34.68	3.81
16	0.29	1.017271	34.66	3.94
17	0.29	1.017784	34.73	4.26
18	0.29	1.016136	34.94	4.35
19	0.29	1.016395	35.00	4.52
20	0.29	1.01574	34.75	4.76
21	0.29	1.018654	34.90	4.82
22	0.29	1.017745	35.05	5.01
23	0.29	1.016675	34.81	5.15
24	0.29	1.0165	34.83	5.29

25	0.29	1.016021	34.92	5.46
26	0.29	1.016677	35.07	5.57
27	0.29	1.018517	34.82	5.63
28	0.29	1.015825	34.83	5.83
29	0.29	1.015603	34.86	5.98
30	0.29	1.016657	34.90	6.06
31	0.29	1.016923	34.92	6.16
32	0.29	1.018439	35.02	6.26
33	0.29	1.018333	34.94	6.36
34	0.29	1.017749	34.79	6.47
35	0.29	1.01824	34.76	6.60
36	0.29	1.018473	34.71	6.72
37	0.29	1.019109	34.69	6.81
38	0.29	1.019665	34.67	6.86
39	0.29	1.020094	34.63	7.00
40	0.29	1.019764	34.58	7.09
41	0.29	1.020227	34.63	7.19
42	0.29	1.020971	34.70	7.29
43	0.29	1.020513	34.82	7.45
44	0.29	1.020513	34.90	7.52
45	0.29	1.022273	34.99	7.53
46	0.29	1.022098	34.90	7.65
47	0.29	1.022949	34.82	7.70
48	0.29	1.023875	34.87	7.75
49	0.29	1.023959	34.97	7.80
50	0.29	1.024962	34.96	7.87
51	0.29	1.025251	34.81	7.94
52	0.29	1.025945	34.76	7.99
53	0.29	1.026109	34.76	8.10
54	0.29	1.02765	34.76	8.12
55	0.28	1.028356	34.76	8.11
56	0.00	1.028367	34.39	8.07
57	0.00	1.028409	33.96	8.08
58	0.00	1.028227	33.54	8.09
59	0.00	1.028091	33.25	8.12
60	0.00	1.027766	32.92	8.14
61	0.00	1.027877	32.66	8.18
62	0.00	1.027877	32.45	8.18
63	0.00	1.027877	32.25	8.18
64	0.00	1.027127	32.04	8.24
65	0.00	1.027078	31.73	8.24
66	0.00	1.027069	31.69	8.25
67	0.00	1.026787	31.74	8.28
68	0.00	1.026495	31.83	8.31
69	0.00	1.026456	31.91	8.32

70	0.00	1.026276	31.91	8.34
71	0.00	1.026091	31.99	8.37
72	0.00	1.02596	31.99	8.39

A.1.5 Experiment 5

The results of Experiment 5 are shown in Table A5. This experiment used an increased amount of yeast compared to the previous experiments, and it can be seen that the initial decline in the SG is faster than for the previous experiments. The Feedrate in this experiment was set to the same level as for experiment 4; however, the rubber tubing in the peristaltic pump became damaged and could no longer feed the sugar solution at a constant rate; hence the remaining feed vessel was added at approximately 27 hours. The addition of the large volume of feed resulted in a sudden drop in the temperature; however, after adding the feed, the temperature returned to the setpoint. There is a period of constant SG values measured at 40 hours due to the iSpindle being unable to connect to the MQTT server. Despite the fast initial fermentation, the last stages followed a similar profile to those found in Experiments 1, 2 and 4.

Table A5: Data for Experiment 5

Time h	Vol added /h	SG	Ferm Temp C	total sugar consumed
0	0.00	1.044221	35.19	-0.49
1	0.00	1.042747	35.66	-0.41
2	0.00	1.033019	35.64	0.72
3	0.00	1.029647	35.60	1.08
4	0.00	1.025483	35.51	1.53
5	0.00	1.020793	35.20	1.93
6	0.00	1.017983	34.65	2.26
7	0.00	1.013885	34.65	2.57
8	0.00	1.010875	35.17	2.95
9	0.14	1.008394	34.46	3.24
10	0.27	1.006967	34.23	3.46
11	0.27	1.00452	34.54	3.79
12	0.27	1.003924	34.83	4.06
13	0.27	1.002056	35.12	4.26
14	0.27	1.002436	35.11	4.52
15	0.27	0.99977	34.03	4.67
16	0.27	1.000525	33.80	4.92
17	0.27	0.998563	33.81	5.13
18	0.27	1.000528	33.91	5.21

19	0.27	0.999224	33.99	5.44
20	0.27	0.997594	34.01	5.65
21	0.27	0.996241	34.06	5.80
22	0.27	0.997222	34.12	5.95
23	0.26	0.998567	34.15	6.15
24	0.53	0.99916	34.15	6.31
25	0.53	1.000233	34.17	6.47
26	0.53	1.000745	34.30	6.66
27	9.55	1.034016	31.67	7.05
28	0.00	1.038824	33.44	6.67
29	0.00	1.039052	34.21	6.84
30	0.00	1.036134	34.70	7.05
31	0.00	1.035405	35.06	7.23
32	0.00	1.034017	34.71	7.38
33	0.00	1.033391	34.89	7.56
34	0.00	1.030863	34.93	7.71
35	0.00	1.030013	34.66	7.84
36	0.00	1.029246	34.70	7.98
37	0.00	1.028808	34.92	8.08
38	0.00	1.027404	34.89	8.21
39	0.00	1.027159	34.68	8.23
40	0.00	1.027159	34.66	8.25
41	0.00	1.027159	34.80	8.25
42	0.00	1.024499	34.95	8.58
43	0.00	1.023971	34.96	8.67
44	0.00	1.023117	34.80	8.73
45	0.00	1.022913	34.79	8.80
46	0.00	1.02235	34.87	8.87
47	0.00	1.021856	34.95	8.93
48	0.00	1.02144	34.98	8.97
49	0.00	1.020954	34.93	9.05
50	0.00	1.020482	34.90	9.08
51	0.00	1.020428	34.83	9.12
52	0.00	1.020011	34.55	9.15
53	0.00	1.020011	34.69	9.17
54	0.00	1.019391	34.85	9.21
55	0.00	1.019266	35.04	9.26
56	0.00	1.01904	34.90	9.30
57	0.00	1.018998	34.94	9.29
58	0.00	1.018576	34.99	9.34
59	0.00	1.018597	34.72	9.34
60	0.00	1.018339	34.45	9.36

A.1.6 Experiment 6

The results for Experiment 6 can be seen in Table A6. This batch also used a larger mass of yeast and a larger mass of yeast extract compared to the initial experiments. It can be seen that the initial rate of fermentation was very fast as the SG curve declined sharply. Due to the fast fermentation, the initial feed rate was not adequate to increase the SG, so to prevent the fermentation from slowing down, as was seen in Experiment 3, the feed rate was increased. As shown in the figure, the feed rate was increased at approximately 20 hours, and the SG showed a noticeable increase. The break in the SG readings at 33 hours was caused by a power failure in the lab, causing the controllers to go offline. The control system was offline, which also caused the fermenter's temperature to decline. Once the temperature controllers were restarted, at 44 hours, the temperature increased but did not return to the setpoint. The fermentation ended after approximately 65 hours, after which the fermenter's temperature again declined.

Table A6: Data for Experiment 6

Time h	Vol added /h	SG	Ferm Temp C	total sugar consumed
0	0.00	1.051039	36.03	-1.44
1	0.00	1.043946	36.10	-0.43
2	0.00	1.040254	34.73	0.27
3	0.00	1.036833	34.19	0.69
4	0.00	1.026768	34.66	1.43
5	0.00	1.027156	35.21	1.73
6	0.12	1.019882	34.66	2.29
7	0.42	1.019337	34.58	2.46
8	0.42	1.014873	34.79	3.06
9	0.42	1.014006	35.17	3.26
10	0.42	1.015172	34.82	3.63
11	0.42	1.008862	34.48	3.93
12	0.42	1.009778	34.51	4.23
13	0.42	1.011007	34.58	4.56
14	0.42	1.009912	34.72	4.78
15	0.42	1.00846	34.88	5.12
16	0.42	1.006695	35.03	5.42
17	0.42	1.005946	34.85	5.62

18	0.42	1.007495	34.68	5.84
19	0.54	1.007649	34.53	6.08
20	0.83	1.010103	34.48	6.35
21	0.83	1.011134	34.57	6.47
22	0.83	1.014772	34.70	6.69
23	0.83	1.014917	34.87	6.93
24	0.83	1.01665	35.05	7.15
25	0.83	1.016685	34.80	7.34
26	0.83	1.019341	34.55	7.50
27	0.83	1.022083	34.37	7.65
28	0.83	1.023883	34.32	7.85
29	0.83	1.02607	34.30	7.93
30	0.57	1.026547	34.25	8.10
31	0.00	1.025692	34.20	8.26
32	0.00	1.024379	34.38	8.43
33	0.00	1.023283	34.39	8.97
34	0.00	1.022504	33.97	8.97
35	0.00	1.021725	33.55	8.97
36	0.00	1.020947	33.13	8.97
37	0.00	1.020168	32.70	8.97
38	0.00	1.019389	32.28	8.97
39	0.00	1.01861	31.86	8.98
40	0.00	1.017831	31.43	8.98
41	0.00	1.017053	31.01	8.98
42	0.00	1.016306	30.57	9.31
43	0.00	1.015681	30.08	9.50
44	0.00	1.01559	29.58	9.52
45	0.00	1.015162	29.55	9.57
46	0.00	1.014789	29.94	9.68
47	0.00	1.014722	30.50	9.71
48	0.00	1.014722	31.13	9.71
49	0.00	1.013084	31.71	9.89
50	0.00	1.012727	32.17	9.93
51	0.00	1.011852	32.35	9.96
52	0.00	1.011269	32.46	10.08
53	0.00	1.010514	32.60	10.15
54	0.00	1.010162	32.70	10.21
55	0.00	1.010162	32.73	10.21
56	0.00	1.00956	32.76	10.30
57	0.00	1.008946	32.69	10.36
58	0.00	1.008345	32.63	10.40
59	0.00	1.008412	32.59	10.43
60	0.00	1.008369	32.56	10.44

A.1.7 Experiment 7

Experiment 7 was performed with the largest mass of yeast added, 300 g and 300 g of yeast extract. The feed rate was set to the maximum to increase the sugar concentration during the fermentation. At the start of the fermentation, as can be seen in Table A7, the temperature of the fermenter was lower than in the previous experiments, as the addition of the yeast was delayed, and the fermenter cooled below the target temperature. Once the fermenter temperature reached the setpoint, the temperature was maintained until the fermentation was completed.

Table A7: Data for Experiment 7

Time h	Vol added /h	SG	Ferm Temp C	total sugar consumed
0	0.00	1.049649	25.65	-1.68
1	0.00	1.04946	26.58	-1.17
2	0.00	1.046617	27.11	-0.27
3	0.00	1.037942	27.97	0.23
4	0.00	1.036166	28.98	0.61
5	0.00	1.035689	29.95	0.85
6	0.00	1.026212	30.87	1.43
7	0.36	1.017796	31.58	2.33
8	2.50	1.028879	32.03	2.74
9	2.50	1.031045	32.36	3.46
10	2.50	1.034987	32.63	4.51
11	2.50	1.034987	33.14	5.09
12	2.50	1.034987	33.64	5.11
13	1.80	1.048847	34.17	5.55
14	0.00	1.052479	34.70	4.90
15	0.00	1.059968	35.05	4.40
16	0.00	1.06339	33.88	3.71
17	0.00	1.060996	34.08	3.83
18	0.00	1.057253	34.73	4.42
19	0.00	1.051923	34.65	4.88
20	0.00	1.046947	34.05	5.33
21	0.00	1.04446	34.30	5.83
22	0.00	1.039963	34.79	6.24
23	0.00	1.038471	34.67	6.58
24	0.00	1.038471	34.10	6.98
25	0.00	1.037012	34.38	7.04

26	0.00	1.03146	34.83	7.26
27	0.00	1.032407	34.67	7.55
28	0.00	1.02914	34.69	7.83
29	0.00	1.027299	35.00	8.04
30	0.00	1.027032	34.34	8.16
31	0.00	1.024518	34.51	8.44
32	0.00	1.023325	34.89	8.57
33	0.00	1.021327	34.50	8.72
34	0.00	1.021144	34.23	8.91
35	0.00	1.020195	34.51	8.95
36	0.00	1.018751	34.90	9.04
37	0.00	1.018033	34.53	9.23
38	0.00	1.018338	34.15	9.29
39	0.00	1.017023	34.12	9.44
40	0.00	1.017023	33.52	9.44
41	0.00	1.017023	32.91	9.44
42	0.00	1.017023	32.31	9.44
43	0.00	1.017023	31.71	9.44
44	0.00	1.017023	31.10	9.44
45	0.00	1.017023	30.50	9.44
46	0.00	1.017023	29.90	9.44
47	0.00	1.015628	29.31	9.58
48	0.00	1.015278	29.18	9.59
49	0.00	1.014912	29.32	9.63
50	0.00	1.014866	29.53	9.65
51	0.00	1.014335	29.81	9.68
52	0.00	1.014149	30.04	9.71
53	0.00	1.014798	30.12	9.73
54	0.00	1.013945	30.31	9.76
55	0.00	1.013454	30.43	9.82
56	0.00	1.01361	30.53	9.83
57	0.00	1.012817	30.60	9.89
58	0.00	1.013365	30.66	9.87
59	0.00	1.013147	30.67	9.89
60	0.00	1.012621	30.66	9.92
61	0.00	1.012211	30.21	9.95
62	0.00	1.012421	29.58	9.96
63	0.00	1.012267	28.95	9.98
64	0.00	1.012217	28.33	10.00
65	0.00	1.012189	27.82	10.00
66	0.00	1.012162	27.31	10.00
67	0.00	1.012134	26.80	10.00
68	0.00	1.012106	26.29	10.00
69	0.00	1.012079	25.77	10.00
70	0.00	1.012051	25.26	10.00

71	0.00	1.012038	24.68	10.01
72	0.00	1.012038	24.33	10.01
73	0.00	1.012038	23.96	10.01
74	0.00	1.012038	23.62	10.02
75	0.00	1.012038	23.39	10.02
76	0.00	1.012038	23.16	10.02

4.3.8 Experiment 8

Experiment 8 differed from the previous experiments in that a density control loop was added to maintain the SG at a value of 1.010. the controller was a simple on/off controller, where if the density measurement was below the setpoint, a relay was closed, and the feed was added to the fermenter at the maximum feed rate. Once the density rose above the setpoint, the relay was opened again. The feed added was recorded based on the amount of time the relay was closed and corrected based on the mass measurements of the feed vessel.

The temperature control for this experiment was not fully functional, as seen from the temperature profile in Table A8, due to a malfunctioning pump. While the temperature was not maintained at the setpoint, the temperature of the fermenter remained above 28°C for the duration of the experiment until the fermentation was complete.

Table A8: Data for Experiment 8

Time h	Vol added /h	SG	Ferm Temp C	total sugar consumed
0	0.00	1.046	40.20	-0.35
1	0.00	1.046	39.69	-0.35
2	0.00	1.046	38.57	-0.35
3	0.00	1.046	37.68	0.16
4	0.00	1.030451	36.93	1.16
5	0.00	1.028612	36.20	1.35
6	0.00	1.023546	36.01	1.74
7	0.00	1.024182	35.60	1.90
8	0.00	1.016741	35.23	2.22
9	0.00	1.014731	34.90	2.33
10	0.00	1.014706	34.56	2.60
11	0.00	1.014055	34.21	2.86
12	0.45	1.008995	33.82	3.20
13	0.37	1.010752	33.44	3.46
14	0.61	1.00748	32.92	3.51
15	0.29	1.0103	32.55	3.90
16	0.73	1.011026	32.05	4.11
17	0.00	1.011478	31.78	4.18
18	0.41	1.011948	31.36	4.28
19	0.00	1.010505	31.07	4.42
20	0.00	1.009396	30.40	4.60

21	0.82	1.011871	29.70	4.69
22	0.00	1.010461	29.79	4.84
23	0.41	1.010213	30.06	5.00
24	0.35	1.007668	30.37	5.08
25	0.05	1.009823	30.85	5.24
26	0.41	1.008461	31.26	5.48
27	0.00	1.008521	31.67	5.62
28	0.41	1.008975	31.98	5.76
29	0.64	1.011366	32.21	5.98
30	0.00	1.010172	32.37	5.98
31	0.00	1.008879	32.51	6.11
32	0.40	1.009102	32.63	6.27
33	0.41	1.009232	32.80	6.51
34	0.00	1.009232	32.76	6.51
35	0.41	1.009485	32.47	6.62
36	0.00	1.007851	32.16	6.79
37	0.41	1.007695	31.71	6.91
38	0.00	1.0076	31.50	6.93
39	0.41	1.008835	31.20	7.06
40	0.00	1.00932	30.97	7.15
41	0.41	1.008539	30.72	7.25
42	0.00	1.008233	30.53	7.27
43	0.00	1.008512	30.38	7.32
44	0.41	1.008732	30.12	7.62
45	0.00	1.008732	30.11	7.62
46	0.41	1.009418	30.00	7.68
47	0.17	1.006509	30.09	7.83
48	0.24	1.007694	30.16	7.89
49	0.00	1.008363	30.23	7.95
50	0.00	1.007668	30.28	8.01
51	0.00	1.006758	30.33	8.14
52	0.41	1.008058	30.31	8.19
53	0.23	1.006464	30.35	8.31
54	0.00	1.007725	30.44	8.34
55	0.00	1.007135	30.42	8.41
56	0.39	1.007917	30.25	8.51
57	0.00	1.007402	30.22	8.56
58	0.41	1.00884	30.04	8.65
59	0.00	1.007821	29.92	8.73
60	0.00	1.007222	29.85	8.77
61	0.00	1.006491	29.72	8.88
62	0.20	1.006848	29.67	8.94
63	0.24	1.007453	29.55	8.96
64	0.00	1.006868	29.42	9.05
65	0.00	1.006356	29.32	9.12

66	0.41	1.007807	29.16	9.17
67	0.00	1.007212	29.07	9.22
68	0.00	1.006757	28.98	9.31
69	0.41	1.007732	28.81	9.35
70	0.00	1.007388	28.75	9.44
71	0.00	1.006993	28.32	9.47
72	0.00	1.006993	27.82	9.47
73	0.41	1.007203	27.11	9.60
74	0.00	1.0076	26.84	9.61
75	0.00	1.007027	26.74	9.70
76	0.00	1.006909	26.59	9.71
77	0.00	1.005916	26.48	9.76
78	0.20	1.005652	26.42	9.82
79	0.00	1.005639	26.45	9.86
80	0.40	1.007385	26.34	9.87
81	0.00	1.007267	26.39	9.96
82	0.00	1.006158	26.40	10.00
83	0.00	1.006304	26.39	10.07
84	0.02	1.006316	26.41	10.12
85	0.38	1.006898	26.33	10.15
86	0.00	1.006794	26.30	10.19
87	0.00	1.006653	26.30	10.24
88	0.00	1.006234	26.29	10.26
89	0.02	1.005472	26.20	10.30
90	0.00	1.00553	26.15	10.32
91	0.01	1.005428	26.15	10.30
92	0.00	1.006225	26.17	10.31
93	0.00	1.006109	26.16	10.29
94	0.00	1.005232	26.30	10.34
95	0.00	1.004699	26.25	10.40
96	0.00	1.005775	26.04	10.42
97	0.00	1.004892	26.09	10.46
98	0.00	1.00414	26.19	10.50
99	0.00	1.003245	26.35	10.56
100	0.00	1.00354	26.50	10.60
101	0.00	1.003098	26.59	10.67
102	0.00	1.003064	26.68	10.70
103	0.00	1.003008	26.71	10.70
104	0.00	1.002181	26.75	10.77
105	0.00	1.00205	26.72	10.78
106	0.00	1.001433	26.68	10.85
107	0.00	1.001346	26.65	10.88
108	0.00	1.00053	26.53	10.94
109	0.00	1.000849	26.51	10.97
110	0.00	1.00059	26.46	10.96

111	0.00	0.999943	26.33	11.01
112	0.00	0.999916	26.30	11.05
113	0.00	0.999354	26.20	11.09
114	0.00	0.99904	26.17	11.16
115	0.00	0.998934	26.11	11.17
116	0.00	0.999048	26.04	11.20

A.1.9 Experiment 9

This experiment consisted of 2 parts, the first being the initial phase from the start of the fermentation to 42 hours, and the second phase continuing until the end of the fermentation at 114 hours, as seen in Table A9. The initial stage was run similarly to experiment 8, with the feedback controller used to maintain the sugar concentration at 50 g/l. The method used to calculate the sugar concentration from the density measurement will be discussed in detail in Chapter 5. The specific gravity measured a static value of 1.001 after 42 hours, where 10.91 kg of the feed had been added. The second phase of the fermentation consisted of adding the remaining feed and 20 kg of water to dilute the ethanol in the fermenter. The fermentation continued once the addition had been made, as shown in Table A9. The fermentation continued until the specific gravity measured a static value of 0.994 after 114 hours. The temperature control maintained the temperature near the setpoint; however, the sudden addition of a large amount of feed and water caused the temperature to drop significantly. It was only after 100 hours that the temperature declined significantly.

Table A9: Data for Experiment 9

Time h	Vol added /h	SG	Ferm Temp C	total sugar consumed
0	0.00	1.038381	39.45	0.43
1	0.00	1.036518	38.32	0.53
2	0.00	1.027345	37.39	1.13
3	0.00	1.019301	36.78	1.74
4	0.00	1.017548	36.47	2.35
5	0.00	1.009824	36.19	2.85
6	0.83	1.01378	35.82	3.31
7	0.42	1.010708	35.55	3.63
8	0.62	1.010311	35.04	3.99
9	0.76	1.007257	34.54	4.27
10	0.10	1.008068	34.23	4.57
11	0.49	1.005511	33.87	4.87
12	0.54	1.008736	33.46	5.16
13	1.23	1.005337	32.95	5.68
14	0.00	1.008721	32.79	5.68
15	0.17	1.006353	32.59	5.90

16	0.60	1.004679	32.25	6.17
17	0.00	1.005476	32.31	6.41
18	0.80	1.00399	32.52	6.49
19	0.24	1.006594	32.87	6.73
20	0.00	1.005821	33.33	6.97
21	0.41	1.005116	33.73	7.23
22	0.13	1.004565	34.17	7.35
23	0.51	1.003098	34.51	7.61
24	0.36	1.002934	34.74	7.81
25	0.00	0.999896	35.08	8.03
26	0.00	1.001258	34.74	8.05
27	0.00	1.001258	34.78	8.03
28	0.00	1.001258	35.04	8.03
29	0.00	1.001258	34.93	8.03
30	0.00	1.001258	34.93	8.20
31	0.00	0.993898	34.89	8.81
32	0.00	0.993909	34.48	8.86
33	0.00	0.993215	33.97	8.91
34	0.00	0.992989	33.45	8.94
35	0.00	0.992989	32.95	8.92
36	0.00	0.992989	32.54	8.91
37	0.00	0.992989	32.16	8.91
38	0.00	0.992989	31.78	8.90
39	0.00	0.992989	31.40	8.90
40	0.00	0.992989	31.01	8.90
41	0.00	0.992989	30.63	8.90
42	0.00	0.992989	30.25	8.90
43	46.79	0.991989	30.42	10.14
44	0.00	1.018672	31.28	11.44
45	0.00	1.01499	32.22	12.60
46	0.00	1.014523	32.67	12.85
47	0.00	1.013399	33.06	13.05
48	0.00	1.012478	33.42	13.20
49	0.00	1.012535	33.66	13.31
50	0.00	1.012097	33.87	13.40
51	0.00	1.011485	34.12	13.50
52	0.00	1.01098	34.23	13.63
53	0.00	1.010231	34.32	14.16
54	0.00	1.010231	34.30	14.16
55	0.00	1.010231	34.29	14.16
56	0.00	1.010231	34.27	14.16
57	0.00	1.010231	34.25	14.16
58	0.00	1.010231	34.23	14.17
59	0.00	1.010231	34.22	14.17
60	0.00	1.010231	34.20	14.17

61	0.00	1.010231	34.18	14.17
62	0.00	1.010231	34.16	14.17
63	0.00	1.010231	34.15	14.17
64	0.00	1.006072	34.03	14.74
65	0.00	1.005867	33.95	14.80
66	0.00	1.004921	33.87	14.90
67	0.00	1.004996	33.85	14.99
68	0.00	1.004318	33.96	15.09
69	0.00	1.003899	34.14	15.18
70	0.00	1.003598	34.33	15.27
71	0.00	1.002876	34.36	15.38
72	0.00	1.002725	34.37	15.46
73	0.00	1.002273	34.36	15.65
74	0.00	1.0019	34.35	15.65
75	0.00	1.001527	34.34	15.65
76	0.00	1.000746	34.29	15.83
77	0.00	1.000625	34.24	15.89
78	0.00	1.000581	34.23	15.91
79	0.00	0.999807	34.22	16.06
80	0.00	0.999556	34.07	16.14
81	0.00	0.999199	34.02	16.19
82	0.00	0.998896	33.95	16.24
83	0.00	0.998641	33.82	16.33
84	0.00	0.998712	33.80	16.39
85	0.00	0.997883	33.61	16.47
86	0.00	0.998018	33.49	16.52
87	0.00	0.998018	33.32	16.52
88	0.00	0.997734	33.21	16.55
89	0.00	0.997237	33.09	16.65
90	0.00	0.996699	32.92	16.75
91	0.00	0.996577	32.95	16.77
92	0.00	0.996435	32.96	16.83
93	0.00	0.996105	33.11	16.88
94	0.00	0.995723	33.34	16.99
95	0.00	0.995603	33.44	16.99
96	0.00	0.995761	33.45	16.93
97	0.00	0.995542	33.45	17.01
98	0.00	0.995161	33.47	17.14
99	0.00	0.994724	33.41	17.20
100	0.00	0.994724	33.28	17.20
101	0.00	0.994724	33.23	17.21
102	0.00	0.994297	32.94	17.28
103	0.00	0.994062	32.18	17.32
104	0.00	0.994399	31.33	17.30
105	0.00	0.994151	30.52	17.31

106	0.00	0.994346	29.73	17.31
107	0.00	0.994065	28.96	17.34
108	0.00	0.99399	28.15	17.35
109	0.00	0.99399	27.43	17.36
110	0.00	0.99399	26.71	17.36
111	0.00	0.99399	26.04	17.36
112	0.00	0.99399	25.37	17.36
113	0.00	0.99399	24.73	17.36

A.1.10 Experiment 10

The final experiment was also performed in 2 phases, with the initial phase starting using the same initial mass of yeast and yeast extract as the first four experiments. The fermentation was initially run as a batch reaction containing 50 kg of water, 15 kg of sugar, 100 g of yeast extract and 100 g of dried yeast. The fermentation continued until the specific gravity measured a static value of 1.022 after 38 hours, as shown in Table A10. The second phase of the fermentation was initiated by adding 42.7 kg of water into the fermenter. The mass of water was calculated to allow all sugar to be converted into ethanol, with the ethanol concentration being the same at which the fermentation initially stalled in the initial phase. The fermentation continued until the specific gravity measured a static value of 0.993 after 128 hours. The method used to calculate the ethanol concentration will be discussed in detail in Chapter 5. The temperature of the fermentation is shown in Table A10.

Table A10: Data for Experiment 10

Time h	Vol added /h	SG	Ferm Temp C	total sugar consumed
0	0.00	1.106759	37.69	-2.25
1	0.00	1.113194	34.69	-2.87
2	0.00	1.10481	34.73	-2.27
3	0.00	1.105767	35.12	-1.97
4	0.00	1.104398	34.22	-1.79
5	0.00	1.102058	34.37	-1.53
6	0.00	1.100424	34.76	-1.20
7	0.00	1.097258	35.11	-0.81
8	0.00	1.09374	34.49	-0.37
9	0.00	1.092841	34.51	-0.21
10	0.00	1.091283	34.56	0.11
11	0.00	1.087162	34.81	0.34
12	0.00	1.085967	35.02	0.56
13	0.00	1.083899	33.81	0.81
14	0.00	1.08483	33.45	0.87
15	0.00	1.082408	33.48	1.15
16	0.00	1.080211	33.63	1.47
17	0.00	1.078261	33.66	1.75

18	0.00	1.074246	33.77	1.97
19	0.00	1.0731	33.91	2.42
20	0.00	1.070874	33.96	2.52
21	0.00	1.06905	33.99	2.87
22	0.00	1.066972	34.07	3.15
23	0.00	1.063625	34.17	3.40
24	0.00	1.061985	34.19	3.73
25	0.00	1.059764	34.35	3.98
26	0.00	1.05719	34.54	4.26
27	0.00	1.056838	34.83	4.46
28	0.00	1.054405	35.04	4.73
29	0.00	1.052648	34.74	4.92
30	0.00	1.050747	34.72	5.19
31	0.00	1.04918	34.74	5.42
32	0.00	1.04747	34.75	5.62
33	0.00	1.045538	34.67	5.85
34	0.00	1.045117	34.53	5.99
35	0.00	1.042861	34.42	6.18
36	0.00	1.042255	34.34	6.32
37	0.00	1.041188	34.28	6.46
38	0.00	1.03984	34.12	6.63
39	0.00	1.038677	34.02	6.75
40	0.00	1.038201	33.94	6.82
41	0.00	1.03716	33.68	6.96
42	0.00	1.036513	33.50	7.15
43	0.00	1.036158	33.31	7.15
44	0.00	1.035816	33.10	7.17
45	0.00	1.033721	32.86	7.38
46	0.00	1.033041	32.59	7.47
47	0.00	1.032466	32.29	7.54
48	0.00	1.032265	31.92	7.63
49	0.00	1.031776	31.64	7.68
50	0.00	1.031013	31.48	7.75
51	0.00	1.030395	31.45	7.83
52	0.00	1.029786	31.34	7.90
53	0.00	1.029332	31.19	7.96
54	0.00	1.029108	31.07	8.01
55	0.00	1.028388	30.92	8.07
56	0.00	1.028018	30.82	8.14
57	0.00	1.02755	30.63	8.19
58	0.00	1.027	30.43	8.25
59	0.00	1.026761	30.21	8.31
60	0.00	1.026326	30.04	8.35
61	0.00	1.026099	29.85	8.41
62	0.00	1.025786	29.65	8.43

63	0.00	1.02515	29.52	8.48
64	0.00	1.024968	29.34	8.53
65	0.00	1.024752	29.10	8.55
66	0.00	1.024338	28.91	8.61
67	0.00	1.02393	28.70	8.62
68	0.00	1.02363	28.50	8.68
69	0.00	1.023078	28.29	8.74
70	0.00	1.023003	28.11	8.76
71	0.00	1.02266	28.04	8.80
72	0.00	1.022677	27.93	8.84
73	0.00	1.022249	27.96	8.87
74	0.00	1.022249	28.08	8.89
75	0.00	1.021811	28.16	8.83
76	42.70	1.022657	28.15	6.65
77	0.00	1.032366	28.22	6.23
78	0.00	1.010519	29.22	9.36
79	0.00	1.009525	29.59	9.60
80	0.00	1.00935	29.94	9.74
81	0.00	1.008543	30.18	9.84
82	0.00	1.007835	30.47	9.96
83	0.00	1.006899	30.65	10.19
84	0.00	1.006884	30.85	10.26
85	0.00	1.005781	31.02	10.42
86	0.00	1.005826	31.19	10.50
87	0.00	1.004556	31.30	10.60
88	0.00	1.004754	31.42	10.70
89	0.00	1.004521	31.60	10.71
90	0.00	1.004521	31.63	10.71
91	0.00	1.004521	31.75	10.71
92	0.00	1.004521	31.84	10.71
93	0.00	1.001372	31.90	11.24
94	0.00	1.001747	31.98	11.32
95	0.00	1.001358	32.01	11.46
96	0.00	1.000388	32.06	11.62
97	0.00	0.999756	32.17	11.74
98	0.00	0.999806	32.37	11.86
99	0.00	0.999094	32.49	11.87
100	0.00	0.998823	32.63	11.96
101	0.00	0.998714	32.73	11.96
102	0.00	0.997864	32.80	12.10
103	0.00	0.997607	32.88	12.24
104	0.00	0.996573	32.88	12.36
105	0.00	0.996905	32.88	12.40
106	0.00	0.995994	32.77	12.54
107	0.00	0.996106	32.78	12.62

108	0.00	0.995396	32.74	12.67
109	0.00	0.994956	32.65	12.72
110	0.00	0.995351	32.56	12.69
111	0.00	0.995019	32.40	12.75
112	0.00	0.994785	32.27	12.80
113	0.00	0.994636	32.14	12.89
114	0.00	0.994244	32.01	12.95
115	0.00	0.994327	31.88	13.00
116	0.00	0.99356	31.70	13.02
117	0.00	0.993869	31.58	13.01
118	0.00	0.993347	31.43	13.10
119	0.00	0.993193	31.33	13.17
120	0.00	0.992864	31.17	13.20
121	0.00	0.992861	31.14	13.21
122	0.00	0.992979	31.10	13.22
123	0.00	0.992825	31.07	13.22
124	0.00	0.992694	31.00	13.23
125	0.00	0.993298	30.95	13.21
126	0.00	0.993058	30.92	13.19
127	0.00	0.993376	30.77	13.15
128	0.00	0.993206	30.63	13.17

A.1.13 Optimisation strategy tests

The methods used to produce these results will be discussed in detail in Chapters 5, 6 and 7.

The dilution strategy was demonstrated as effective in Experiment 9 and Experiment 10, shown in previous chapters. The total ethanol production is calculated based on online density measurements. The total ethanol produced in Experiment 9 and Experiment 10 is shown in Figure A.1 and Figure A.2 respectively. In both cases, adding water increases the ethanol produced from where the fermentation had initially stopped at approximately 4000 g to over 7000 g. Excess water allowed the yeast to consume as much sugar as possible, increasing the sugar consumed from 59.6% and 58.5% to 100% and 87.7% for Experiment 9 and experiment 10.

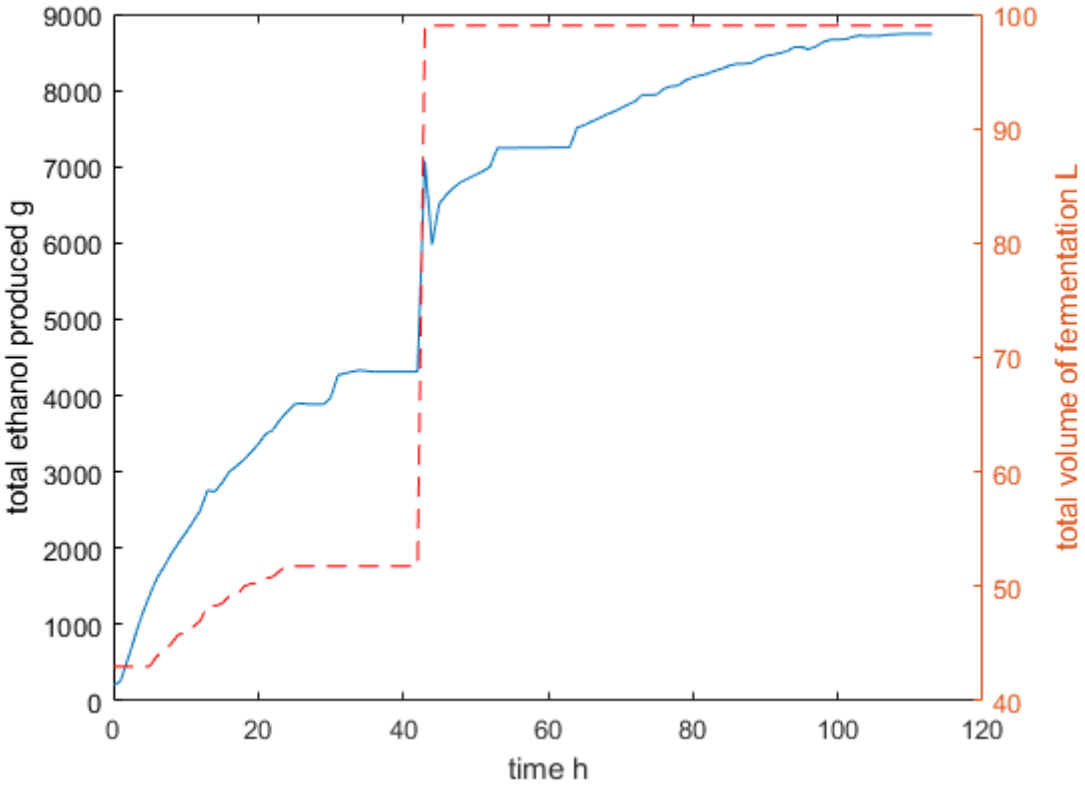

Figure A.0.1: Total ethanol production during experiment 9

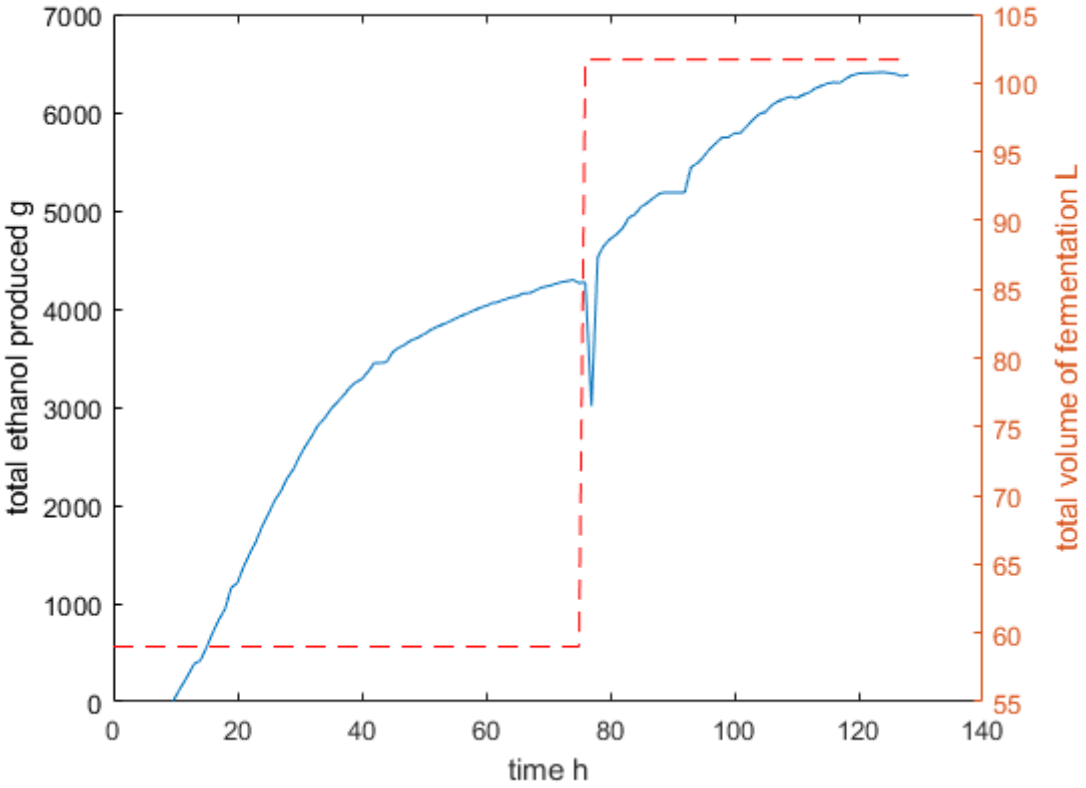

Figure A.0.2: Total ethanol production during experiment 10

The optimisation strategy was refined and tested in 2 optimisation tests. In the first test, the fermentation progressed until the ethanol concentration caused the fermentation to cease, as shown in Figure A.3. The ethanol concentration at the point the fermentation stalled, calculated from the density measurements, was assumed to be P_{max} for the fermentation. The value of P_{max} was then used to determine the volume of dilution water required to convert the sugar to ethanol completely. The water was heated to 35°C to avoid any temperature changes in the fermenter.

In the second test, the same volume of water was added. However, it was added after 17 h while the yeast was still active.

Figure A.0.3 shows the effect of adding the dilution water after the fermentation had stopped. In the case where the dilution water was added after the fermentation had stalled, the final ethanol concentration was lower; hence the

total ethanol produced was lower, and the sugar conversion was 92.4% and a final ethanol concentration of 91.6 g/L.

Figure A.4 shows the effect of adding the dilution water earlier. When the dilution water was added earlier in the fermentation, the final ethanol concentration increased to 96.37 g/L, and the sugar conversion increased to 98.2%. The results demonstrate that the optimal operation of the fermenter would be achieved by adding the dilution water early. Early addition of the dilution water also shortened the fermentation time, as the second test completed the fermentation 50 h faster than the first.

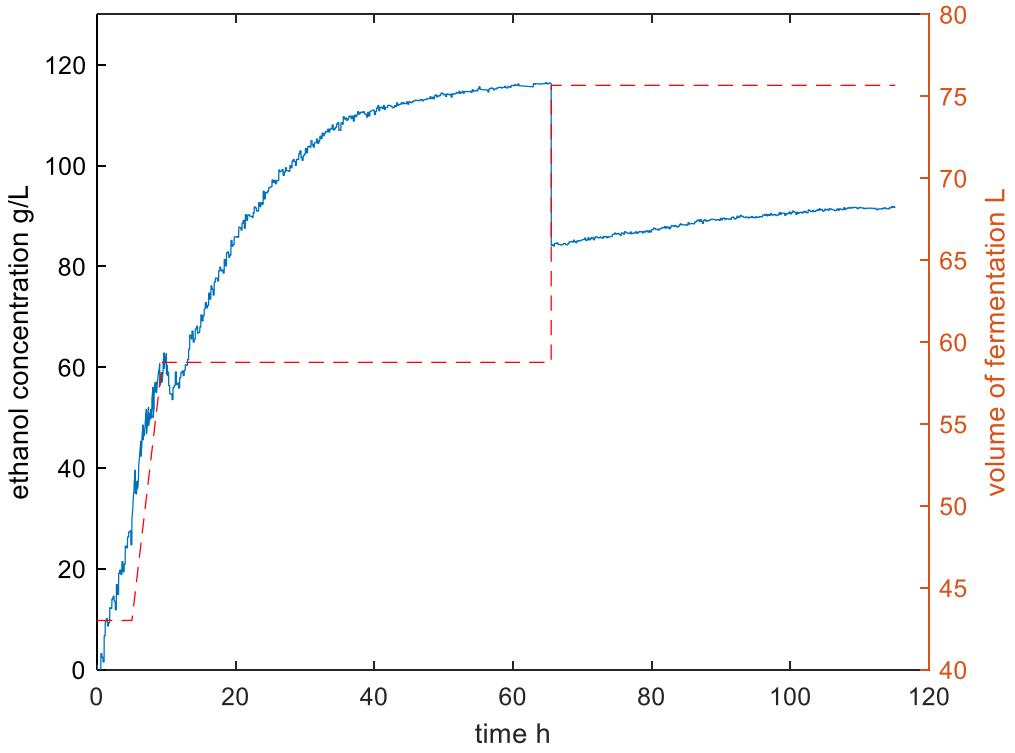

Figure A.0.3: Ethanol concentration and volume of fermentation during first optimisation test

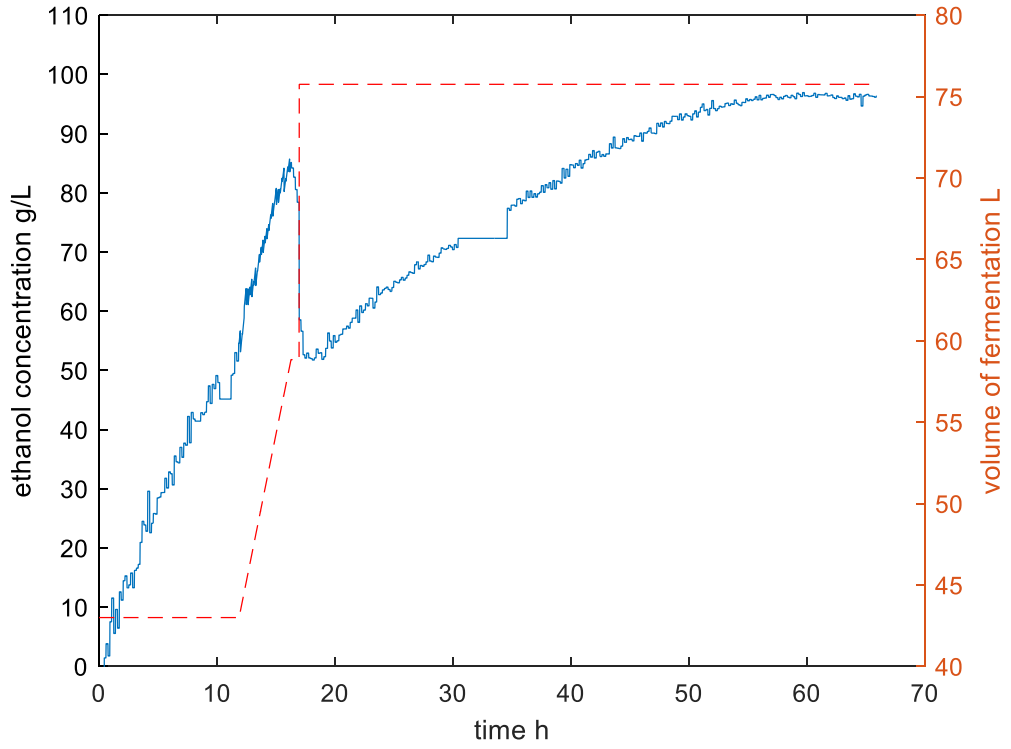

Figure A.0.4: Ethanol concentration and volume of fermentation during second optimisation test

Appendix B-Matlab Code

MATLAB code for determining model parameters

```
clear;
clc;
load("all_variables.mat");
et=a;
tt=b;
ft=c;
Stt=Stot;
y0=[0  42.5 ];

Para0=[ 0.5 100  1 ];

a=et.x1;
b=tt.x1;
c=ft.x1;
Stot=Stt.x1;

tspan=[0: b(end)];

d=@(Para) slvr(Para,tspan,a,b,c,y0,Stot);
%EXP1
[Para1,fval] = fminsearch(d,Para0);
%[Para1,fval] = ga(d,3,[],[],[],[],[0.1 50 0.5],[2
150 1.5]);
p=tiledlayout(5,2);
nexttile
[plt1, V1]=slvrplt(Para1,b,a,b,c,y0);
err=(Stot-plt1);
err2=err.^2;
rmse1=sqrt(mean(err2))/mean(Stot);
R1=corr2(Stot,plt1)^2;
plot(b,Stot,'r.')
hold on
plot(b,plt1,'k')
hold off
title('EXP 1')
xlabel('time h')
```

```
ylabel('Sugar consumed g')
ylim([0 15])


% Exp 2
nexttile

a=et.x2;
b=tt.x2;
c=ft.x2;
Stot=Stt.x2;

tspan=[0: b(end)];
d=@(Para) slvr(Para,tspan,a,b,c,y0,Stot);
[Para2,fval] = fminsearch(d,Para0);
%[Para2,fval] = ga(d,3,[],[],[],[],[0.1 50 0.5],[2
150 1.5]);
[plt2, V2]=slvrplt(Para2,b,a,b,c,y0);
err=(Stot-plt2);
err2=err.^2;
rmse2=sqrt(mean(err2))/mean(Stot);
R2=corr2(Stot,plt2)^2;
plot(b,Stot,'r.')
hold on
plot(b,plt2,'k')
hold off
title('EXP 2')
xlabel('time h')
ylabel('Sugar consumed g')
ylim([0 15])
% Exp 3
nexttile

a=et.x3;
b=tt.x3;
c=ft.x3;
Stot=Stt.x3;

tspan=[0: b(end)];
d=@(Para) slvr(Para,tspan,a,b,c,y0,Stot);
[Para3,fval] = fminsearch(d,Para0);
%[Para3,fval] = ga(d,3,[],[],[],[],[0.1 50 0.5],[2
150 1.5]);
[plt3, V3]=slvrplt(Para3,b,a,b,c,y0);
err=(Stot-plt3);
err2=err.^2;
```

```
rmse3=sqrt(mean(err2))/mean(Stot);
R3=corr2(Stot,plt3)^2;
plot(b,Stot,'r.')
hold on
plot(b,plt3,'k')
hold off
title('EXP 3')
xlabel('time h')
ylabel('Sugar consumed g')
ylim([0 15])
% Exp 4
nexttile

a=et.x4;
b=tt.x4;
c=ft.x4;
Stot=Stt.x4;

tspan=[0: b(end)];
d=@(Para) slvr(Para,tspan,a,b,c,y0,Stot);

[Para4,fval] = fminsearch(d,Para0);
%[Para4,fval] = ga(d,3,[],[],[],[],[0.1 50 0.5],[2
150 1.5]);
[plt4, V4]=slvrplt(Para4,b,a,b,c,y0);
err=(Stot-plt4);
err2=err.^2;
rmse4=sqrt(mean(err2))/mean(Stot);
R4=corr2(Stot,plt4)^2
plot(b,Stot,'r.')
hold on
plot(b,plt4,'k')
hold off
title('EXP 4')
xlabel('time h')
ylabel('Sugar consumed g')
ylim([0 15])
% Exp 5
nexttile

a=et.x5;
b=tt.x5;
c=ft.x5;
Stot=Stt.x5;

tspan=[0: b(end)];
```

```
d=@(Para) slvr(Para,tspan,a,b,c,y0,Stot);
[Para5,fval] = fminsearch(d,Para0);
%[Para5,fval] = ga(d,3,[],[],[],[],[0.1 50 0.5],[2
150 1.5]);
[plt5, V5]=slvrplt(Para5,b,a,b,c,y0);
err=(Stot-plt5);
err2=err.^2;
rmse5=sqrt(mean(err2))/mean(Stot);
R5=corr2(Stot,plt5)^2
plot(b,Stot,'r.')
hold on
plot(b,plt5,'k')
hold off
title('EXP 5')
xlabel('time h')
ylabel('Sugar consumed g')
ylim([0 15])
% Exp 6
nexttile

a=et.x6;
b=tt.x6;
c=ft.x6;
Stot=Stt.x6;

tspan=[0: b(end)];
d=@(Para) slvr(Para,tspan,a,b,c,y0,Stot);
[Para6,fval] = fminsearch(d,Para0);
%[Para6,fval] = ga(d,3,[],[],[],[],[0.1 50 0.5],[2
150 1.5]);
[plt6, V6]=slvrplt(Para6,b,a,b,c,y0);
err=(Stot-plt6);
err2=err.^2;
rmse6=sqrt(mean(err2))/mean(Stot);
R6=corr2(Stot,plt6)^2;
plot(b,Stot,'r.')
hold on
plot(b,plt6,'k')
hold off
title('EXP 6')
xlabel('time h')
ylabel('Sugar consumed g')
ylim([0 15])

% Exp 7
```

```
nexttile

a=et.x7;
b=tt.x7;
c=ft.x7;
Stot=Stt.x7;

tspan=[0: b(end)];
d=@(Para) slvr(Para,tspan,a,b,c,y0,Stot);
[Para7,fval] = fminsearch(d,Para0);
%[Para7,fval] = ga(d,4,[],[],[],[],[0.1 50 0.5],[2
150 1.5]);
[plt7, V7]=slvrplt(Para7,b,a,b,c,y0);
err=(Stot-plt7);
err2=err.^2;
rmse7=sqrt(mean(err2))/mean(Stot);
R7=corr2(Stot,plt7)^2;
plot(b,Stot,'r.')
hold on
plot(b,plt7,'k')
hold off
title('EXP 7')
xlabel('time h')
ylabel('Sugar consumed g')
ylim([0 15])
% Exp 8
nexttile

a=et.x8;
b=tt.x8;
c=ft.x8;
Stot=Stt.x8;

tspan=[0: b(end)];
d=@(Para) slvr(Para,tspan,a,b,c,y0,Stot);
[Para8,fval] = fminsearch(d,Para0);
%[Para8,fval] = ga(d,3,[],[],[],[],[0.1 50 0.5],[2
150 1.5]);
[plt8, V8]=slvrplt(Para8,b,a,b,c,y0);
err=(Stot-plt8);
err2=err.^2;
rmse8=sqrt(mean(err2))/mean(Stot);
R8=corr2(Stot,plt8)^2;
plot(b,Stot,'r.')
hold on
```

```
plot(b,plt8,'k')
hold off
title('EXP 8')
xlabel('time h')
ylabel('Sugar consumed g')
ylim([0 15])
% Exp 9
nexttile

a=et.x9;
b=tt.x9;
c=ft.x9;
Stot=Stt.x9;

tspan=[0: b(end)];
d=@(Para) slvr(Para,tspan,a,b,c,y0,Stot);
[Para9,fval] = fminsearch(d,Para0);
%[Para9,fval] = ga(d,3,[],[],[],[],[0.1 50 0.5],[2
150 1.5]);
[plt9, V9]=slvrplt(Para9,b,a,b,c,y0);
err=(Stot-plt9);
err2=err.^2;
rmse9=sqrt(mean(err2))/mean(Stot);
R9=corr2(Stot,plt9)^2;
plot(b,Stot,'r.')
hold on
plot(b,plt9,'k')
hold off
title('EXP 9')
xlabel('time h')
ylabel('Sugar consumed g')
ylim([0 15])
% Exp 10
nexttile

a=et.x10;
b=tt.x10;
c=ft.x10;
Stot=Stt.x10;

tspan=[0: b(end)];
d=@(Para) slvr(Para,tspan,a,b,c,y0,Stot);
[Para10,fval] = fminsearch(d,Para0);
%[Para10,fval] = ga(d,3,[],[],[],[],[0.1 50
0.5],[2 150 1.5]);
```

```
[plt10, V10]=slvrplt(Para10,b,a,b,c,y0);
err=(Stot-plt10);
err2=err.^2;
rmse10=sqrt(mean(err2))/mean(Stot);
R10=corr2(Stot,plt10)^2;
plot(b,Stot,'r.')
hold on
plot(b,plt10,'k')
hold off
title('EXP 10')
xlabel('time h')
ylabel('Sugar consumed g')
ylim([0 15])
paraf=[Para1 rmse1 R1;Para2 rmse2 R2;Para3 rmse3
R3;Para4 rmse4 R4;Para5 rmse5 R5;Para6 rmse6
R6;Para7 rmse7 R7;Para8 rmse8 R8;Para9 rmse9
R9;Para10 rmse10 R10];
function dydt=ode(t,y,Para,a,b,c,y0)

  Vmax=Para(1);
  Pmax=Para(2);
  n=Para(3);



  dydt=zeros(2,1);
  Ft=interp1(b,c,t,'linear');
  %P=interp1(b,a,t,'linear');
  P=378.1*y(1)/y(2);
  dydt(1)=Vmax*(1-(P/Pmax))^n;
if dydt(1)<0
    dydt(1)=0;
 end
  dydt(2)=Ft;


end

function St=slvr(Para,tspan,a,b,c,y0,Stot)

y0=[0 42.5];

[t,y]=ode45(@(t,y)
ode(t,y,Para,a,b,c,y0),tspan,y0);

St=norm(y(:,1)-Stot,2).^2;
```

```
end

function [St, V]=slvrplt(Para,tspan,a,b,c,y0)

y0=[0 42.5];
[t,y]=ode45(@(t,y)
ode(t,y,Para,a,b,c,y0),tspan,y0);

St=(y(:,1));
V=(y(:,2));
end
```

MATLAB code for training Neural network

```
% create a neural network
net = feedforwardnet([ 2 5  ]);
% train net
net.divideParam.trainRatio = 0.7; % training set
[%]
net.divideParam.valRatio = 0.15; % validation set
[%]
net.divideParam.testRatio = 0.15; % test set [%]

 net1.layers{1}.transferFcn='tansig';
 net1.layers{2}.transferFcn='tansig';
 net1.layers{3}.transferFcn='tansig';

% train a neural network
net = trainlm(net,inputs2',Utp');
% show network
view(net);
genFunction(net,'MLP_NN.m','MatrixOnly','yes')
```

Neural network Model used to predict final ethanol concentration

```
function [Y,Xf,Af] = MLP_NN(X,~,~)
%MLP_NN neural network simulation function.
%
% Auto-generated by MATLAB, 01-Oct-2022 16:40:39.
%
% [Y] = MLP_NN(X,~,~) takes these arguments:
%
%   X = 1xTS cell, 1 inputs over TS timesteps
%   Each X{1,ts} = 11xQ matrix, input #1 at
timestep ts.
%
% and returns:
%   Y = 1xTS cell of 1 outputs over TS timesteps.
%   Each Y{1,ts} = 1xQ matrix, output #1 at
timestep ts.
%
% where Q is number of samples (or series) and TS
is the number of timesteps.

%#ok<*RPMT0>

% ===== NEURAL NETWORK CONSTANTS =====

% Input 1
x1_step1.xoffset = [-2.3201027028354;-
2.3201027028354;-2.3201027028354;-
2.3201027028354;-2.3201027028354;-
2.3201027028354;-2.3201027028354;-
1.69336949183638;-0.222985415032497];
x1_step1.gain =
[0.36621370428329;0.36621370428329;0.3662137042832
9;0.36621370428329;0.36621370428329;0.366213704283
29;0.36621370428329;0.36621370428329;0.36621370428
329;0.0208828370870072;0.0425424170187972];
x1_step1.ymin = -1;

% Layer 1
b1 = [1.5704825828536714827;-
1.7467180074850785498;1.7999615673827700224;-
0.589826393661032843955;0.84575182777078383722;-
0.87821617070175983510;-0.20935302306935069105;-
0.029450969911164949495;0.15873820125663087865;-
0.29767622138393190490;-
```

```
0.042038967109596196703;0.12283962195333994472;-
0.010714047684200601537;-
0.76452359467715125252;1.2091575983925648696;-
1.31949735502430964483;-1.13742099358826620482;-
1.0823288419227325985;1.5187247406015018658;1.7245
810742754681399;1.46964173431090205920];
IW1_1 = [-0.81750443152282459280 -
0.59354183264929982755 0.88830310243374732693
0.80725932543791134588 -0.59151088877270763255
0.41331577400798663602 -0.43440160433727481593 -
0.26106811642316679611 0.26370225489251170048
0.77249448103221496353
0.98433555687600449158;0.68619767368581430222 -
0.42470558367157890123 0.84874424517434277071
0.65690618545645529380 -0.22348060652505127854 -
0.31817960069269557444 -0.52780060590664557019
0.65724819577450932506 0.47862978804935218946
0.46869188532926525648 0.47805748092904026825;-
0.70822434667023215216 -0.50347628102277730555 -
0.95214534121649685439 -0.70675373808141006560
0.014291460985233130077 -0.34893038640220808144 -
0.33422983145811491212 0.25941135993991859543
0.47396209269337086223 0.055764831501441042283 -
0.31335308347280121932;1.0859771286109842769 -
0.34929141986723855062 -0.62538579838855912207 -
0.62801421812940472211 0.96773434027529681156
0.049712039033887975292 0.24242562771002829081
0.89684193284595092877 1.1365944526194913244
0.6210104308560693287 -0.403377842789008733369;-
0.055145759983072521748 -0.677093025067114107070
0.583805644017902025670 -0.962315350176320749580 -
0.548731468407942513110 1.0080743864922043773 -
1.09162118752593739760 -0.640749274147757730270 -
0.32865487281007310649 -0.054648050458443189759
0.051017267998181028976;0.69888278716639073984 -
0.97233489099508008113 -0.603456209856499725670
0.54920595017018258854 -0.935206313598573646400 -
0.20112691428325640830 0.033698978670713822248
0.51163261171917950865 -0.088479719954654548197 -
0.30081477070417023123 -
0.88284433492460812065;0.670290957460029201980
0.30090463932473487940 0.756070712019342838770 -
0.019236617250825177594 0.325386206302442027030
1.05976220338100790560 0.860251207390529737400
0.504812084126762372630 0.342078175648197757570
```

```
0.86953913603827781564 -
0.18882121641832350 09;0.62245239776358773 92
1.03992092412084158 33 -0.13130400248516532757 -
1.65701982258828772 74 -0.79300677360542304317 -
0.71279774862328337814 -0.47990387106873810819
0.12070988129079575357 -0.109498041497979412
0.04372350153743881362 4 0.39013554693954799468;-
0.58344795941038618547 -0.70715439193971851 85 -
0.77841743280037922759 -1.61498250855202329 92 -
1.35994450121007481 87 -1.76334480640964663 68 -
1.89698784013094168 27 -1.83476325976380261 2 -
1.79880308273385169 93 -1.00191569311650918 73
0.74658706428716281 6;-0.68589649308298417107 -
0.91388328524956508048 -0.60295821557016326953 -
0.17892021267957750053 0.62713234786546989685 -
0.04405301715823561 1983 -0.70247865942992804289 -
1.10459951220931418 27 -0.19909957733131894431 -
1.01630858331871687 38 -0.22874881723878676132;-
0.98086136453754035891 -1.50942201275068388 36 -
1.65451771981951556 43 0.31578108520581116281 -
0.41323582427963417851 0.10846197416421989035 -
1.24765472291788892 53 1.00559998061360844 62
0.33087172659534391794 -0.82946765628941621085 -
0.65856712664007532876;0.66076286539663031672
0.21966969646160630636 -0.70141006842984321423
0.64201438033693536411 0.04466158982823401763
0.78392719110207953 47 0.64560500471599890915 -
0.71045974170183345819 -0.52265189255510358102
0.03743949425313966 5725
0.94401061881987657909;0.08045980098061408 7917
0.63692799389461740578 -0.68176493921686687205 -
0.06475704906640923630 4 0.62313275828193936956
0.75846546666607872478 -0.42328775852087985321
0.69681384169587612387 -0.28061385816464334 83 -
1.88202869269708483 73 0.16549221019031648 55;-
1.69151716659011586 15 -2.01794532394911207 97 -
0.64578178531417840258 -0.95127893552591324955 -
1.23112284022665763 32 -0.51075447199777412877 -
0.91911336771330431894 -0.84998837504678304011 -
1.49038823917410434 56 0.77406469844178171 78
0.74565481409853517913;0.84047799853761373523
0.90785411544015581775 0.60485291361989357295
0.10684037842238693072 -0.20659110897018170827
0.28582143627957601328 0.26162951166907078004 -
0.62584645088580637129 -1.46657792365282269 03 -
```

```
3.2454989027400187318 -0.35810640299290968924;-
1.4099074413661329963 -1.2345835973394934104
1.2407864466549802795 0.55963572244339976347 -
0.10612416936998969597 1.34646892255590611114
0.56375898933042889460 0.37769300908138753181 -
0.24257105006190604612 0.20396646415183999901 -
1.18976778118516191010;-0.28843774086862222772
0.01513557367495553876 4 0.74482006376524545477
0.93578538781558562309 1.05908621041091399740
0.42844942184178863576 0.17175089594688178196
0.01940995167151167780 1 0.36103884535862201810 -
0.19374751444066665163 0.73038631791723618303;-
0.56209605208707380530 -0.15553010649002940724 -
0.73235467119419994653 1.24142288317413429510
0.52757547383968994570 0.67431227643598845578
0.52716826619981160817 0.86836314191409547103
0.30761616311872419516 1.08371648402399434200 -
1.10834176581284382660;0.23075609773090249854
0.67115061576264167797 0.18503024200766146623 -
0.46268384824568531410 -0.62115270406141920301
0.73144301277599099720 -0.63918060343582605576
0.52238233854873927786 0.75484246274605781846
0.41410515671063080623 -
0.39041980943012538630;0.15122520542976930491 -
0.63577160342135796700 0.59368779761757939362
0.77509987593095475145 -0.53518750607325193958 -
0.35290070673846513083 1.03156032285888987770 -
0.03105956793520172482 0.17069370533023964231
0.38710098291645211876 -
0.24569142226323900657;0.28012077750911162921
0.61956990877263329320 0.92321368208373755238 -
0.19962011503730611728 -0.03486415576078819023 -
0.69600626465878456806 0.21015271707674126889 -
0.49282306712657403258 0.12014411761101119469 -
1.00031374654742277740 -1.08844701268451760080];

% Layer 2
b2 = [-
1.12857482056975522160;0.68161488265456060542;-
0.31059949191609154129;0.58656538060394758372;0.93
83981016311733203110;1.55738025647230271530];
LW2_1 = [0.86017377741728506813
0.08385231685206945284 0.57009738346005733867
0.23228660744766477242 0.59689514607393889811
0.51640333231237034450 -0.31516795862151214536 -
```

```
0.64361132037552137852 -2.21033375011317589991 -
0.013880149303162907584 -1.34051456589702810971 -
0.58962707422171645177 0.38385987976189150928 -
1.16657278263881725171 -2.1590192390824936021
1.13417827590714415111 -0.606845414524356474571
1.31913393572765036411 0.756878935988817169721
0.610466507699505500641 -0.051643571938184751335;-
0.481079536801634288781 0.081697499719677268981 -
0.65667328274641811881 0.066563026295675994937
0.121547915826254501751 0.099299490289129835331 -
0.131537231664259235411 -0.185978639333345657781
0.686902185418058697231 0.404431684427773940891 -
0.128024724753422580741 0.483211622321543687871
0.180226038722399201091 0.889667239879572413491 -
1.048030282663575674101 0.128047048437383959031
0.602954822373221177581 0.271236707844418056811 -
0.480350215321637519231 0.336242529529922340451 -
0.447755797000522925981;0.639638063840478388041
0.026310982523231662977 0.157185805355679164561 -
0.307380428523396476151 -0.928950516366626843911 -
0.244331380898903882671 1.024539298970241096901 -
0.905933389395714105951 -2.106305457795580871 -
0.678783983658015954711 0.576298594379357709271
0.053619534977490806931 -0.771228607522682629851 -
1.164306791622311321201 -1.747055718281086411601 -
0.382472712736419528931 -0.419221963721728152491 -
0.128164657855060509781 0.464903260473663815231
0.059585799137524433421
0.387099426364864052111;0.540695196465316940681 -
0.305636875963972931561 -0.184069612496379292341
0.859122331827222640581 0.114556048595149506661 -
0.492894816008692671081 1.000143997335172230101
0.964819022493899502991 -1.9655894808812031105 -
1.042218721126565439401 -1.29889590731185511351
0.173507399819682411881 -1.43289313433911669191 -
2.621573940464763108311 0.364223541966058050881
1.337012844354560581201 0.226566103766897064541
0.772560433969054827231 0.481656486183943910451
0.417428603078866533591 -
0.219334362428852125421;0.410844440147974054871
0.228633100528808447251 -0.337425474551344528611 -
0.309571936883075271571 -0.141297368996022382201 -
0.751508704933700921741 0.764791399193703203 -
0.753772214862006961771 -0.647361196498124180641 -
0.468617386991472706371 0.297658595713936435791
```

```
0.61942332850204850914 -0.28738674686047727125 -
0.37432189540357385666 0.00318426413116616562 06
0.47912934604393153659 0.20459956527185402253 -
0.25817607173859302705 -0.40598575883902759953
0.38177018676735724467
0.648809577010634241920;1713309902108679505 5 -
0.27605322811280735840 -0.38459243315592872570
0.098852253054050362446 0.33798537376843351687 -
0.10984975012140810180 0.19786463441148904874 -
0.28527195756984408126 -0.52206369868126367706 -
0.42613641990328199327 -0.54338448188512544768 -
0.62505346571738451544 -0.24211890058658655511 -
0.14669707018143490762 -0.30115552198320932886
0.19407642397072180640 0.19027627523321305469 -
0.27138951663787408419 0.40008411576544061772 -
0.13806140925573293088 -0.28110560169644971396];

% Layer 3
b3 = 0.515811982884857744840;
LW3_2 = [1.7736345670590196733
0.954099630570123591330 -1.9564168325048938435
1.0276974980091853062 -0.95471770848016801470
0.893502947711923845020];

% Output 1
y1_step1.ymin = -1;
y1_step1.gain = 0.0733115934786222;
y1_step1.xoffset = 66.7982432243897;

% ===== SIMULATION ========

% Format Input Arguments
isCellX = iscell(X);
if ~isCellX
  X = {X};
end

% Dimensions
TS = size(X,2); % timesteps
if ~isempty(X)
  Q = size(X{1},2); % samples/series
else
  Q = 0;
end

% Allocate Outputs
```

```
Y = cell(1,TS);

% Time loop
for ts=1:TS

    % Input 1
    Xp1 = mapminmax_apply(X{1,ts},x1_step1);

    % Layer 1
    a1 = tansig_apply(repmat(b1,1,Q) + IW1_1*Xp1);

    % Layer 2
    a2 = tansig_apply(repmat(b2,1,Q) + LW2_1*a1);

    % Layer 3
    a3 = repmat(b3,1,Q) + LW3_2*a2;

    % Output 1
    Y{1,ts} = mapminmax_reverse(a3,y1_step1);
end

% Final Delay States
Xf = cell(1,0);
Af = cell(3,0);

% Format Output Arguments
if ~isCellX
  Y = cell2mat(Y);
end
end

% ===== MODULE FUNCTIONS ========

% Map Minimum and Maximum Input Processing
Function
function y = mapminmax_apply(x,settings)
  y = bsxfun(@minus,x,settings.xoffset);
  y = bsxfun(@times,y,settings.gain);
  y = bsxfun(@plus,y,settings.ymin);
end

% Sigmoid Symmetric Transfer Function
function a = tansig_apply(n,~)
  a = 2 ./ (1 + exp(-2*n)) - 1;
end
```

```
% Map Minimum and Maximum Output Reverse-
Processing Function
function x = mapminmax_reverse(y,settings)
  x = bsxfun(@minus,y,settings.ymin);
  x = bsxfun(@rdivide,x,settings.gain);
  x = bsxfun(@plus,x,settings.xoffset);
end
```